The constraint-mechanism of the human tarsus

A roentgenological experimental study

Robert Jan Benink

ACTA ORTHOPAEDICA SCANDINAVICA SUPPLEMENTUM NO. 215, VOL. 56, 1985

MUNKSGAARD · COPENHAGEN

THE CONSTRAINT-MECHANISM OF THE HUMAN TARSUS

A Roentgenological Experimental Study

This study has been accepted as doctoral thesis by the State University of Leiden, The Netherlands

Promotiecommissie:

Promotor	: Prof. Dr. A. Huson
Referent	: Prof. Dr. R.H. Rozendal (Vrije Universiteit Amsterdam)
Overige leden	: Prof. Dr. Ir. J.D. Janssen (Technische Hogeschool Eindhoven)
	Prof. Dr. A. Cats
	Prof. Dr. J.D. Mulder

The following figures were reprinted with permission: Figures 2.8., 2.9., 2.10., from Benink, R.J. (1978), Radiology (The Radiological Society of North-America, Inc.) Figure 3.3a., from Langelaan, E.J. van (1983), Thesis Leiden, (Munksgaard).

The production of this book was handled by Palm Produkties, Nieuwerkerk a/d IJssel, The Netherlands.

ISBN: 87-16-06322-8
ISSN: 0300-8827

To my family

CONTENTS

ONE

Introduction, definition of the problem, arrangement of the study, and review of the literature

1.1. Introduction

Looking at the tarsal bones one by one, it is difficult to conceive that, together, they constitute a functional unit capable of supple movement. Yet, the tarsus is a part of the locomotor system that combines an excellent weight-bearing capacity with a surprisingly good flexibility. The foot can bear the weight of the entire body and more with apparently little if any deformation of its vault. When the surface on which the foot is placed changes its spatial orientation or shape, the foot is capable, within certain limits, of adapting itself easily to these changes and remain in optimal contact via a combination of movements in the talo-crural, tarsal and tarso-metatarsal articulations.

Huson (1961, 1966, 1973, a.o. 1977, 1982), has described the interdependence of the tarsal bones using the principle of the"closed kinematic chain". In Huson's model, the movements of the tarsal bones are interlinked in such a way that any movement of any bone in relation to another will initiate movements of all the other bones, according to a fixed pattern, with only one degree of freedom of motion. In view of the short, closed kinematic chain of the tarsus, this interlinkage would necessarily imply the presence of polyaxial articulations rather than the previously postulated hinge movements.

With a view to testing this kinematic model of Huson's, Van Langelaan and Spoor (1975), and Van Langelaan (1983) studied the interrupted, stepwise tarsal supination of vertically loaded lower leg foot-preparations. To this end, the tibia was exorotated *stepwise* (discontinuously) while the forefoot was prevented from following. The tarsal bones were marked with steel pellets, and the foot-preparation X-rayed in two projections. Using photogrammetry, it was then possible to calculate the spatial co-ordinates of the displaced pellets, and from these deduce the absolute and relative helical axes of the rotations of the tarsal bones.

This established that the tarsal movements were indeed polyaxial, apparently confirming Huson's views. It should be noted however, that so far the theory had only been proved for *interrupted* movements, broken up into a sequence of positions. The obvious next step (the first step in our study) was to test the theory also for a movement carried out *continuously without interruption*. The methods used and the findings of the study are described in Chapter 2.

The main question to be answered by our entire study was to what extent Huson's model, based on analysis of osteo-ligamentous material fixed post mortem, is also valid for motions in-vivo. This part of the work is described in Chapters 3 and 4, and compared with the findings of Van Langelaan (1983). It appears fair to assume that interindividual morphological variations of the foot do not affect the basic principle of the tarsal mechanism of the closed kinematic chain system.

While performing the experiments, we discovered fairly soon that there were sometimes considerable differences in the magnitude of the input moment that had to be applied to the tibia to supinate the tarsus. In addition, there appeared to be a relationship between the magnitude of the moment and the simultaneous vertical tibial translation that practically always accompanies the tarsal supination.

Since a follow-up of these observations might improve our understanding of the complicated biomechanical behaviour of the tarsus, the test setup was modified to include a momentmeter and a meter to register the vertical translation of the tibia.

We also wished to consider the biomechanical behaviour of the tarsus in the light of its roentgen-morphometric characteristics. Since the standard roentgen indexes (Stewart, 1970, and others) were found inadequate, we worked out a new index (i_t) in a lateral X-ray with the aid of a standardized radiographic technique.

$$i_t = 100 \times \frac{P_C}{L_T} \times \operatorname{tg} \epsilon_{TC}$$

P_C is a measure of the overlap of the anterior upper part of the calcaneus and the head of the talus,

L_T is the length of the talus for correction of foot size, and

ϵ_{TC} is the talo-calcaneal angle of inclination.

In this tarsal index formula, the talo-calcaneal relation is the central factor.

1.2. Definition of the problem

We postulated that our ultimate goal, which was to test the applicability of the findings of Huson (1961), Ambagtsheer (1978) and Van Langelaan (1983) to the living leg, necessitated finding answers to the following questions:

1. Is there an essential difference between a tarsal supination that is carried out in steps (discontinuously) and a supination that is carried out uninterruptedly or continuously in fixed osteo-ligamentous preparations?

The viscous-elastic behaviour which is often displayed by biological materials, prompted the second question:

2. How is the pattern of tarsal movements affected by differences in
   a. the vertical loading of the tibia?
   b. the speed of the imposed continuous movement?

In addition to the influence of the material's properties, the influence of variations in shape had also to be considered. This inspired the third question:

3. a. What is the relationship between the morphological parameters of the bones of the foot that can be deduced from a roentgen projection, and the biomechanical behaviour of the tarsus?
   b. To what extent are the results of the experiments reproducible?

By way of transition to in vivo studies, the following question may be asked:

4. How do the methods for processing and preserving fresh amputation preparations affect the biomechanical behaviour of the tarsus?

Finally, the comparability with in vivo registrations had to be considered:

5. a. Is it possible to design an experimental setup in which living subjects perform movements in a manner comparable with the post-mortem experiments, and how can these movements be recorded without the use of intra-osseous marker pellets?
   b. Are the movements that are made in vivo and recorded with this test setup comparable with the movements recorded during experiments with cadaver preparations?

1.3. Arrangement of the study

The study that was to provide answers to these questions was divided in three parts:

The first part (Chapter 2) deals with the first three questions. The positions of the measuring pellets in tibia and tarsal bones were recorded in roentgenograms of 6 osteo-ligamentous preparations under different experimental circumstances, and then compared. To make this possible we made both multiple-exposure instantaneous roentgenograms of the stepwise movement as well as time-exposure roentgenograms of the same tarsal supination movement carried out continuously. This part also includes measurement of the "input" moments that had to be applied to the tibia to supinate the foot, and measurements of the vertical tibial translations that accompanied the tarsal supination movements, using a total of 36 preparations which include 5 of the 6 preparations mentioned above and 31 others which were processed in the same way but not marked with measuring pellets.

The second part (Chapter 3) discusses the fourth question. Two amputation preparations were studied in a fresh, unprocessed condition. The findings this yielded were compared with the results of an analysis of the behaviour of the preparations after they had been dissected into osteo-ligamentous preparations. Before and after the dissection, the discrete, absolute and relative helical axes of the moving tarsal bones were calculated for both legs, using roentgen-photogrammetry.

The first two parts of the study are closely related to the work of Van Langelaan (1983).

In the third part (Chapter 4), the last question is considered and an attempt is made to demonstrate a relationship between the results obtained with cadaver material and the results obtained with living test subjects, using an analysis of outlines of the roentgen projections of the tarsal bones.

In Chapter 5 we reflect upon the things we have said in the previous chapters and try to place them in a clinical context with respect to the strain of the lateral ligaments that results from forced supination.

1.4. Review of the literature

There are few published studies which have a direct relation to our work, so that this review of the literature is necessarily brief. It is somewhat confusing, as Van Langelaan (1983) has pointed out, that analogous kinematic concepts are used and interpreted by different authors in different ways.

In defining the problem as we have, we realized that, by limiting our study to the complex of tarsal articulations, we might give the impression that we regard the functional relationship between the tarsus and the talo-crural joint as less important. This is certainly not our view; we fully realize that in practice the ankle joint and the tarsus nearly always move conjointly. However, we stop short of the assertion made by Inman (1976) that, because of the close relationship of these joints, neither of them can be studied without the other. This assertion appears to be basically correct but it might wrongly lead to the view that any functional study of one of these two systems of articulations, or even of any part of them, would be useless.

That the subject matter actually does lend itself to a separate investigation is apparent from the work of Barnett and Napier (1952) and De Vogel (1970) who analysed the tibio-tarsal joint.

Other investigators, Manter (1941), Jones (1945), Close and Inman (1953), Elftman (1960), Huson (1961) and Van Langelaan, Spoor and Huson (1974), on the other hand, focused their attention on the tarsal articulations. Authors who included both in their considerations are Hicks (1953, 1954, 1955), Sammarco et al. (1973), Inman (1976) and Schmidt (1981).

Huson's conception (1961, 1973) that the moving tarsus behaves as a closed kinematic chain with one degree of freedom of motion and, in consequence, may be regarded and analysed as an autonomous entity, justifies our studies (Benink, 1977, 1978, 1982) as well as those of others.

Huson (1961) and Van Langelaan (1983), in their doctoral theses, have presented extensive, detailed surveys of the published studies on the constructive-functional relationships of the tarsal articulations.

Our own study is concerned to a considerable extent with the correlations between the biomechanical behaviour of the tarsus and its roentgen-morphometric image, a subject on which we were not able to locate published information.

Certain authors, have, however, attempted to classify the foot or its skeleton, with the aid of the time-honoured sub-division, into "cavus", "normal" and "flat". The roentgenological classification of Stewart (1970) appeals to us most. He used a talar, a navicular and a cuboid index. In contrast Sachers (1949) made a classification with the external aspect of the foot and attached great value to the shape of the calcaneus. Because of the great variability, however, the measuring was not easy. Neither author described a relationship between (roentgen) morphometric findings and biomechanical behaviour of the tarsus.

TWO

Kinematic analysis and biomechanical behaviour of the tarsus of fixed osteo-ligamentous preparations: Part 1 of the study

2.1. Introduction

The objective of this part of the study was to provide answers to the following three questions:

1. Is there an essential difference between tarsal supination which is carried out in steps (discontinuously) and a tarsal supination which is carried out uninterruptedly (continuously) in fixed osteo-ligamentous preparations?
2. How is the pattern of tarsal movements affected by differences in
   a. the vertical loading of the tibia?
   b. the speed of the imposed continuous movement?
3. a. What is the relationship between the morphological parameters of the bones of the foot that can be deduced from an X-ray projection, and the biomechanical behaviour of the tarsus?
   b. To what extent are the results of the experiments reproducible?

To compare the stepwise tarsal supination with the same movement carried out continuously, helical axes are not suitable as kinematic parameters of the biomechanical behaviour. Whereas these axes can be determined for the step-by-step movement, they cannot be determined for the continuous movement. A different method was therefore needed. We decided to compare the trajectories of steel pellets in the tarsal bones on time-exposure roentgenograms in two projections with the positions of the same pellets projected on multiple-exposure roentgenograms during the step-by-step movement (Fig. 2.1.).

The biomechanical behaviour of the preparations was investigated in four different ways by recording:

a. the projections of successive positions of the markers of tarsal bones moving stepwise;

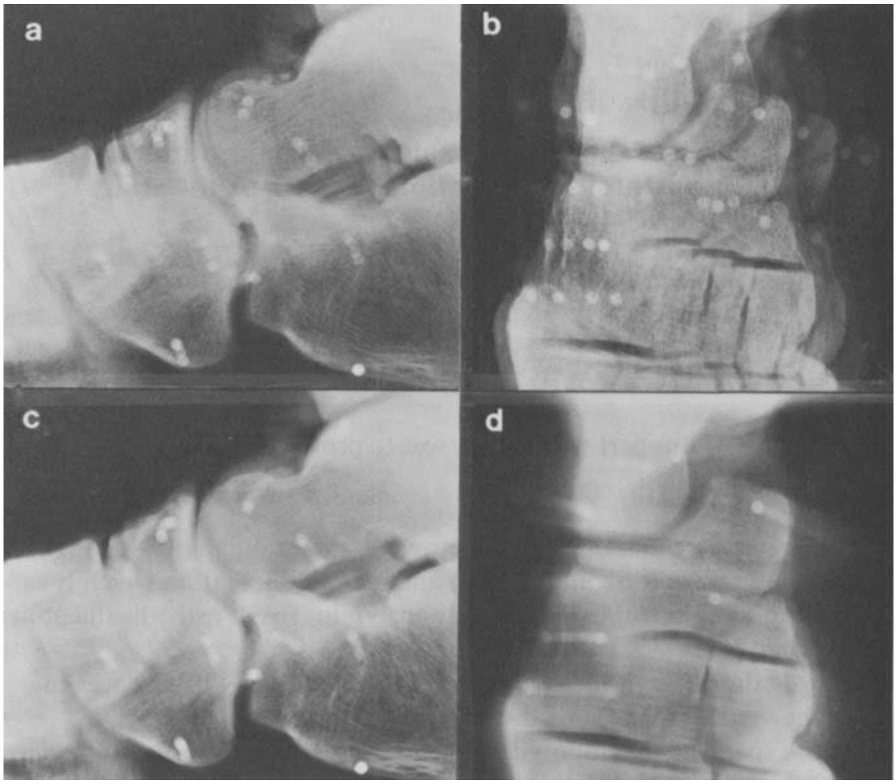

Fig. 2.1. Composite photograph of X-rays in two projections (horizontal and dorso-plantar) of supination of the tarsus. a and b show the multiple exposure registration of the supination of the tarsus carried out stepwise, c and d show the time exposure registration of the supination of the tarsus carried out continuously.

b. trajectories of the markers of tarsal bones moving continuously;
c. the magnitude of the input moment on the tibia as a function of the angle of rotation;
d. the vertical tibial translation during supination as a function of the angle of rotation.

This behaviour was examined on several preparations using three different loads and two different speeds.

In addition, morphological characteristics of the arch of the foot of the preparations were determined. This necessitated the development of a new roentgen index and an examination of the relationship between this index and the results of c and d (above).

2.2. Material used

To record the motions described under a and b above we used 6 fixed lower leg foot-preparations (two left feet and four right feet) from dissecting-room material (Table 2.1.). They originated from one woman and five men, averaging 63 years of age (range 43–80 years).

We used the same procedure as Van Langelaan.

The preparations were taken from cadavers preserved in toto (intravascular fixation) using the socalled "vin d'Alsace", composition: chloral hydrate 300 g, sol. Carolinum facticium 500 g, formalin 36% 750 ml, alcohol 96% 500 ml, glycerin 100 ml, phenol 100 ml; add water to 10 l.

The lower leg foot-preparations were obtained by exarticulation at knee level. The skin and the subcutaneous tissue were removed, after which the musculature of the lower leg was detached from the foot by severing the tendons at the level of the ankle joint. Good care was taken to ensure that during these manipulations, the capsule and ligaments of the ankle joint were not damaged. The proximal tibio-fibular joint was left in situ.

The subcutaneous tissue and the fatty mass below the plantar surface of the calcaneus were removed (Van Langelaan, 1983, p. 33.).

One preparation (cad. nr 342) came from Van Langelaan's collection and contained already roentgen marking-pellets.

In our preparations, the steel pellets were introduced into the tarsal bones in a slightly different manner, viz. directly subcortically, and as much as possible at corresponding sites in the different feet. Conspicuous, easily accessible sites were selected (Fig. 2.2.) and holes made with a dental drill. The pellets were fixed by means of a rapid-bonding adhesive (alpha-cyanolite) (Fig. 2.3.).

Whenever the test roentgenogram revealed arthrosis or other pathol-

TABLE 2.1.

Data for anatomical specimens

Specimen number (cad. nr)	sex	age (yrs)	L/R	catalogue number
342	m	79	R	4056
349	f	80	L	4081
492	m	52	R	5411
506	m	73	R	5538
511	m	43	R	5576
548	m	50	L	5838

TABLE 2.2.

Data for anatomical specimens

Specimen number (cad. nr)	sex	age (yrs)	L/R	catalogue number
248	f	75	R	1684
331	m	54	L	3985
338	m	80	L	4036
342	m	79	R	4056
345	m	70	R	4066
345	m	70	L	4066
349	f	80	L	4081
349	f	80	R	4081
355	m	59	L	4123
355	m	59	R	4123
400	f	84	R	4656
427	m	59	R	4973
456	m	75	R	5188
457	f	76	R	5187
465	f	84	R	5264
499	m	89	R	5457
492	m	52	R	5411
502	m	63	R	5503
504	m	68	L	5505
506	m	73	R	5538
516	f	75	R	5615
521	m	70	R	5681
529	m	76	R	5719
530	f	93	R	5747
537	m	67	R	5770
541	m	78	L	5793
541	m	78	R	5793
542	m	91	R	5794
543	f	78	R	5795
544	m	66	L	5799
545	m	74	L	5800
545	m	74	R	5800
546	f	81	L	5801
547	m	85	R	5824
548	m	50	L	5838
548	m	50	R	5838

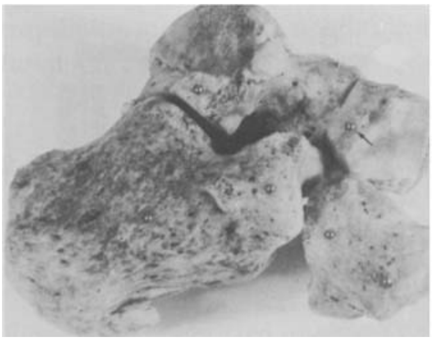

Fig. 2.2. Lateral aspect of the tarsus. Marker pellets in-situ.

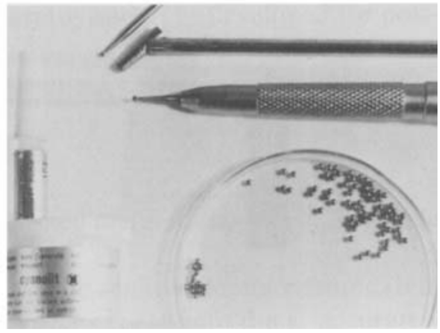

Fig. 2.3. Tools used to introduce the markers.

ogical alterations of bones, the preparation was rejected.

For the observations described in c and d above, 36 preparations were used, viz. 5 of the 6 already mentioned (cad. nrs 342, 349, 492, 506 and 548), together with 31 others which were prepared in the same way but not fitted with marker pellets. The magnitudes of the moment and the vertical tibial translation were measured as functions of the angle of exorotation (Table 2.2.).

Of cad. nrs 345, 349, 355, 541, 545 and 548, both the left and the right leg were measured. It should be kept in mind that although 36 legs have been measured, only 30 of these measurements can be regarded definitely as independent. Six preparations constituted pairs and are possibly not independent on the basis of an acceptable left-right comparison. We have not found data in the literature concerning such pairs and the parameters we have used.

The experiments with cad. nrs 338, 457, 492, 530 and 541R, chosen at random, were repeated as a check.

The material originated from 9 women and 21 men, averaging 73 years of age (range 50–93 years), and consisted of 11 left feet and 25 right feet, of which 6 constituted pairs (Table 2.3.).

TABLE 2.3.

Male-female and left-right distributions

Sex	nr	L	R
f	9	2	8 (1 pair)
m	21	9	17 (5 pair)

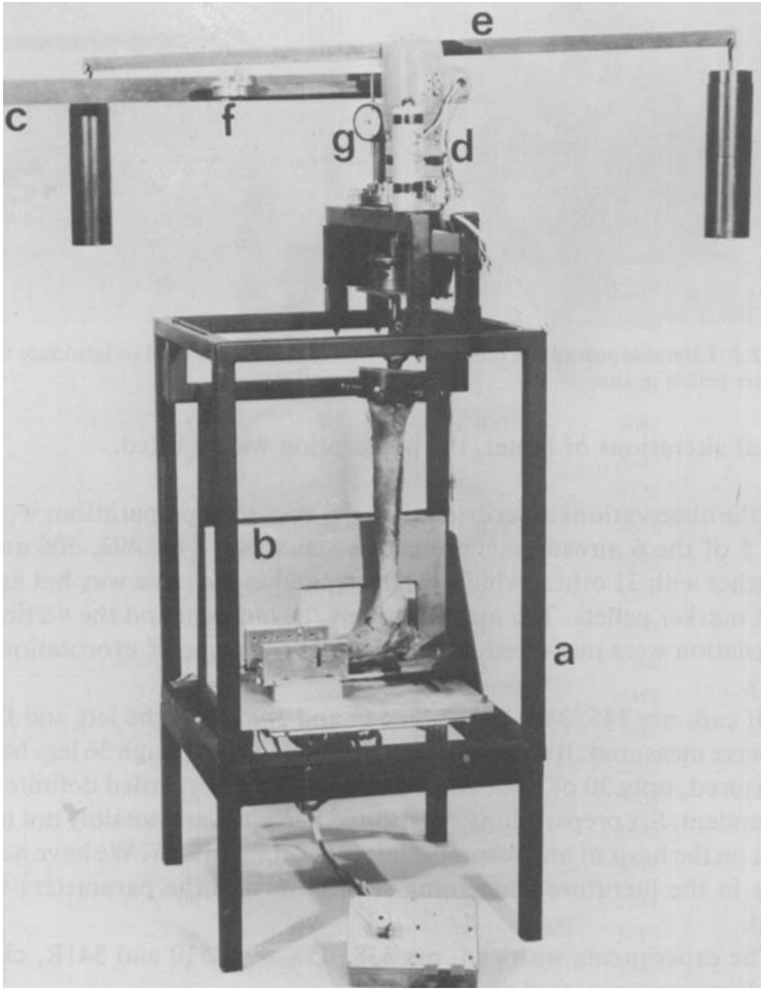

Fig. 2.4. Experimental setup with foot-lower leg preparation, with external (a) and internal (b) frames, manual (c) and electric (d) drive with variable vertical loading (e) and continuously adjustable rotation speed, momentmeter (f) and meter for the vertical tibial translation (g).

2.3. The measuring equipment and the sighting system

The experiments were carried out with an experimental setup, called the 'cage' (Fig. 2.4.). The prototype was designed by Ambagtsheer (1978), and Van Langelaan (1983) adapted it extensively so that it could be used for roentgen-photogrammetry. For our investigation, this cage had to be altered only slightly. It was equipped with a moment meter and a vertical translation meter. Also, a sighting apparatus had to be developed for positioning the roentgen sources.

2.3.1. Outer and inner frame of the cage

The outer frame was constructed of cornered metal tubing, 30 × 30 mm (a in Fig. 2.4.).

The measuring system was attached to the removable inner frame (b in Fig. 2.4.). It consisted of two aluminium plates, 13 mm thick, accurately placed at right angles, one horizontal and one vertical. Openings in these plates allowed the roentgen rays to pass through. Both plates were equipped with a brass reference system, consisting of three bars at right angles to each other (X, Y and Z axes). Fixed to the plates were two flattened roentgen cassettes (make ENRAF), with detachable lids. This part of the equipment was attached separately to the inner frame. Also attached to this inner frame was the support for the heel of the preparation.

Thanks to this arrangement, the pressure of the calcaneus during axial weighting of the tibia was not transmitted directly to the vertical plate. The forefoot was supported by an aluminium platform attached to the thick aluminium base plate. The pressure transmitted through the forefoot during the heaviest axial loading of the tibia that was used caused only negligible deformation of this plate.

To prevent slipping of the calcaneus and to let the movements take place as naturally as possible, a thin layer of coarse sand was glued to the heel platform with waterproof glue. On the sand layer was placed a cube of elastic foam plastic of 70 × 70 × 25 mm, which supported the calcaneus. This took the place of the fat pad below the tuber calcanei prepared off before fixation. Turning away (or abduction) of the forefoot during the tilting of the foot was prevented by fitting two vertical blocks of aluminium, horizontally movable, between which the forefoot could be placed (not too tightly). A separate small block (not visible in Fig. 2.4.), attached to one of the two vertical blocks (depending on the left or right foot), prevented the capitulum of the first metatarsal bone from rising.

2.3.2. Fittings for applying exorotating moment and vertical loading

The foot was made to tilt by applying an exorotating moment to the tibia. Both the vertical loading and the exorotating moment to initiate movement were applied to a vertical shaft attached by a universal joint coupling to a ring with 8 screws for fixing the proximal tibia. A known vertical load could

Fig. 2.5. Close-up of bellows, microswitches, and pawl.

be applied with a weight-bearing yoke that could be placed on top of the shaft. A ballbearing between them kept it from being turned by the shaft.

The shaft was connected by a bellows to a bearing which, with very little friction, allowed rotation in the (detachable) upper structure. Using a bellows also made possible translation in the vertical direction.

a. Discontinuous rotation

In the wide base ring of the bellows (Fig. 2.5.) there are holes at 5° (0.72 rad) distance from each other. A pawl attached to the upper structure makes possible movements in steps of exactly 5° (or a multiple), using a pinhole mechanism, enabling us to perform discontinuous rotation of the tibia.

b. Continuous rotation

The rotating moment could also be applied by an electric motor which, via a gear-wheel mechanism, could impart a moment to the base ring of the bellows. This motor (a combination motor of the firm of Groschopp und Co (Wild) type DM 80–60 and W.KM 80–60 used in heart-lung machines) could be continuously adjusted to various speeds, so that the rotation speed of the vertical shaft ranged from 0 rad/sec to 0.5 rad/sec. The magnitude of the angle of rotation could be adjusted by means of two microswitches (Fig. 2.5.).

2.3.3. Moment meter and vertical tibial translation meter

A calibrated *moment meter* was attached to the vertical shaft immediately below the ballbearing supporting the yoke.

The moment meter consisted of a long flexible steel arm and a short rigid rod, attached to a brass block of each side of the vertical shaft. Attached to the end of the short rod was a micrometer, the feeler point

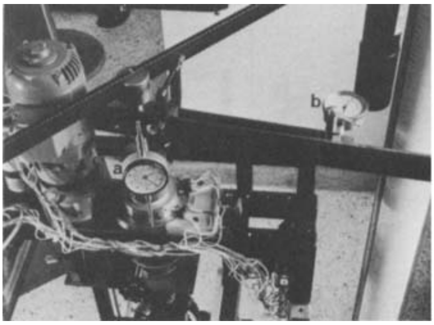

Fig. 2.6. Vertical tibial translation meter (a) and momentmeter (b) in the starting situation (before the exorotation of the lower leg resulting in the supination of the tarsus).

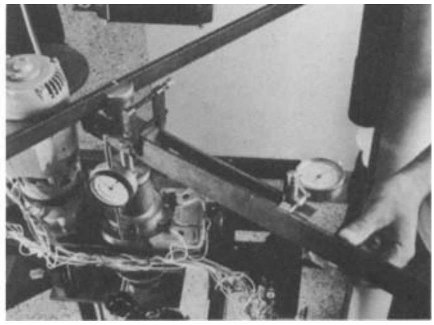

Fig. 2.7. Exorotation of the lower leg and supination of the tarsus induced by pressure against the rod. Vertical tibial translation and moment can be read.

of which pressed against a small brass block on the flexible arm (Fig. 2.6.). The long rod served to apply the force required to exorotate the tibia (Fig. 2.7.).

Calibration of the apparatus was simple since a virtually linear relationship was observed between the exo- (or endo-)rotating moment and the angular displacement.

The *vertical tibial translation meter* (also a micrometer) was attached to the upper ring of the bellows. Its feeler rested on the wide base ring. Since the bellows transmission allowed translation, the vertical tibial displacement could be measured to an accuracy of 0.01 mm.

2.3.4. Some critical notes on frictional and deformational resistances

The moment to be applied to overcome the rotation friction of the vertical shaft was found to be less than 0.05 Nm. The effect of this friction on the measurements appears negligible and moreover is constant. Some influence by the vertical friction between the shaft and the shaft bearing is to be expected, on the other hand. Calculations show it to be 9 N and constant.

When the spring constant of the bellows connection was determined, it was found that a rise of the shaft of 1 mm, 10 mm and 13 mm during supination corresponded to an increase of the vertical charge of $\approx$ 5.7 N, $\approx$ 57 N and $\approx$ 77 N respectively. Hence, this influence is not constant but increases linearly.

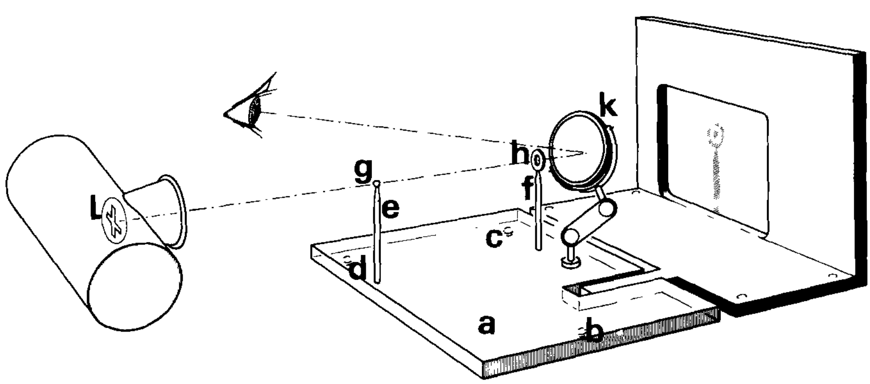

Fig. 2.8. Schematic diagram showing the positioning of the X-ray source, localizing device and cassette.

2.3.5. The X-ray equipment

The X-ray projections were made with two travelling roentgen tubes type 'Facilis 90/40' of the firm of Enraf Nonius in Delft. They consisted of a four-valve roentgen unit 'Elinos 90/40', mounted on the travelling column stand X315. The source-cassette distance was 106 cm for the horizontal projection and 110 cm for the dorsoplantar projection. These distances correspond to the cinematograph used for the in-vivo experiments (Chapter 4), in which the distance between source and intensifying screen is fixed.

2.3.6. The sighting system

Since the planning involved work with different X-ray apparatuses in various locations, as well as repeated roentgenography of the same preparations, a fixed setup was not feasible. Nevertheless, a standard roentgen technique was required for comparability. In order to achieve standardization, we developed a sighting system which allowes highly accurate positioning of the roentgen source in the desired direction at a fixed distance. The description of the sighting system has been published elsewhere (Benink 1978), but is included here for the sake of completeness.

For stability, three steel pellets 3 mm in diameter (Fig. 2.8. b, c and d) are partially countersunk in the lower surface of a Perspex plate (Fig. 2.8a). The plate is also provided with a rectangular slot into which a tongue

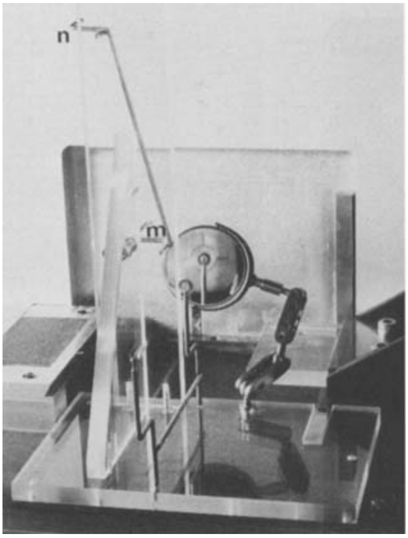

Fig. 2.9. The mark on the tube shield as seen in the mirror by the investigator through the localizing device.

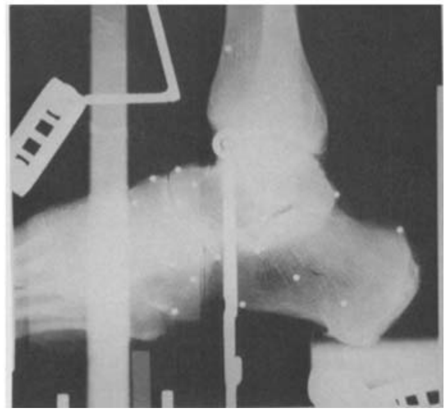

Fig. 2.10. Localizing device radiographed together with a specimen of the lower leg in the desired position.

attached to the cassette holder can be inserted to ensure proper positioning. Under the guidance of an optical sighting system, two small rods (Fig. 2.8e and f) are fixed in the Perspex plate 12 cm apart. A small pellet (diameter 2 mm) (Fig. 2.8g) is placed on top of rod e and a small ring (inner diameter 4 mm) (Fig. 2.8h) is placed on top of rod f. The rods are positioned such that the optical axis through the centers of the pellet and ring strikes the film in the cassette in the required direction (in this case, perpendicular to the vertical cassette). The central beam of the X-ray apparatus can then easily be made to coincide with the optical axis of the sighting system by means of a small mirror (k) situated behind bar f. The focal position of the tube shield can be brought into line with the pellet and ring while the operator keeps his eye on the mirror in the most convenient direction (Fig. 2.9.). Further refinement can be achieved by attaching a second mirror to the tube directly in front of the port; in this way even a slight deviation of the optical axis can be detected immediately by the observer, who will see a long row of pellets and rings. Ideally, the source is now perfectly positioned, but in using the device I invariably check the exposure of the device together with the specimen (Fig. 2.10.) or experimental subject, so that minor corrections can be carried out if necessary. The accuracy of this method is such that a 1–2 mm shift of a tube placed 1 meter from an object (living foot or specimen)

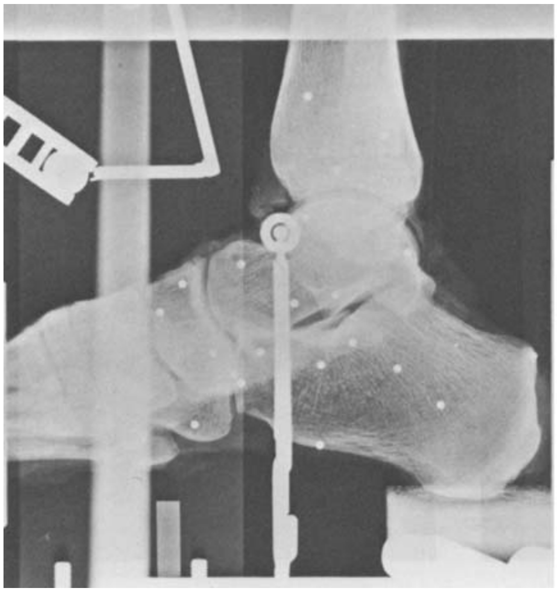

Fig. 2.11. Close-up of the central beam for the horizontal projection.

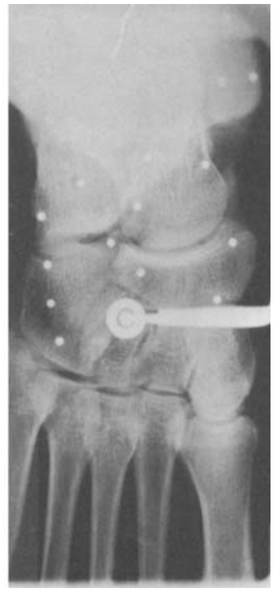

Fig. 2.12. Direction of the central beam for the dorso-plantar exposures.

can be detected from the position of the pellet in the ring.

For these studies, dorso-plantar radiographs taken at an angle of 75° with respect to a horizontal cassette lying parallel to the Perspex plate were also needed. For this purpose, a second set of rods (Fig. 2.9m and n) was incorporated into the device; a more universal apparatus could undoubtedly be constructed with rods that could be moved and adjusted in a plane parallel to the cassette according to any desired centre-point.

2.4. Experimental procedure

The tarsus was roentgenographed (time exposures), in the horizontal direction, perpendicular to the vertical cassette, and, in the dorso-plantar direction, at an angle of 75° to the horizontal cassette. These directions are the same as those used by Van Langelaan in his photogrammetric studies.

Of each foot we first made a 'standardized' X-ray in the experimental setup. The 'close-packed position' (Barnett et al. 1961), with a vertical loading of 340N, was chosen as the starting position. The foot was positioned in such a way that the two margins of the talar trochlea were projected superimposed on each other. A test X-ray was made to check this. Using the sighting system, the roentgen source was placed at a fixed distance

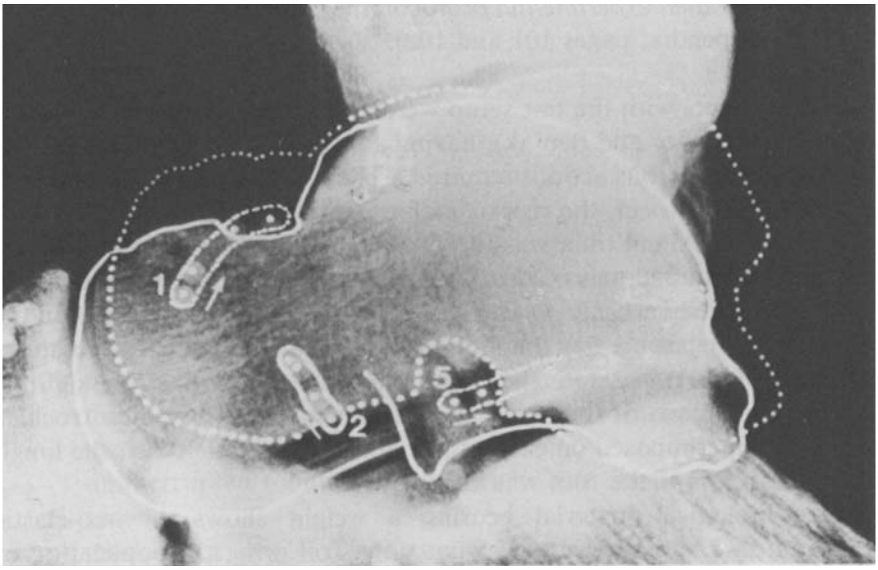

Fig. 2.13. Composite photograph of projection of pellet path with centre line and projection of the 4 pellet positions of the continuous movement of the talus in the horizontal projection.

of 106 cm. The horizontal central beam was aimed in front of the body of the talus, just above the neck, as shown in Fig. 2.11.. Fig. 2.12. shows the direction of the central beam for the dorso-plantar X-rays.

Next, we made multiple instantaneous exposures of the same field with a vertical loading of 160N. (Note. Van Langelaan used a separate film for each instantaneous exposure).

The vertical and horizontal X-ray projections were recorded simultaneously with the 0° position and the 10°, 20° and 30° exorotation positions superimposed on each other. The return movement was recorded in the same way in two other X-rays. We opted for steps of 10°, because with steps of 5° the pellets are very difficult to distinguish. Each film would then have had to be exposed 7 times instead of 4 times.

We then made time exposures with a vertical loading of 160N. The movement was imparted by the electric motor, and the changing positions of the marker pellets from 0° to 30° were recorded continuously in horizontal and vertical X-rays. The continuous return movement from 30° to 0° was likewise recorded.

This procedure caused the pellets to make, as it were, a 'tracing' or a 'trajectory' in the X-rays (Fig. 2.13., see also Fig. 2.1.). The continuous movement was recorded at two speeds: first at 6°/sec., then 0.5°/sec. Finally, the entire experiment was repeated with a heavier loading (340N).

2.4.1. Abbreviated experimental protocol (the complete protocol is included in the Appendix, pages 101 and 102).

The experiments with the test setup were always carried out by the same two persons (Spoor and Benink), having a fixed division of tasks. By performing the numerous actions required according to a strict time schedule experimental protocol, the risk of making mistakes was minimized.

First, the proximal tibia was locked in position, taking care to ensure that the longitudinal axis of the tibia was the precise continuation of the centre-line of the vertical rotation shaft. The calcaneus was placed on the heel platform in such a way that it did not slip off during the trial rotation.

The roentgen tubes were then positioned with the aid of the sighting system. The images of the two semicircular margins of the talar trochlea had to be superimposed on each other. Following a test X-ray, the longitudinal position of the foot was adjusted.

Since biological material bearing a weight shows a visco-elastic behaviour, we had to decide at what time, following the application of the vertical loading, the measurements were to start. Thus we waited until the rate of descent of the tibia was approx 0.01 mm per 14 seconds.

One series of measurements comprised:

1. *Adjustment*, i.e. mounting the yoke with weights (160N) and determining the starting position or the 0° position.
2. *Recording* of the *exorating moment* (M) and the *vertical tibial translation* (S) as functions of the angle of rotation from 0° to 30° and from 30° to 0°.
3. *Recording of the marker positions of the stepwise movement.*
4. *Recording of the marker trajectory of the continuous movement at two speeds* (6°/sec. and 0.5°/sec.)

Following this, the vertical loading was increased to 340N. After a wait of approx 5 minutes, the rate of descent or subsidence was approx 0.01 mm/14 seconds. The experiment was then repeated with this load.

Since the microswitches at this stage were still adjusted to the slow continuous movement, the slow movement was now roentgenographed first and the rapid movement second.

At the end of the experiment the magnitude of the moment and the vertical tibial translation as functions of the angle of rotation were determined with this load.

2.5. Data processing

List of symbols used:

I : vertical loading of 50N
II : vertical loading of 160N
III : vertical loading of 340N
i_s : interrupted (stepwise) supination
i_r : interrupted (stepwise) return to the starting position
u_{s5} : uninterrupted (continuous) supination in 5 seconds
u_{s8} : uninterrupted (continuous) supination in 8 seconds
u_{s60} : uninterrupted (continuous) supination in 60 seconds
u_{r5} : uninterrupted (continuous) return to the starting position in 5 seconds
u_{r60} : uninterrupted (continuous) return to the starting position in 60 seconds
* : marker not visible. (Used as a symbol in Tables A.1. to A.10. inclusive and A.34. and A.35. Appendix.)

2.5.1. Comparison of stepwise and continuous movement (questions 1 and 2)

By comparing the stepwise supination of the tarsus, made in steps of 10 degrees and recorded in both directions in two X-rays, with the continuous movement, also recorded in two X-rays, we ought to be able to demonstrate any existing differences, since a standard X-ray technique was used and the two movements were carried out in succession. Van Langelaan (1983) demonstrated the good reproducibility of the stepwise movements.

Transparencies (PR-OHP foil, 210 × 297 × 0.1 mm), with the centres of the pellet projections of the stepwise movement reproduced on them, were placed on top of those showing the outlines of the pellet trajectory projections of the continuous supination. The positions 0° and 30°, photographed separately, aided in the determination of the pellets or pellet trajectories in the X-rays of the stepwise and continuous movements.

Both transparencies were projected, 5 times magnified, by means of an overhead projector, and the distance from the centre of the pellet to the centre-line of the pellet trajectory was measured, divided by 5, and entered in mm in a number of frequency tables (See Tables A.1.-A.10., Appendix). The centre of the pellet is the point of intersection of the two lines connecting 4 points of contact of two pairs of parallel tangents running at right angles (Fig. 2.14.). In the tables, a + or − sign was added to the figures to indicate the position in relation to the centre-line according to the

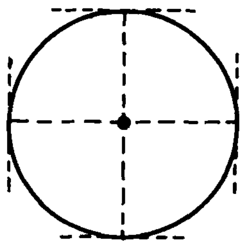

Fig. 2.14. Determination of the centre of the marker.

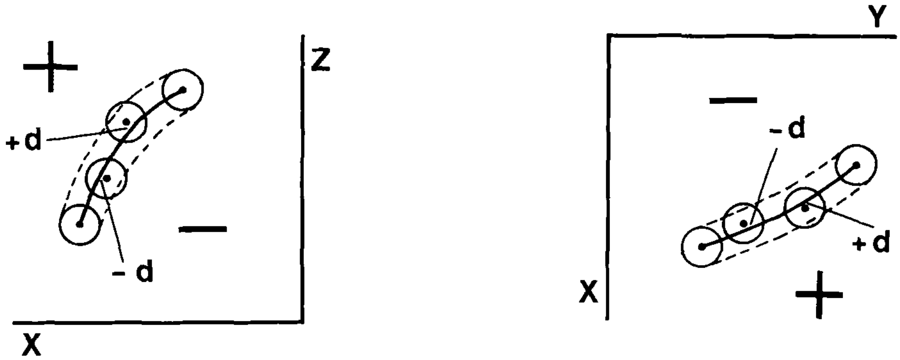

Fig. 2.15. Practical example of sign distribution of deviation from centre-line.

diagrams in Fig. 2.15., which show an example of the sign distribution for the projections of the horizontal and dorso-plantar beams, respectively, on the vertical and horizontal planes (Y = 0) and (Z = 0).

Since we were interested in movements of and in the tarsus, only the movement of one pellet of the tibia was recorded.

Additional information about the tibia was obtained by measuring the vertical translation as a function of the angle of rotation. The figures in the tables represent projections of distances from pellet centre to centre-line of the pellet trajectory in space, with the reservation that they have been measured in only two dimensions. Now there are three possibilities:

1. The centre of the pellet lies on the centre-line of the pellet trajectory in both directions. The distance, therefore, is 0.0.
2. The centre of the pellet lies in the centre-line of the pellet trajectory in one direction. The measured distance in the other direction then is the real distance (Fig. 2.16a.).
3. The centre of the pellet does not coincide with the centre-line of the pellet trajectory in either direction. In that case, the measured distance is smaller than the real distance. The maximal multiplication factor is $\sqrt{2}$ (Fig. 2.16b.).

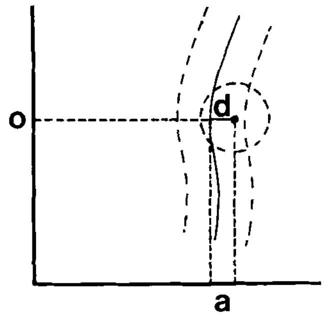

Fig. 2.16a. Real distance from the pellet centre to the centre-line. d = a.

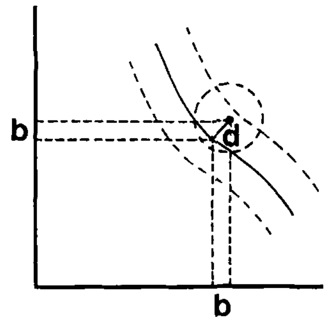

Fig. 2.16b. The distance (d) from the pellet centre to the centre-line is $b\sqrt{2}$.

The fact that the real value often exceeds the measured value is cancelled in part by the magnification factor introduced by the relationship: source–object–cassette. The distance from the middle of the foot to the vertical cassette is approx 8 cm (width of the foot at navicular level approx 7 cm) for the horizontal projection (source – cassette distance 106 cm). In the starting position, the pellet's distance is at least 5 cm, at most 11 cm.

For right legs this means that during supination, all distances between the marker pellets and the film grow slightly smaller, while for left legs they grow larger (max. approx 2%).

The influence of the distance between the pellet and the film is slightly more pronounced in the dorso-plantar direction. The pellet situated near the base of the calcaneus is at a distance of approximately 5 cm from the horizontal cassette, but in the tibia this distance may be as much as 14 cm (source – cassette distance 110 cm).

Before starting out, in Chapter 2.6., on the interpretation of the data, a few remarks are in order.

Initially we believed that if we should introduce the marker pellets into the tarsal bones at corresponding sites, the shapes of the movement trajectories would also be similar. However, because the material used showed not only interindividual differences in shape and structure, but also inter-individual differences in the physical behaviour of the tissues, there were quite pronounced differences to be expected in the biomechanical behaviour of the tarsi as well. Therefore, the movement patterns of the tarsal bones will be comparable intra-individually but not inter-individually. A second factor that renders inter-individual comparability difficult is the fact that the positions of the pellets in the bones were as uniform as we could make them, but yet not always perfectly uniform. Moreover, some bones contained more than three pellets. Of these, we used only those three pellets that were best visible in both projections.

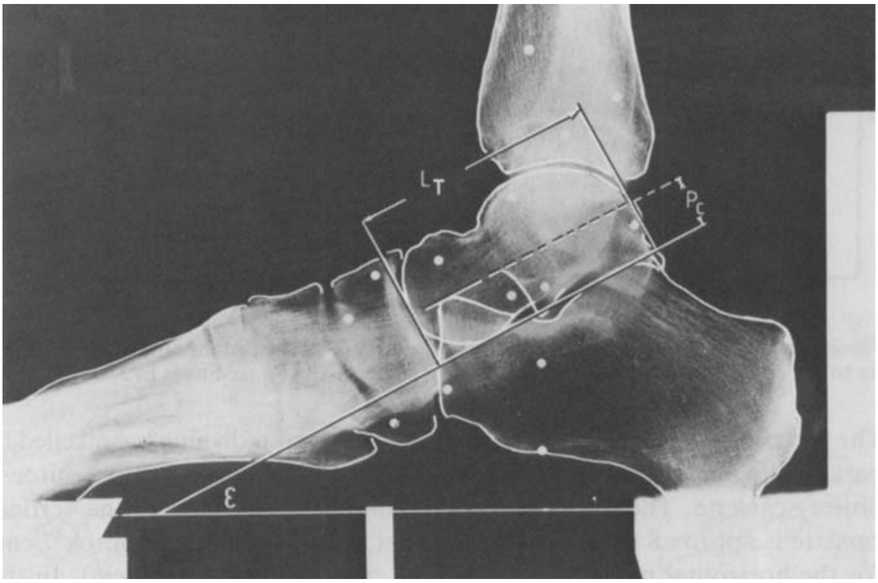

Fig. 2.17. Talo-calcaneal superprojection (overlap P_C), angle of talo-calcaneal inclination (ϵ_{TC}) and length of talus (L_T) for determining the tarsal index i_t.

Occasionally, the centre-line of the pellet trajectory could not be determined with adequate accuracy, owing to superprojection during the movement or to insufficient difference in contrast. Consequently, it was not always possible to determine the distance from the centre-point of the projection of the pellet to the corresponding centre-line of the projection of the pellet trajectory. These instances are marked with a *. For one preparation (cad. nr 548), the frequency tables show the observed differences of all measurements, with two different loads, for the supination movement as well as for the pronating return movement. For the other preparations, the tables show the comparison of the stepwise supinating movement with the continuous movements, fast and slow, performed with only one load (160N). The measurements of the lower leg foot-preparation of cad. nr 492 were carried out 3 years earlier than the others.

Also, in this preparation, unlike the others, the slow continuous supinatory deformation (u_{s60}) with load II (160N) was recorded prior to the fast movement (u_{s5}).

Of cad. nr 349, two series of X-rays were made in practically identical experiments (i_sII compared with u_{s5}II and i_sII compared with u_{s8}II) with an interval of 2 years. The speed difference was only 2.25°/sec. Initially the experiments were carried out at an 8-second speed. However, in view

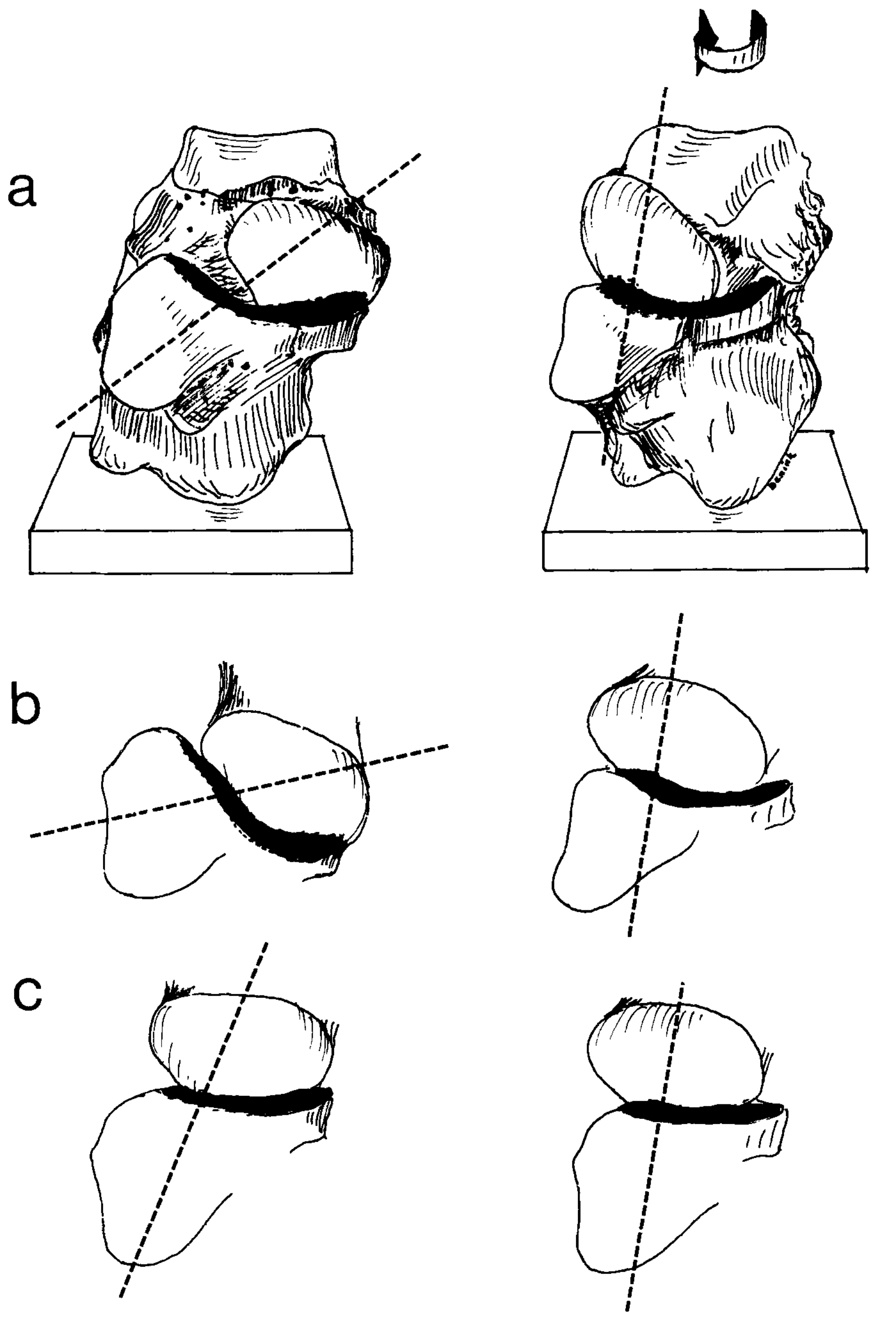

Fig. 2.18. A frontal view on the talo-calcaneal joint complex before and after supination of a 'normal' (a) a 'flat' (b) and a 'cavus' (c) foot.

Note the climbing of the talar head, rotation of talus and calcaneus, a slight eversion of the talus and inversion of the calcaneus.

of the differences in contrast, we subsequently opted for a 5-second speed.

2.5.2. *Tarsal index (i_t)* (question 3a)

Because the standard indexing criteria (Stewart 1970) proved inadequate to establish a relationship between X-ray and mechanical behaviour, we had to invent a new index. This required standardization of the roentgenographic technique, which we could accomplish with the aid of the sighting system (2.3.5.).

The new tarsal index (i_t) was determined as follows: The angle of inclination of the talo-calcaneal joint (ϵ_{TC}) was determined by measuring the angle (ϵ) of the tangent to the clearly visible posterior articular surface of the calcaneus (facies articularis talaris posterior) and the equally clearly visible anterior articular surface at the underside of the head of the talus (facies articularis calcanea anterior and media) (Fig. 2.17.).

The front of the calcaneus overlaps to a greater or lesser extent the head of the talus. The extent of the overlap determines the relative angle of inclination of talus and calcaneus in relation to each other in the longitudinal direction of the foot. This angle, represented in the *lateral projection* by ϵ_{TC}, changes during supination, to a degree which depends on the extent of the overlap. This overlap is named P_C and shows often a marked individual variability. It is mostly large in flat feet and small in cavus feet (Fig. 2.18.).

Our new index was based on ϵ_{TC} and P_C. In order to obtain a dimensionless figure that is independent of the dimensions of the foot, the overlap (P_C) in mm was divided by the length of the talus (L_T) in mm. The talus length was found by drawing tangents at the anterior and posterior aspects of the talus, perpendicular to the line through the talo-calcaneal joint, and measuring the distance between them (Fig. 2.19.).

Finally, a mutiplication factor of 100 was introduced to make the index an integer. This gives the following equation for the roentgenological index of the tarsus:

$$i_t = 100 \times \frac{P_C}{L_T} \times \text{tg}\ \epsilon_{TC}$$

in which:

i_t = tarsal index
P_C = talo-calcaneal overlap in mm
L_T = length of talus in mm

ϵ_{TC} = the talo-calcaneal inclination angle in the longitudinal direction of the foot.

The tarsal indexes of the six preparations were:

TABLE 2.4.
Range 10–23, $\bar{x}$ = 13.5, SD = 4.9

specimen number	tarsal index $i_t = 100 \times \frac{P_C}{L_T} \times \text{tg}\ \epsilon_{TC}$
342	11
349	10
492	14
506	13
511	23
548	10

2.5.3. Recording the moment and the vertical tibial translation as functions of the angle of rotation. Correlation with the roentgenological tarsal index (questions 3a and 3b)

The magnitudes of the moment and the vertical tibial translation were plotted in two series of graphs (Fig. 2.19.) showing the input moment (M) required for the supination of the tarsus as a function of the angle of rotation α; and the vertical tibial translation (S) as a function of the angle of rotation α.

Numerical values were deduced from the shape of the curves as follows:

Moment (M)
The curves that show the magnitude of the exorotating moment as a function of the angle of exorotation can be arranged in a sequence showing a more or less gradual transition. The upper half of Figure 2.19. shows three examples representing three types of foot, viz. feet with low (a), 'normal' (b) and high (c) arch.

In interpreting the graphs we have to keep in mind that the mechanical properties of the experimental apparatus also influence the shape of the curves. The principal one, viz. the spring constant of the bellows, is mentioned in Chapter 2.3.3.

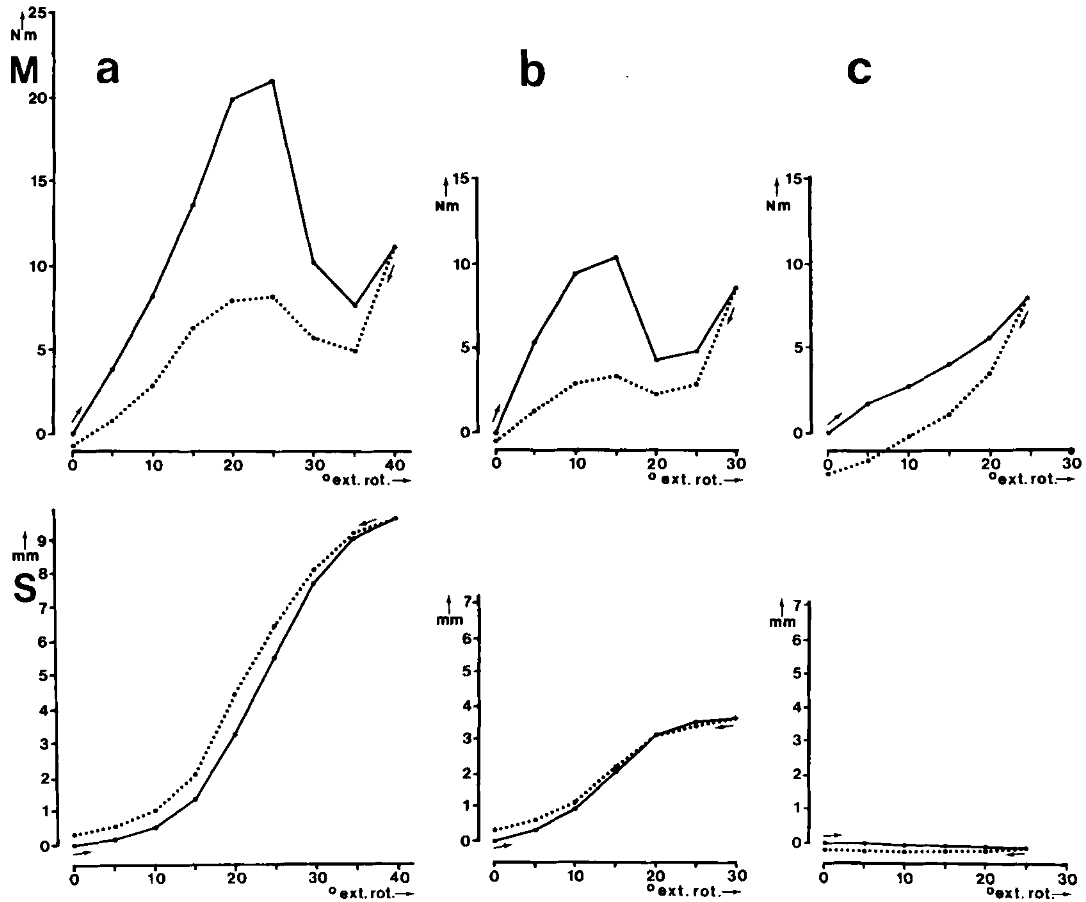

Fig. 2.19. Moment curves (top) and tibial translation curves (bottom) of supination at a vertical pressure of 340N.
a. 'flat' foot, b. 'normal' foot and c. 'cavus' foot. Solid line: movement from 0 to supination; dotted line: reverse movement.

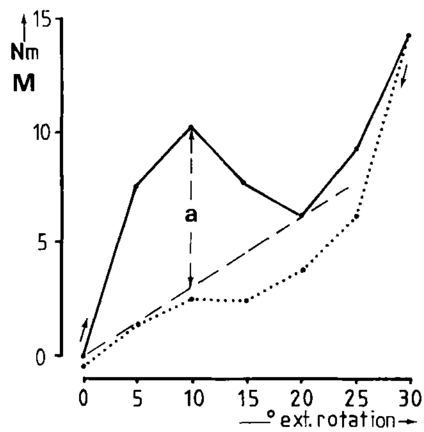

Fig. 2.20. Determination of distance a in the moment curve. Solid line: movement from 0 to supination; dotted line: reverse movement.

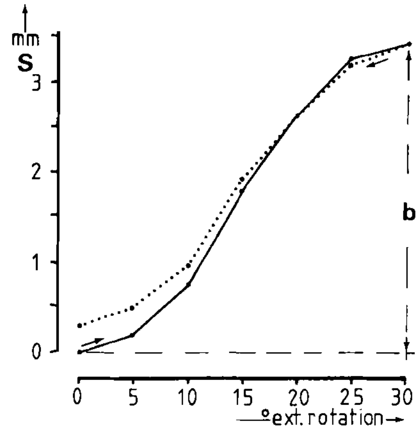

Fig. 2.21. Determination of distance b in the tibial translation curve. Solid line: movement from 0 to supination; dotted line: reverse movement.

Consequently, it seems to be incorrect to classify the *moment-exorotation angle curves* of the 36 preparations by their shapes, on the basis of visual impressions. In particular, longer tibias are affected relatively more by the increase of the spring constant of the bellows transmission than are shorter ones in spite of identical tarsal indexes. In other words, the vertical loading is slightly heavier. In order to find a reliable classification criterion, which as much as possible eliminates differences in size without requiring complex mathematical calculations, we opted for the following solution: We noted that nearly all moment curves followed a similar, S-shaped pattern (Fig. 2.20.). The moment initially increases and reaches a maximum at the first inflexion point. It is only in a few curves, approximately of type c (Fig. 2.19c.) that this inflexion point is missing.

Thereafter, the moment decreases until a second inflexion point. Beyond this, the moment increases again. (If we were to exorotate farther, the heel in our test setup would slip away before a ligament would rupture.)

The curve accordingly runs a fixed course with two inflexion points which vary from one individual to another both in magnitude, height and relative position. Thus, the curves reflect a varying biomechanical behaviour which, as will become apparent, is closely correlated with the tarsal index and the vertical tibial translation.

In order to find a figure which imparts information about both inflexion points, we connected the starting point of the curve and the second inflexion point with a straight line, and drew a line from the first inflexion point perpendicular to the horizontal axis, intersecting with the first line. The distance a between the first inflexion point and the point of intersection was then measured (Fig. 2.20.).

A correction factor was introduced by dividing this figure by the talar length (in millimeters) and multiplying it by 10, giving for each individual a dimension-free number discribing the moment graphs (column M in Table 2.5.). Thus $M = \frac{a}{L_T} \times 10$. As the load increased, the inflexion points moved higher up and farther to the right.

Vertical tibial translation (S)

The recorded *vertical tibial translation* was also represented as a function of the exorotation angle. These curves proved to be more or less S-shaped (Fig. 2.21.).

The same reservations mentioned for the moment curves also are true for

TABLE 2.5.

Tarsal indexes and corresponding values of the moment and the tibial translation for 36 preparations

Cad. nr	L/R	i_t	M	S	Cad. nr	L/R	i_t	M	S
338	R	0	0.9	0	457	R	11	12.2	5.7
504	L	0	0.9	0	342	R	11	13.2	7
502	R	2	0.0	0	456	R	12	14.8	6.4
547	R	3	1.8	0	506	R	13	10.2	5.1
516	R	3	2.1	0	492	R	13	16.5	7.1
248	R	5	2.4	1	355	R	14	9.9	6.2
355	L	7	2.2	0.6	427	R	15	15.2	4.5
545	L	8	5.6	2.6	546	L	19	19.8	10.2
545	R	8	6.6	4.5	465	R	20	15.4	7.9
400	R	9	7.0	4	530	R	22	14.0	12.6
541	R	9	9.2	5.1	345	L	22	17.6	11.1
541	L	9	8.0	4.3	345	R	25	18.9	10.8
543	R	9	8.7	3.2	529	R	25	17.2	11.2
548	R	9	8.5	3.7	544	L	26	23.2	11.5
548	L	10	8.6	4.5	537	R	27	22.4	12.8
349	L	10	10.0	5.3	521	R	43	19.0	11.6
349	R	10	10.0	5.6	542	R	44	25.5	14.7
331	L	11	9.7	3.2	499	L	49	>24.6	>16.4

these curves. In order to find a reasonably simple representation by a single figure, we opted for the maximal tibial climbing b in Fig. 2.2.1., which was practically invariably towards the end of the supinatory deformation.

This figure – ranging from 0 to 12 mm in our series – was also corrected for the dimensions of the preparation by dividing by talar length and multiplying by 100. The value obtained is dimensionless (column S in Table 2.5.). Therefore $S = \frac{b}{L_T} \times 100$.

2.6. Results and discussion

2.6.1. Comparison of stepwise and continuous supination (questions 1 and 2)

It is difficult to interpret the frequency tables (See Tables A.1.-A.10., Appendix) in terms of the intra- and interindividual comparability of stepwise and continuous supinatory deformation.

However, if we enter the entire data set (1352 observations) in a new frequency table (Table 2.6.) (the insufficiently comparable observations are marked with *), a quite clear impression of the differences between stepwise and continuous supination is obtained for each individual bone. When we consider the 0.0/0.0 pairs, i.e. the pairs in which pellet centre and centre-line of pellet trajectory coincide perfectly (in two directions), we find that the average proportion of the tarsal pellets that meets these conditions is 69% for the supinatory and 57% for the pronatory movement.

When we examine the tables for 0.1 mm deviation, i.e. the 0.0/0.1 pairs, we find that on the average 24% and 27%, respectively, of the tarsal pellets answer this description. When we add these averages to those for the 0.0/0.0 pairs, we find that for all tarsal pellets together, 93% and 84%, respectively, of the projections deviate no more than 0.1 mm in one projection direction (Table 2.7.).

On the whole, the differences between the stepwise and the continuous movement are thus very small, and there are no significant differences between the individual bones. This implies that tarsal supination proceeds according to a fixed pattern.

Let us consider certain aspects in more detail. Interestingly, preparations (548, 349) with the tarsal index $i_t = 10$, for both, i.e. feet with higher arches, show smaller differences between stepwise and continuous movement than the leg with a higher index (511: $i_t = 23$), i.e. a foot with a fairly low arch. However, we have to keep in mind that the latter is only one single preparation. The differences are generally smallest for the rapidly performed deformation (s5). It should be remembered, however, that this is also the move-

TABLE 2.6.

Frequency table of measured distances from pellet centre to centre-line during supination of 6 preparations with a load of 160N at 6 and 60 seconds, respectively. One preparation (349L) had also been measured 2 years previously. The + and − signs have been omitted*

Cad. nr + R/L		548 L		349 L		342 R		506 R		492 R		511 R		349L*
Index (i_t)		10		10		11		13		14		23		10
Speed (sec.)		5	60	5	60	5	60	5	60	5	60	5	50	8
	0	6	3	5	4	2	—	3	3	4	4	3	1	5
Tibia	0.1	1	2	2	2	4	3	4	3	3	2	2	4	2
(1 pellet)	0.2	1	2	1	2	1	3	1	2	1	2	3	3	1
	0.3		—	1	—	—	1	2	—	—	—	—	—	—
	0.4	—	—	—	—	—	—	—	—	—	—	—	—	—
	*	—	—	—	—	—	—	—	—	—	—	—	—	—
	0	18	16	14	12	15	6	16	14	17	17	17	13	16
	0.1	5	5	6	6	7	7	4	6	4	4	7	10	4
Talus	0.2	1	3	—	2	—	7	—	—	—	—	—	1	—
	0.3	—	—	—	—	—	2	—	—	—	—	—	—	—
	0.4	—	—	—	—	—	—	—	—	—	—	—	—	
	*	—	—	4	4	2	2	4	4	3	3	—	—	4
	0	17	14	19	16	14	11	14	13	17	19	17	17	19
	0.1	7	9	2	5	9	10	1	1	7	5	7	5	4
Calcaneus	0.2	—	1	2	1	—	2	1	2	—	—	—	2	—
	0.3	—	—	—	1	—	—	—	—	—	—	—	—	—
	0.4	—	—	—	—	—	—	—	—	—	—	—	—	—
	*	—	—	1	1	1	1	8	8	—	—	—	—	1
	0	21	20	13	12	15	9	20	10	18	15	12	11	17
	0.1	2	3	8	8	7	9	4	8	6	8	9	8	6
Navicular	0.2	1	1	1	2	1	5	—	5	—	1	—	2	1
	0.3	—	—	—	—	—	—	—	—	—	—	—	—	—
	0.4	—	—	—	—	—	—	—	—	—	—	—	—	—
	*	—	—	2	2	1	1	—	1	—	—	3	3	—
	0	19	19	22	15	18	10	17	18	20	20	9	1	24
	0.1	5	5	1	8	4	11	7	5	4	4	13	8	—
Cuboid	0.2	—	—	1	1	2	3	—	1	—	—	2	9	—
	0.3	—	—	—	—	—	—	—	—	—	—	—	5	—
	0.4	—	—	—	—	—	—	—	—	—	—	—	1	—
	*	—	—	—	—	—	—	—	—	—	—	—	—	—
	0	81	72	73	59	64	36	70	58	76	75	58	43	81
	0.1	20	24	19	29	31	40	20	23	24	23	38	35	36
Total	0.2	3	7	5	8	4	20	2	10	1	3	5	17	2
	0.3	—	1	—	1	1	4	—	—	—	—	—	5	—
	0.4	—	—	—	—	—	—	—	—	—	—	—	1	—
	*	—	—	7	7	4	4	12	13	3	3	3	3	5

ment that was carried out first, following the stepwise deformation (except for cad. nr 492). The speed had to be adjusted (s60) and the positions of the microswitches changed before the experiment could be repeated for the slow movement. The observed variations can be attributed to the complex setup and to working with biological material. Between the stepwise slow movement and the continuous slow movement the leg has been subjected to rapid continuous rotation, so that, the foot not being absolutely fixed, the leg may have shifted a fraction. This manifests itself in the figures in Table 2.6.

Interestingly, however, this does not apply to cad. nr 492, which may possibly be explained by the fact that the experiments with this leg were carried out 3 years before the others. During those 3 years, the experimental apparatus was in regular use and subject to wear. During the final experiments, we noted that the play between the wormwheel – cogwheel transmission between the motor and the vertical shaft had increased a little so that the continuous rapid movement sometimes started with a slight jerk. This may also have been the cause of the slight differences between the columns of figures for leg 349, this being the first experiment carried out.

There is a greater difference between columns 5 and 60 of cad. nr 342 (i_t = 11). During this experiment, however, we succeeded in achieving the optimal setting of the microswitches (cut-off in the starting position at 0° and at 30° exorotation) only after rotating five times. As a rule this took only one or two times with other preparations. In view of the above, it is remarkable that, statistically, the differences are not significant. We conclude that a change of speed does not greatly affect the motion pattern.

Apart from frequency tables concerning the tarsal supination with load II (160N) for the 6 preparations, the appendix includes, for one leg (cad. nr 548), a table for the *continuous return* movement to the starting position in 5 and 60 seconds, which is compared with the step-by-

TABLE 2.7.

0.0/0.0 + 0.0/0.1 scores for each tarsal bone and averages for all tarsal bones for the supinatory movement and return to the neutral position

	supination	return
Talus	90%	80%
Calcaneus	91%	86%
Navicular	94%	84%
Cuboid	97%	86%
	average 93%	average 84%

TABLE 2.8a. TABLE 2.8b.
Frequency tables of comparison of return movement (2.8a.) and after increasing load (2.8b.)

Cad. nr R/L		548 L			548 L		548 L	
Index (i_f)		10			10		10	
Load II (160N)		r5	r60	Load III (360N)	s5	s60	r60	r5
Tibia	0	4	4		6	5	6	6
	0.1	2	4		1	2	1	2
	0.2	2	—		1	1	1	1
	0.3	—	—		—	—	—	—
	0.4	—	—		—	—	—	—
	*	—	—		—	—	—	—
Talus	0	21	24		16	20	20	21
	0.1	2	—		8	4	2	1
	0.2	1	—		—	—	—	—
	0.3	—	—		—	—	—	—
	0.4	—	—		—	—	—	—
	*	—	—		—	—	—	—
Calcaneus	0	22	22		19	21	22	17
	0.1	2	2		5	3	—	5
	0.2	—	—		—	—	—	—
	0.3	—	—		—	—	—	—
	0.4	—	—		—	—	—	—
	*	—	—		—	—	2	2
Navicular	0	21	22		18	23	22	24
	0.1	3	2		6	1	2	—
	0.2	—	—		—	—	—	—
	0.3	—	—		—	—	—	—
	0.4	—	—		—	—	—	—
	*	—	—		—	—	—	—
Cuboid	0	22	24		17	20	24	24
	0.1	2	—		6	4	—	—
	0.2	—	—		1	—	—	—
	0.3	—	—		—	—	—	—
	0.4	—	—		—	—	—	—
	*	—	—		—	—	—	—
Total	0	90	96		76	89	94	82
	0.1	11	8		26	14	5	8
	0.2	3	—		2	1	1	1
	0.3	—	—		—	—	—	—
	0.4	—	—		—	—	—	—
	*	—	—		—	—	4	4

step return movement under the same load (160N). Table 2.7. summarizes the findings.

Here again, as for the supinatory movement, (Table 2.6.), we noticed a clear similarity between the two speeds, even more so than for the

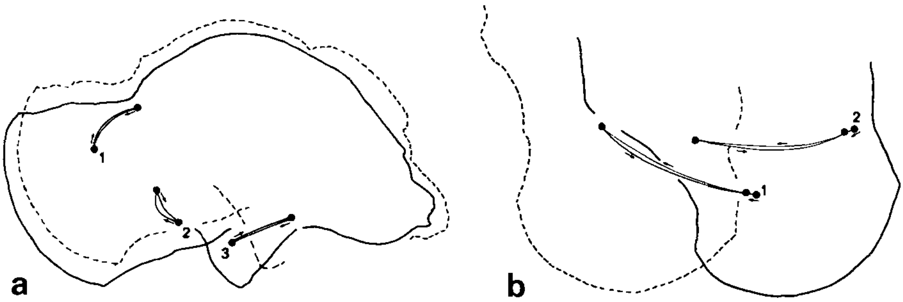

Fig. 2.22. The hysteresis pattern of respectively 3 and 2 pellets in the talus for the horizontal (a) and dorso-plantar (b) projections.

supination. Comparison of the roentgenograms of the other preparations, which although recorded have not been included in the table, leaves the same impression. We cannot satisfactorily explain this. The supinatory and pronatory movements of cad. nr 548 under load III (340N) are compared with the corresponding step-by-step movements listed in Tables 2.11. and 2.12. and summarized in Tables 2.8a. and 2.8b. Under load II, r5 was carried out first, while under load III, r60 was done first.

Looking at the (0.0/0.0 + 0.0/0.1) pairs of the return movement for the two speeds, 5 and 60 seconds, respectively, Table 2.8a., we find for the talus: 96–100%, for the calcaneus: 100–100%, for the navicular: 100–100% and for the cuboid: 100–100% scores. As Table 2.8b. shows, increasing the load to 340N leads to virtually the same values for the two speeds, both for the supinatory and for the return movement.

In this preparation, increasing the load and changing the speed have had no discernible effect on the very slight difference between stepwise and continuous movements.

Hysteresis. While comparing the X-rays of the continuous forward (supination) and return (pronation) movements, we noticed an interesting phenomenon which we could observe in all fixed preparations and later also in fresh material.

The projections of the pellet trajectories of the supinatory and return movements were mostly not completely congruent. There was nearly always a relatively constant difference which, with analogy to the phenomenon known in engineering, and which has also been observed in, for instance, tensile strength tests of ligaments, we shall call *hysteresis*.

An example for the talus is shown in Fig. 2.22.

In spite of the difference, the shapes of the trajectories remained virtually unchanged as speed and load were varied.

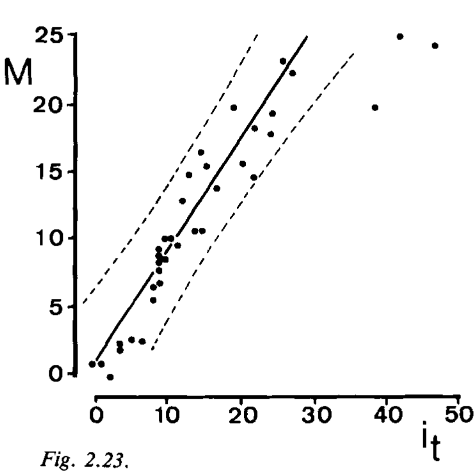

Fig. 2.23.

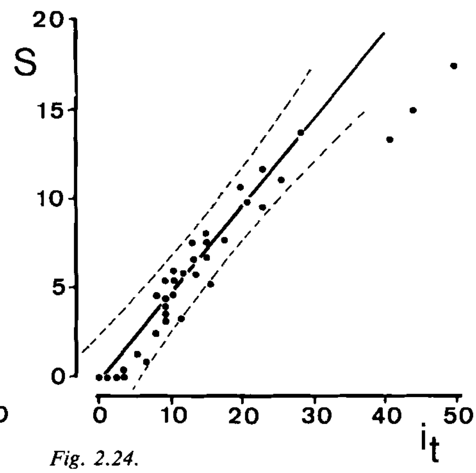

Fig. 2.24.

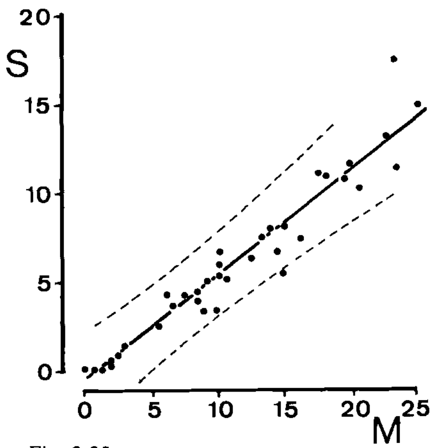

Fig. 2.25.

Fig. 2.23. The moment indexes of 36 fixed lower leg foot-preparations plotted against the tarsal indexes. The regression line and the 95% confidence limits are indicated.

Fig. 2.24. The vertical tibial translation indexes of 36 fixed lower leg foot-preparations plotted against the tarsal indexes. The regression line and the 95% confidence limits are indicated.

Fig. 2.25. The vertical tibial translation indexes of 36 fixed lower leg foot-preparations plotted against the moment indexes. The regression line and the 95% confidence limits are indicated.

We encountered this phenomenon again while recording the moment and the vertical tibial translation as functions of the angle of rotation (Fig. 2.19.).

2.6.2. *Interpretation of the relationships between moment index and tarsal index, between tibial translation and tarsal index, and between tibial translation and moment* (question 3)

By plotting the figures of Table 2.5., we can compare in two different ways the biomechanical behaviour of the tarsus with the roentgen-morphometric findings as expressed with the tarsal index i_t (Figs. 2.23. and 2.24.).

Also, the two recordings of biomechanical behaviour are compared in Fig. 2.25.

These figures show that the exorotating moment (M) required for supination, and the vertical tibial translation (S) in the test setup, are correlated not only with each other but also with the roentgen-morphometric relationships in the tarsus (tarsal index i_t).

Figure 2.23. represents the relationship between the tarsal index (i_t) and the supinatory moment (M).

The correlation coefficient, including all points, is 0.88. Above $i_t = 13$ and $M = 10$, the deviation increases. This is due to the fact that the moment could not be recorded continuously, but was recorded once every 5°. This means that feet with a higher index (i.e. mostly the lower and low vaults) behave more critically where the recording of the two inflexion points is concerned. This holds true in particular of the first inflexion point, the true position of which may be higher than indicated by the measured values. This explains the fact that the three points with $i_t > 40$ fall outside the area of variation. In determining the regression lines in Figs 2.23., 2.24. and 2.25. these have been excluded, resulting in a correlation coefficient of 0.93.

That this variation is less in the relationship between the maximal tibial climbing (S) and the tarsal index (i_t) can be seen in Fig. 2.24.

The correlation coefficient is 0.93 when all points are included and 0.95 if the three points with $i_t > 40$ are excluded. Here again the higher indexes (> 40) deviate more. During the tibial climbing the bellows connection is stretched so that the load increases slightly (page 23), exerting a negative effect on the tibial climbing.

The increase of the load might also play a part in the recording of the moment, thereby partially cancelling the effect of the graphically lower inflexion point. However, the effect of the load is much less because, as a rule, the first inflexion point lies between 10° and 20° exorotation. We have found that, in most cases, the inflexion point is situated at the level of that part of the S-shaped curve of the tibial climbing that has the widest angle of inclination.

The tibia at this point is at most half way towards its maximal translation. The effect of increasing the vertical load (spring constant + friction force in bellows and shaft) is relatively less in preparations with a high tarsal index than in preparations with lower vaults. This graph shows that there exists a linear relationship between the index and the tibial translation.

The tibias above the tarsi with a low index (as a rule the higher and high vaults, tarsal index < 5) climb little or not, while in contrast those with the higher indexes (low vaults) show a marked vertical translation. Fig. 2.25. shows the relationship between variations of the moment behaviour and the tibial translation, with a correlation coefficient of 0.96, all points included.

The smaller the distance between the two inflexion points in the graphs of the moment recording, the less the tibia climbs.

Comparing the findings for the left and right legs listed in Table 2.5., we find (Table 2.9.) that in five preparations (545, 541, 548, 349 and 345) the tarsal indexes are virtually identical, the moment indexes differ little and the climbing indexes sometimes differ a little more.

We may conclude from these five left-right comparisons that the two tarsi of the same individuals in our test setup behaved practically identically, which showes that 5 of the 36 measurements were not independent. In preparation 355, on the other hand, where we also compared the left and the right leg, we found pronounced differences. Supination of the right tarsus required a much greater moment than of the left (15.2 as against 2.2). There was also a marked difference in vertical tibial translation (6.2 as against 0.6). This different biomechanical behaviour proved to corresponded to a difference in the tarsal index (left 7, right 14) due to differences in the calcaneal overlap and the angle of inclination of the talocalcaneal joint. Talar lengths and shapes were identical. A comparison of the outlines of the other tarsal bones of this preparation revealed no noticeable differences. The two preparations were in similar stages of preparation, with intact ligaments.

With cadavers nr 457, 492, 541R, 338 and 530, the measurements of moment and tibial translations were repeated. With 457, 492 and 530, this was done immediately after the first experiment, with 338 and 541R after an interval of one year. Without exception, curve shapes were virtually identical.

The effect of the rate at which the two measurements were carried out

TABLE 2.9.

The parameters i_t, M and S have been tested for possible L-R differences with a t-test for paired observations. None of the three parameters gave rise to significant differences, all $p > 0.10$

Cad. nr	L/R	i_t	M	S	Cad. nr	L/R	i_t	M	S
355	L	7	2.2	0.6	548	L	10	8.6	3.7
355	R	14	9.9	6.2	548	R	9	8.5	4.5
545	L	8	5.6	2.6	349	L	10	10.0	5.6
545	R	8	6.6	4.5	349	R	10	10.0	5.6
541	L	9	8.0	4.3	345	L	22	17.6	11.1
541	R	9	9.2	5.1	345	R	25	18.9	10.8

was studied in cad. 506. Here again, the graph shapes were practically identical.

Varying speeds, compared with each other and with the step-by-step movement, also showed only barely discernible differences.

2.7. Conclusions

The answer to question 1 is that there is no essential difference between step-by-step supination of the foot and continuous supination in fixed osteo-ligamentous preparations. On the one hand this confirms the conclusions of the discrete axes calculations of Van Langelaan and Spoor. On the other hand it enables us to expand our own study further.

The answer to the second question, viz. whether a change of the vertical loading of the tibia affects the pattern of tarsal movements, is also negative. We have found that these changes are so slight as to be statistically insignificant. Nor does the speed of the imposed continuous movement exert a clearly discernible influence on the tarsal movement pattern.

In answer to question 3, we have observed that with the new tarsal index a clear relationship can be established between the morphometric parameters of the foot skeleton and the biomechanical behaviour of the tarsus. These findings show that the simple classification of 'cavus', 'normal' and 'flat' is no longer satisfactory, because the external shape of the foot does not provide sufficient information about the mutual relationships of the talus and the calcaneus. Our findings show that variations of the moment and the vertical tibial translation during supination can be closely correlated with a new tarsal index that is based on the relative spatial positions of the talus and the calcaneus.

THREE

Study of fresh amputation preparations: determination and verification of biomechanical parameters: Part 2 of the study

3.1. Introduction

In the progress of our study from fixed osteo-ligamentous material to the living leg, the use of fresh intact preparations appeared to be the next logical step. How much do preservation techniques affect physical properties of tissues and, in consequence, the kinematic parameters? And is the stage of dissection of the preparation important? (Question 4, page 11, Chapter 1.2.).

Van Langelaan (1983), together with Spoor, studied *fixed osteo-ligamentous preparations*. They determined absolute and relative helical axes of the tibia and the tarsal bones. Using the same method, we have studied two *unfixed fresh amputation preparations* (Figs. 3.1. and 3.2.). We have used the same parameters and symbols, which are explained in detail in Chapter IX of Van Langelaan's thesis. We shall review them briefly under 'Method' (3.3.2.). In addition to the helical axes of the two preparations, we determined tarsal indexes, moment curves and vertical tibial translation curves. These determinations preceded those of the axes.

3.2. Material

The two amputation preparations were obtained from two patients, one with a malignant osteoma of the pelvis and the other with a tumour in the thigh. Table 3.1. lists the data for the specimens.

TABLE 3.1.

Data for amputated specimens

nr	sex	age (yrs)	L/R
1	f	29	L
2	m	14	R

Fig. 3.1. Amputation preparation ♀ 29. Tarsal index (i_t) = 8, vertical load 340N.

Fig. 3.2. Amputation preparation ♂ 14. Tarsal index (i_t) = 15, vertical load 340N. Visual inspection of the preparation showed the calcaneus to be in the valgus position.

After exarticulation in the knee, the measurements in our test setup could be started within one hour after amputation.

3.3. Method

The method that was used has been described by Van Langelaan and Spoor (Van Langelaan, 1983) and may be summarized as follows:

3.3.1. Principle of the photogrammetry

Two roentgen sources project markers in an object (bones) in two directions onto two X-ray films. The positions of the roentgen sources in relation to a reference system, also roentgenographed, are known. From the positions of the markers projected on the roentgenographs, it is possible to calculate the spatial positions and the helical axes of an object moving step by step in 'space'.

For our study the tarsal bones (as moving objects) were fitted with three instead of four marker pellets each.

3.3.2. Parameters and symbols (Figs. 3.3a. and 3.3b.)

We distinguish between *absolute axes*, which describe the movements of each separate bone in relation to a fixed system of co-ordinates, and *relative axes*, which describe the movements of two bones in relation to each other.

X, Y and Z: the co-ordinate axes (of the reference system) to determine the positions in space of the three pellets per bone
H.A. : helical axis
π : angle between the projection of the axis on the basal plane (XY), and the sagittal plane (XZ) (deviation angle)
φ : angle between the axis and the basal plane (XY) (inclination angle)
(π and φ are the parameters for the helical axis.)
t : translation along this axis
α : angle of rotation round the axis
(t and α are the parameters of the helical movement.)
β : the angle of deviation of the directional vector (apex–angle of cone round H.A.) see Fig. 3.3b.

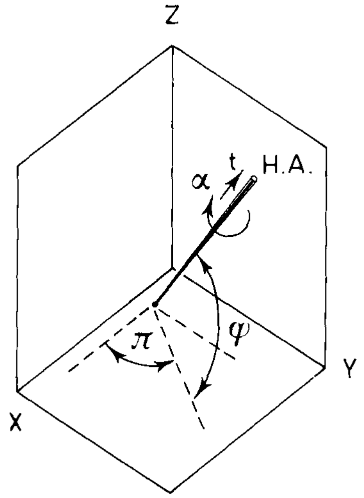

Fig. 3.3a. Helical axes (HA) with deviation angle (π), inclination angle (φ), rotation angle (α) and translation (t).

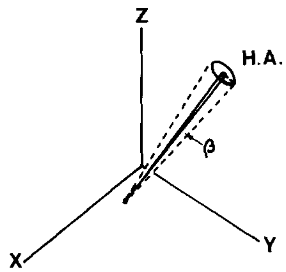

Fig. 3.3b. Spatial representation of deviation angle β.

The following symbols are not shown in the figures:

γ : the angle between the movement axes in relation to each other (in appendix Tables 3–5, 3–8, 3–11, 3–14 and 3–17)
γ 1–6 = 0°–10° supination compared with 10°–0° return movement,
γ 1–2 = 0°–10° supination compared with 10°–20° supination movement, etc.

ϱ : square root of the mean square of the distances of the pellets to the rotation axis through the centre of gravity, in mm.

σ : standard deviation per co-ordinate, in mm.

For the two specimens we calculated the mean rotation angles ($\bar{\alpha}$) of the relative and absolute movement axes, π and φ (angles of deviation and inclination, respectively) of the relative movement axes and γ, the angle between the relative axes. The movements were carried out with the specimens still intact, under loads of 50N and 340N (indicated in the tables with $50N_i$ and $340N_i$, respectively) and then, after removal of skin and muscles, under a load of 340N (indicated in the tables as $340N_0$). The return movements of the intact specimens were studied only with loads of 340N ($340N_i$). The movement axes were calculated for the movements in the talo-calcaneal joint, the talo-navicular joint and the cuboid-navicular joint, as well as for movements between navicular and calcaneus and between cuboid and calcaneus: TACA, TANA, CUNA, NACA and CUCA, respectively. In Tables A.11. – A.25. (Appendix), phases 1–6 mean:

phase 1: 0° – 10° exorotation
phase 2: 10° – 20° exorotation
phase 3: 20° – 30° exorotation
phase 4: 30° – 20° endorotation
phase 5: 20° – 10° endorotation
phase 6: 10° – 0° endorotation

Accordingly, one helical axis goes with every phase. We have also calculated the angles γ between the helical axes 1 and 6, 2 and 5, and 3 and 4 and those between 1 and 2, 2 and 3, 4 and 5, and 5 and 6; these are listed in Tables A.13., A.16., A.19., A.22. and A.25. (Appendix).

The angles γ 1–6, γ 2–5 and γ 3–4 indicate to what extent the exorotatory and endorotatory movements correspond. The angles γ 1–2, γ 2–3, γ 4–5, and γ 5–6 indicate the degree to which the rotation deviates from a hinge movement.

3.3.3. Accuracy of the method of determining axes

In the experiments, errors occur. These errors are analysed in detail in Van Langelaan's thesis. His Chapter 6 (page 45–53) deals with the 'errors in X-ray photogrammetry'. These are divided into two groups.

a. sources of error in the experimental setup, resulting in systematic errors and
b. sources of error in the measuring of X-ray photographs, resulting in accidental errors.

Systematic errors are caused by:

a. Deviations from the ideal planarity of the X-ray cassette against which the X-ray films are pressed, resulting in a less than ideally planar 'photographic plane'.
b. The angle between the cassettes in the cage deviating from the ideal 90° exactly.
c. Errors in measuring the fixed distances in the cage and the source or focus-locating apparatus.
d. The positioning of the source or focus-locating apparatus against the X- and Y-ribs.
e. Use of X-ray sources not ideally rigidly fixed in relation to the cage.
f. The non-punctiform shape of the X-ray source.

Fig. 3.4a. Fresh lower leg foot-preparation in the experimental setup. The openings for insertion of marker pellets are visible.

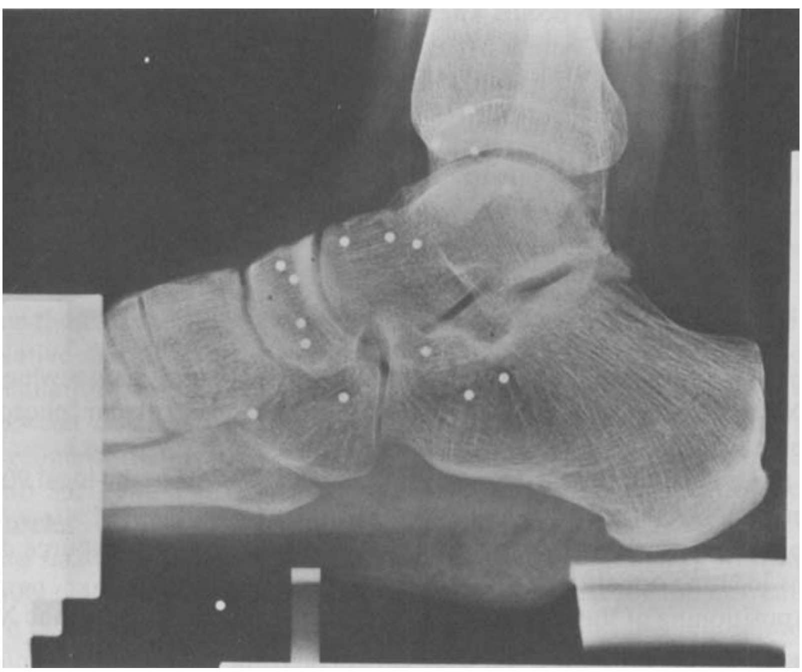

Fig. 3.4b. Amputation preparation ♀ 29 with marker pellets in situ.

Accidental errors result from:

Inaccuracies in making measurements with the comparator on X-ray photographs.

To analyse these errors, a helical movement testing apparatus (HMTA) and a measuring plate were used. The results of this test led to the conclusion that the distance of the pellets from point 0 did not affect the calculated pellet co-ordinates.

Van Langelaan also (in his Chapter 7) presents a detailed analysis of the errors in computation of helical movements, using the HMTA and a computation model into which a known error was introduced. This led to the following findings:

1. During 5° rotation the standard deviation in the direction of the axis of rotation β is less than 1°.
2. The standard deviation of the angle of rotation α is approx 0.1° and the mean standard deviation of the translation is less than 0.05 mm.
3. The standard deviation of the calculated pellet positions ranges from a minimum of 0.01 mm to a maximum of 0.015 mm.

It should also be kept in mind that the accuracy of the helical-axis parameters depends on the angle of rotation α, i.e. on the magnitude of the individual step. Small rotation angles give less accuracy.

Spoor (1984) has presented a more in-depth analysis in his paper 'Explanation, verification and application of helical-axis error propagation formulas'.

Virtually all the statements in Van Langelaan's thesis apply to our work as well, with the restriction that for our study Spoor has adapted the measuring and calculating procedures to the fact that we used three pellets per bone instead of four.

3.4. Procedure

As soon as the leg was locked in the test apparatus, standardized X-rays in the horizontal direction were made of the foot with a vertical load of 340N on the tibia, in order to determine the tarsal index i_t (page 34). Of the two very fresh, intact specimens, the moment curves and the vertical tibial translations were recorded as described in 2.4.1. After measuring the moment and the vertical tibial translation as functions of the angle of rotation, the tarsal bones and the tibias were marked under radiological control with injection needles at the sites where, after freezing, marker pellets (∅ 2 mm) were to be inserted subcortically. The specimens were frozen (−20°C) to enable the pellets to be inserted without damaging the soft tissues too much.

After insertion of the pellets and thawing of the specimen, the supination was recorded radiologically. The starting position (0°) is shown in Fig. 3.4. A comparison of this figure with Fig. 3.1. (without pellets), shows that, with the aid of the sighting system, a sufficiently similar position of the specimen could be reproduced.

The specimen was thawed one day before the experiment to determine the helical axes. After the long tendons had been severed approx 5 cm above the malleoli, the specimen was locked in place in the cage and the measurements were carried out according to the protocol described in Chapter 2.4.1. To determine helical axes of the stepwise movement, the discrete steps had to be photographed on separate X-rays. This was now done in steps of 5° for the input rotation instead of the 10° steps of the protocol of Part 1. The exposures were made with loads of 50N and 340N. These X-rays could also be compared with the X-rays of the movements carried out *continuously* with these loads and at speeds of 5 and 60 seconds, respectively.

After the experiment, the lower leg was removed from the cage and dissected into an osteo-ligamentous preparation, after which the entire procedure was repeated with a vertical load of 340N.

3.5. Results

3.5.1. Introduction

The approximative equation for the standard deviation (σ_α) of the *angle of rotation* α for the *absolute axes* is:

$$\sigma_\alpha \approx \frac{\sigma}{\varrho} \text{ (radians) and } \sigma_\alpha \approx \frac{180\ \sigma}{\pi\ \varrho} \text{ (degrees)}$$

and for the *relative axes*

$$\sigma_\alpha \approx \frac{\sqrt{2}\ \sigma}{\varrho} \text{ (radians) and } \sigma_\alpha \approx \frac{180\ \sqrt{2}\ \sigma}{\pi\ \varrho} \text{ (degrees)}$$

The approximative equation for the standard deviations (σ_β) of the *angle of deviation* β of the directional vector is for the *absolute axes:*

$$\sigma_\beta \approx \frac{\sigma}{\sqrt{3}\varrho \sin \frac{1}{2}\alpha} \text{ (radians) and } \sigma_\beta \approx \frac{180\ \sigma}{\pi\ \sqrt{3}\varrho \sin \frac{1}{2}\alpha} \text{ (degrees)}$$

and for the *relative axes:*

$$\sigma_\beta \approx \frac{\sqrt{2}\,\sigma}{\sqrt{3}\varrho \sin \frac{1}{2}\alpha} \text{ (radians) and } \sigma_\beta \approx \frac{180\sqrt{2}\,\sigma}{\pi\sqrt{3}\varrho \sin \frac{1}{2}\alpha} \text{ (degrees)}$$

ϱ as in Van Langelaan's work, is 9 mm for all bones. (π is not used as a symbol in Van Langelaan's work.)

σ is based on the measurements with the HMTA (helical movement testing apparatus) and amounts to 0.015 mm (Van Langelaan, 1983, p. 48 ff).

When we use these figures in the equations, we find that the standard deviation of the *relative rotation angle* is always 0.14 degrees, σ and ϱ being both independent of the rotation angle.

The standard deviation of the deviation angle is dependent on the rotation angle and is listed in Table 3.2.

TABLE 3.2.

Standard deviations σ of the rotation angle α and the deviation angle β

data for the *relative* tarsal axes

rotation angle (degrees)	σ_α (degrees)	σ_β (degrees)
1°	0.14°	8.93°
2°	0.14°	4.47°
3°	0.14°	2.98°
4°	0.14°	2.23°
5°	0.14°	1.79°
6°	0.14°	1.49°
7°	0.14°	1.28°
8°	0.14°	1.12°
9°	0.14°	0.99°
10°	0.14°	0.89°

3.5.2. *Results of the measurements*

A. *Kinematic parameters* (helical axes)

A. 1. *The rotation angle α of the relative axes*

As can be seen in Tables A.31.-A.33. (Appendix); concerning the *total* rotation angles of the *relative* movement axes, we found that total angles of rotation were different when measured after increasing the load from 50 to 340N and after removing skin and muscles.

These differences were smaller in the woman than in the boy, possibly because their tarsal indexes differed so much (8 and 25, respectively). We have seen before (Chapter 2) that the movements in a 'flatter' foot show larger deflections than in a 'cavus' foot.

Strikingly, $\bar{\alpha}$ in specimen ♀ 29 increased with increasing load, while in ♂ 14 it decreased. The same was true after removing skin and muscles.

We also found that the deflection in the *talo-navicular* joint was very large and between *cuboid and navicular* was smallest. The low mobility (1.1°) in the latter under 340N after removal of skin and muscles in specimen ♂ 14 is particularly noticeable (Table A.33., Appendix, $340N_0$).

Just as Van Langelaan, we also found that the rotation angle α TANA approximately equals the sum of the rotation angles α TACA and α NACA.

From the data in Tables A.11., A.14., A.17., A.20. and A.23. (Appendix), we calculated the mean rotation angles ($\bar{\alpha}$) of the *relative* movement axes for steps of 10° each (Table 3.3.).

Here again we see, without being able to explain it, the difference in behaviour of $\bar{\alpha}$: an increase in ♀ 29 and a decrease in ♂ 14. The $\bar{\alpha}$ values measured at the three processing stages have been compared with each other using Friedman's test. For both preparations there are significant differences ($p < 0.05$): For ♀ 29, it is only after the first processing that $\bar{\alpha}$

TABLE 3.3.

Mean angles of rotation ($\bar{\alpha}$) of the relative movement axes of TACA, TANA, CUNA, NACA and CUCA for 10° steps

	$\bar{\alpha}$			$\bar{\alpha}$		
	♀ 29 $i_t = 8$			♂ 14 $i_t = 25$		
	$50N_i$	$340N_i$	$340N_0$	$50N_i$	$340N_i$	$340N_0$
TACA	6.2	6.5	6.9	9.3	7.4	6.6
TANA	12.1	13.7	14.0	18.2	15.7	10.8
CUNA	2.4	3.0	2.8	3.1	1.9	1.0
NACA	6.4	7.6	7.5	9.3	7.9	4.3
CUCA	4.8	5.6	5.5	7.4	7.1	4.1

is significantly lower than after the other two. For the other preparation the phenomenon is highly systematic in the sense that the $\bar{\alpha}$ is always largest after the first processing intermediate after the second, and always smallest after the third.

The standard deviations of the angle of deviation σ_β deduced from Table 3.3. are listed in Table 3.4.

TABLE 3.4.

Maximum and minimal standard deviations (σ) of the angles of deviation (β) of the directional vectors of TACA, TANA, CUNA, NACA and CUCA

	σ_β max	σ_β min
TACA	1.4	1.0
TANA	0.8	0.5
CUNA	8.9	2.9
NACA	2.1	1.0
CUCA	2.2	1.2

A. 2. *The angles π and φ of the relative axes (together these determine the direction of the rotation axis)*

Next, we subdivided the total relative movement (from 0 to 30 degrees) into smaller steps of 10 degrees each.

The data in Table A.12. (Appendix) for the *talo-calcaneal* joint show that the change of the axial direction (π and φ) in specimen ♀ 29 in the course of the supination followed a similar pattern for both processing stages. During the supination, the axis turned more to the longitudinal direction of the foot, π grew smaller and steeper, and φ grew larger. This is less clear in the other specimen. Van Langelaan (1983) also saw a similar pattern in most of his specimens. For the *talo-calcaneal* joint, a model was constructed of the positions of the axes in space (5° steps), Fig. 3.4c.

As Table A.15. (Appendix) for the *talo-navicular* joint shows, the deviation of the direction of the axis in specimen ♀ 29 was small, and that in specimen ♂ 14 generally slightly larger. There is practically no consistent pattern, as Van Langelaan also concluded.

As to the relative movement in the joint between the *cuboid and the navicular* (Table A.18., Appendix), the values of the rotation angle α are very low. For the three measurements with specimen ♀ 29 the average was 2.7°; with specimen ♂ 14, the average was 2°. Here, there was no consistent

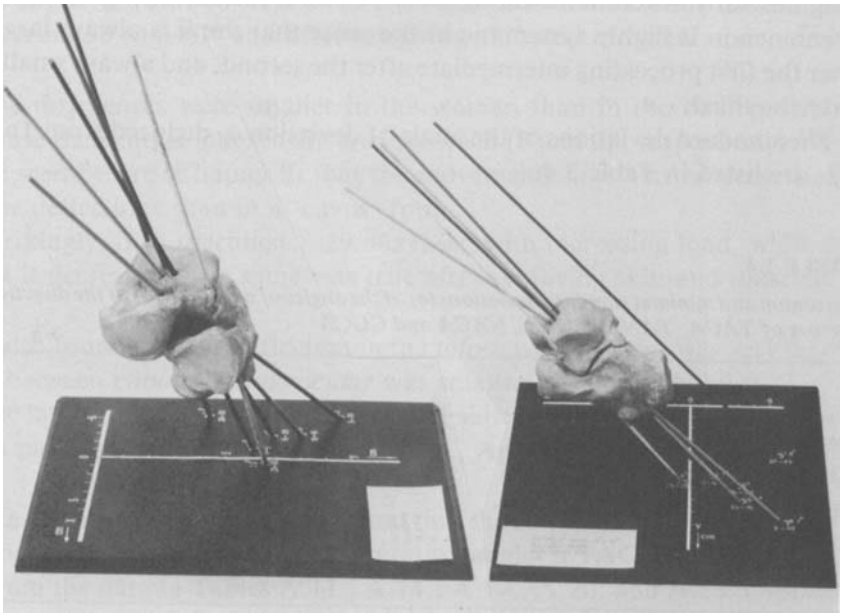

Fig. 3.4c. Model of the relative talo-calcaneal movement axes, representing 5° steps each of the external rotation of the tibia.

pattern either. Consequently, the values of π and φ are not very useful, as was also Van Langelaan's conclusion.

Looking at the figures in Table A.21. (Appendix) for the relative movement between *navicular and calcaneus*, we once more noticed that the inter-experimental differences of the magnitudes of π and φ were smaller for specimen ♀ 29 than for specimen ♂ 14. The same is true for the figures for the relative movement between *cuboid and calcaneus* (Table A.24., Appendix). Van Langelaan observed highly variable values for π and φ of NACA and CUCA in his specimens.

A. 3. *The angle* γ

The angles between the relative movement axes of the corresponding phases (viz. 0°–10° with 10°–0° or 1 with 6, 10°–20° with 20°–10° or 2 with 5 and 10°–30° with 30°–20° or 3 with 4) mostly did not differ significantly from zero. In other words, the supinatory and return movements corresponded well. An exception is the comparison of phase 1 with 6 for specimen ♂ 14, under 340N, both intact and dissected (Tables A.13., A.16. and A.22., Appendix). The larger differences in Table A.19. are explained by the very small α CUNA.

A. 4. *The parameters α and t of the absolute axes*

Tables A.26.-A.30. (Appendix) show a review of the parameters t and α of the *absolute movement axes* of tibia, talus, cuboid, navicular and calcaneus. The translation along the vertical (driving) shaft was read from the translation meter and entered in the table for the tibia (Table A.26. Appendix) under t/direct measurement.

These tables show that in no case was the difference between the calculated values of α and t during the supinatory and return movements very large (max. 2.3° for the experiments during which these two movements were carried out in direct succession). There was also a small difference between t directly measured and t computed. The exception, for $340N_i$ ♀ 29, is due to the fact that during this experiment we did not wait long enough for the subsidence of the tibia to fall below 0.14 mm/min following the application of the heavier vertical load. Occurrence of *torsion* in the tibia explains why the measured rotation angle in the distal part of the tibia is marginally smaller than the imposed rotation angle of the proximal part.

B. *Dynamic parameters* (moment and vertical tibial translation curves)

As we have seen from the Tables A.11.-A.25. as well as the graphs for the moment and the vertical tibial translation included below in this chapter (Figs. 3.6. and 3.7.), show that in the flat foot of the boy, there is much more 'taking place' than in the other specimen. To the eye, the changes of the relative positions of the tarsal bones, visible in the X-rays of the experimental movements, appear larger.

In reality, the tibia of ♂ 14 could rotate much more than 30° and the tarsus could consequently supinate farther. This has intentionally not been represented in the tables since it would make comparison more difficult if not impossible. We believe that the larger deflections may explain the fact that on the whole, the differences between the exo- and endorotatory movements both between the various stages of preparation and at different loads were larger for specimen ♂ 14 (i_t = 25) than for specimen ♀ 29 (i_t = 8). This does not mean that there is also more play. With specimen ♀ 29 as well as with specimen ♂ 14, the movement in the test setup 'turned back' at 30°, but it was only in specimen ♀ 29 that the supinatory movement was then complete. In the lower-arched specimen ♂ 14, the deformation was not yet complete at 30° but only at 40°. This appears clearly, inter alia, in the tibial translation curves in Fig. 3.5.

Also, owing to the flattening of the fat-pad under the calcaneus when the load is increased from 50 to 340N, the difference between corresponding

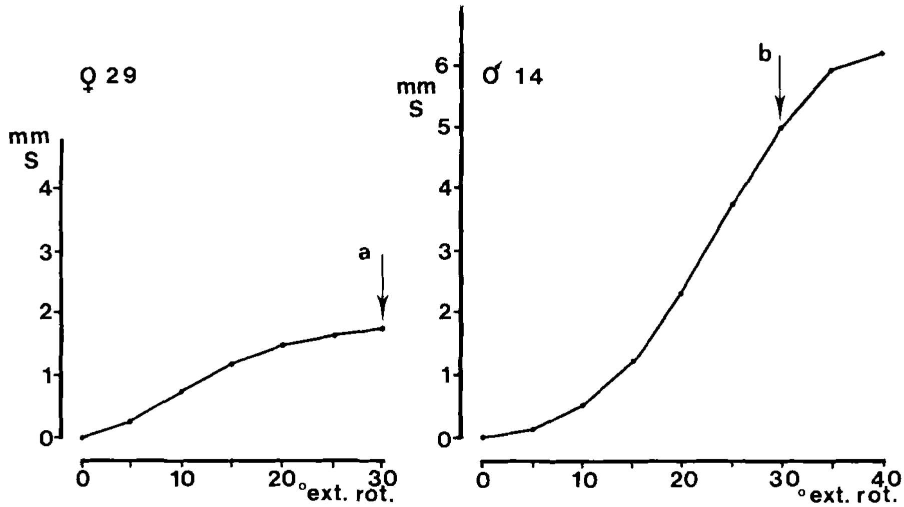

Fig. 3.5. Difference in position of the 'chosen' end of the supination on the tibial translation curves for ♀ 29 (a) and ♂ 14 (b).

registrations was in general slightly larger than the difference between 340N intact and 340N dissected.

When we consider the moment magnitudes and the vertical tibial translations measured in the way described in Chapter 2 in more detail, we find the following:

For both specimen ♀ 29 and specimen ♂ 14, the moment curves and the vertical tibial translation curves under 340N of the intact specimen and the preparation with skin and muscles removed are similar (Figs. 3.6. and 3.7.).

The first inflexion point in the graph of intact ♀ 29, lies at 10° input rotation, and corresponds to a local moment maximum of 10 Nm.

The second inflexion point lies at 20°, corresponding to a local moment minimum of 7 Nm.

Beyond this, the moment increases fairly strongly, and reaches 14 Nm at 30° rotation.

After dissection into an osteoligamentous preparation, the first inflexion point again lies at 10° exorotation, but the moment is now slightly lower, not quite 9 Nm. Beyond 10°, the course is slightly less steep to the second inflexion point which again lies at 20° with a moment of approx 7 Nm, followed by a slower rise to 11 Nm at 30°.

If we compare the *moment indexes* $M = \frac{a}{L_T} \times 10$ (page 35), we find

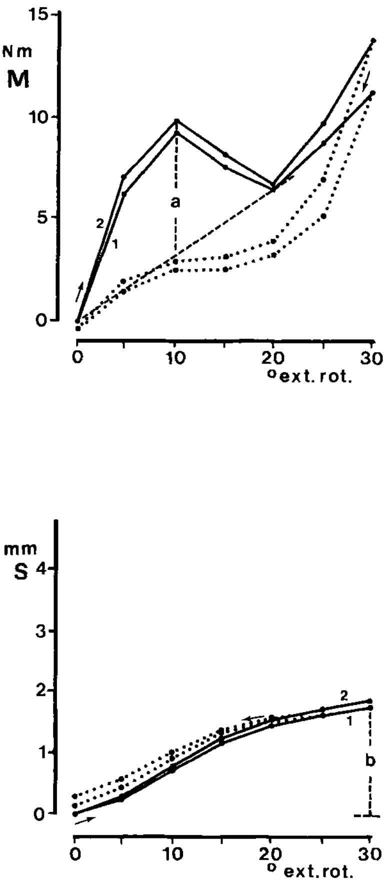

Prep. ♀ 29
i_t = 8
1 = intact 340N
2 = dissected 340N

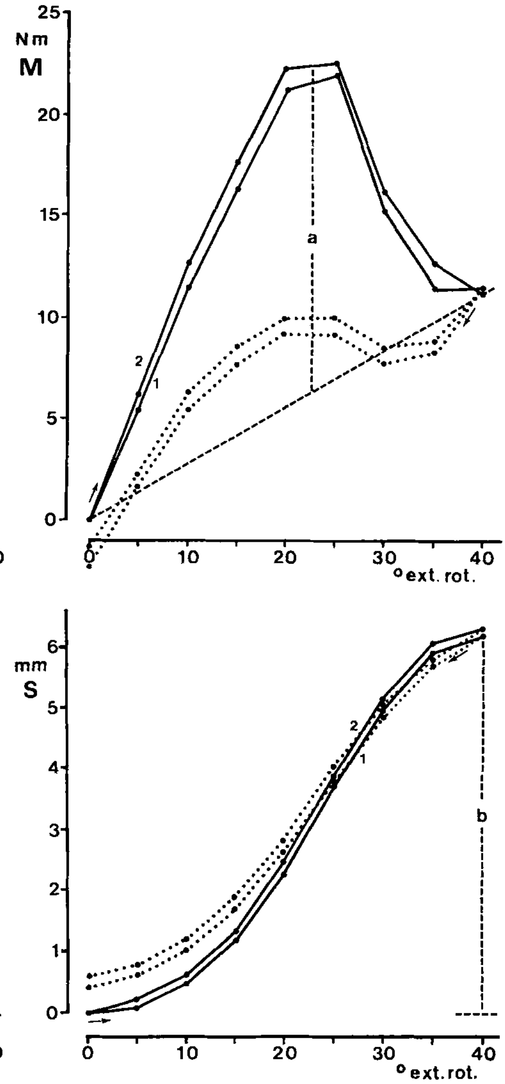

Prep. ♂ 14
i_t = 25
1 = intact 340N
2 = dissected 340N

Fig. 3.6. Moment and tibial translation of preparation ♀ 29 before and after dissection into osteoligamentous preparation. Vertical load 340N.

Fig. 3.7. Moment and tibial translation of preparation ♂ 14 before and after dissection into osteoligamentous preparation. Vertical load 340N.

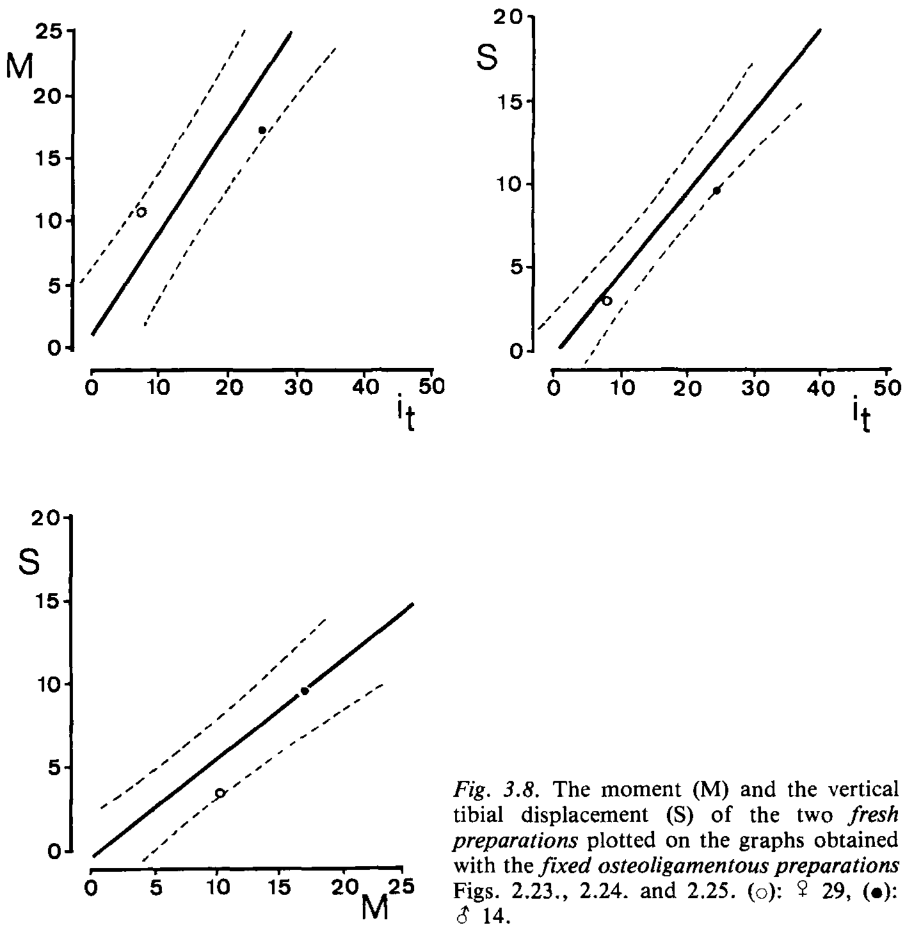

Fig. 3.8. The moment (M) and the vertical tibial displacement (S) of the two *fresh preparations* plotted on the graphs obtained with the *fixed osteoligamentous preparations* Figs. 2.23., 2.24. and 2.25. (○): ♀ 29, (●): ♂ 14.

for the intact specimen $M_1 = 10.7$ and , for the osteo-ligamentous preparation, $M_2 = 10.0$, which are not very different ; $\bar{M} = 10.4 \pm 0.4$. The moment registration of the intact specimen ♂ 14 also shows practically the same curve as the moment registration of the osteo-ligamentous preparation. The first inflexion point lies between 20° and 25° exorotation corresponding to a moment of approximately 23 Nm. The second inflexion point lies at about 40° for both registrations and a moment of 11 Nm. The rising trajectory that follows then was not recorded.

Comparing the moment indexes with each other, we find that M_1 equals $\frac{112}{64} \times 10 = 17.5$ and M_2 equals $\frac{106}{64} \times 10 = 16.6$, so that the difference is again small; $\bar{M} = 17.1 \pm 0.5$.

The *vertical tibial translation* S ($S = \frac{b}{L_T} \times 100$, page 38) did not differ either between the various stages of preparation. It was 1.80 mm and 1.75 mm, respectively for the intact specimen ♀ 29, and 6.01 mm and 5.88 mm, respectively for specimen ♂ 14. Indexed according to the conversion equation:

S ♀ $29 = \frac{b}{L_T} \times 100 = \frac{1.8}{56} \times 100 = 3.2$ and S ♂ $14 = \frac{b}{L_T} \times 100 = \frac{6.0}{64} \times 100 = 9.4$.

As shown in Fig. 3.8., the values of i_t, M and S for the two specimens in Figs. 2.23., 2.24. and 2.25., plotted against each other, fall within the confidence interval of the regression lines that have been calculated for fixed osteo-ligamentous material (page 44).

The curves of the endorotatory movement are also very similar. The hysteresis effect too hardly changes under the influence of the preparation, and is not affected by the soft non ligamentous tissue cover as we can see in Figs. 3.6. and 3.7.

C. *The stepwise and continuous movements*

With specimen ♀ 29 we also studied the difference between continuous and stepwise movements (as described in Chapter 2). We only analysed the test with load 340N at the slow speed. Comparing tests at different loads is not possible because the fat-pad below the calcaneus had not been prepared off in this specimen. As the load increases, therefore, the calcaneus sinks deeper into the fat, so that the positions of the tarsal bones within the reference system of the test set up differ too much from each other. In the fixed osteo-ligamentous specimens of Part 1, the fat under the calcaneus had been prepared off, so that there it was possible indeed to make comparisons.

The frequency Tables A.34. and A.35. (Appendix), summarized in Table 3.5., show that the exo- and endorotatory movements carried out continuously in 60 seconds (s_{60} and r_{60}, respectively) under load 340N with the intact specimen strongly resemble the same movements carried out with the osteo-ligamentous preparation. If we look at the 0.0/0.0 pairs, i.e. those in which the pellet trajectories and pellet projections coincide completely in two directions, we find that these are surprisingly similar. Summarized for all tarsal bones, 69% and 67% coincide for the exo- and endorotatory movements, respectively, of the intact specimen and: 71% and 75% coincide for the exo- and endorotatory movements of the osteo-ligamentous preparation. The slight difference is probably due in part to the fact that without the soft tissues, the pellets show up with better resolution. The

TABLE 3.5.

Frequency table of the differences between the continuous and the stepwise movement with vertical load of 340N, and a speed of 2 sec/degree for both supination (s60) and return to the 0 position (r60)

Spec. ♀ 29 i_t = 8						
state		intact			dissected	
load III (340N)				load III (340N)		
speed (sec.)		s60	r60		s60	r60
Tibia	0	5	7		5	7
(1 pellet)	0.1	3	1		3	1
	0.2	—	—		—	—
	0.3	—	—		—	—
	0.4	—	—		—	—
	*	—	—		—	—
Talus	0	23	20		23	22
	0.1	1	4		1	2
	0.2	—	—		—	—
	0.3	—	—		—	—
	0.4	—	—		—	—
	*	—	—		—	—
Calcaneus	0	18	18		20	18
	0.1	6	6		4	6
	0.2	—	—		—	—
	0.3	—	—		—	—
	0.4	—	—		—	—
	*	—	—		—	—
Navicular	0	20	21		21	22
	0.1	4	3		3	2
	0.2	—	—		—	—
	0.3	—	—		—	—
	0.4	—	—		—	—
	*	—	—		—	—
Cuboid	0	16	18		16	20
	0.1	6	5		6	4
	0.2	2	1		2	—
	0.3	—	—		—	—
	0.4	—	—		—	—
	*	—	—		—	—
Total	0	82	84		85	89
	0.1	20	19		17	15
	0.2	2	1		2	—
	0.3	—	—		—	—
	0.4	—	—		—	—
	*	—	—		—	—

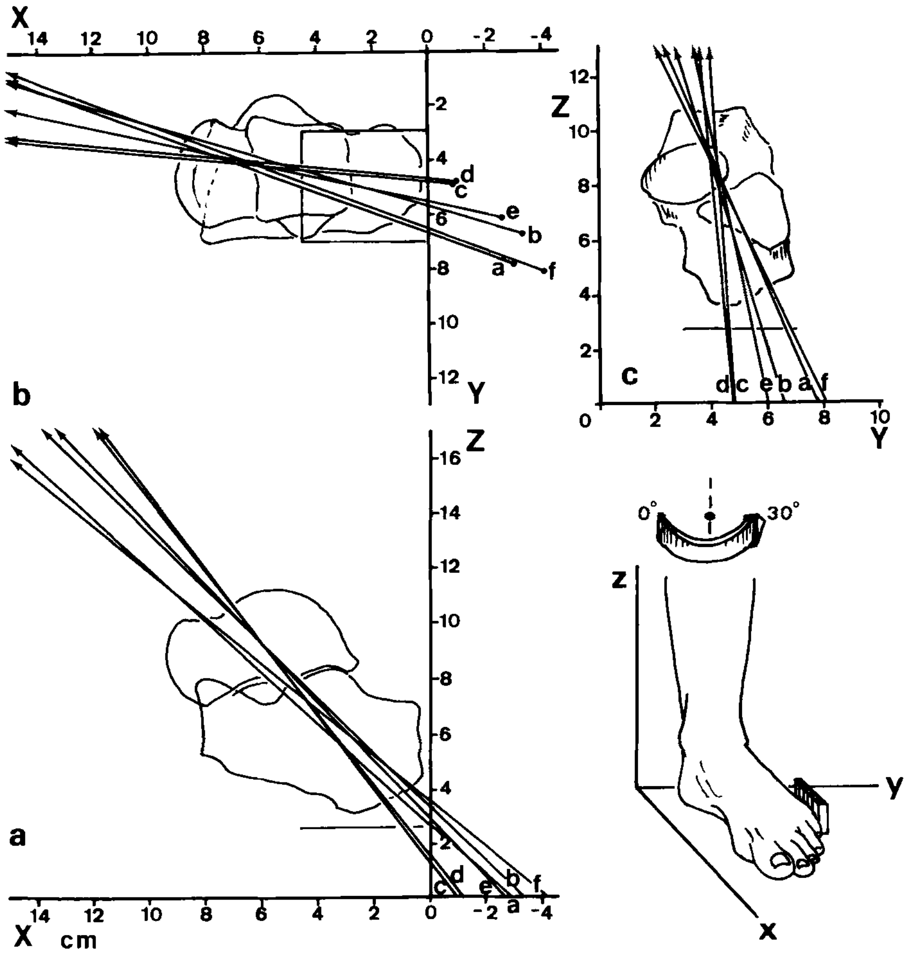

Fig. 3.9. TACA relative axes of ♀ 29 (intact fresh preparation) in 3 different projections. (a: the XZ plane, b: the XY plane, c: the YZ plane).
Load 50N, steps of 10°.
a = 0°–10° (phase 1)
b = 10°–20° (phase 2)
c = 20°–30° (phase 3)
d = 30°–20° (phase 4)
e = 20°–10° (phase 5)
f = 10°– 0° (phase 6)

number of 0.0/0.1 pairs is also very large: 23%, 25% and 23%, 21%, respectively. Accordingly, if we accept a deviation of 0.1 mm in one direction, we find that the similarity between the discontinuous and the continuous movements of specimen ♀ 29 in fresh condition is comparable with that of the fixed specimens examined in Chapter 2.

Note. With the fixed specimens (Chapter 2), the observations were not counted in pairs, but singly. The number of single observations counted (0.0 + 0.1) has to be multiplied by a factor 0.75 to obtain the approximate number of 0.0 pairs.

3.6. Conclusion

Excluding the ligaments, the soft tissues do not materially affect the movement pattern recorded by kinematic and dynamic parameters representing the biomechanical behaviour of the tarsus.

Also, the helical axes of corresponding steps of the exo- and endoratory movement practically coincide.

These results are another step on the way to investigations with the live leg, and justify the work with osteoligamentous material of earlier investigators.

FOUR

In-vivo analysis of the tarsal supination: Part 3 of the study

4.1. Introduction

The tarsal supination under a vertical load was recorded by roentgen-cinematography and studied by outline analysis using eight test subjects (See page 72), the amputation specimen ♀ 29, and the lower leg foot-preparation nr 492. The latter two had been the subject of earlier measurements (Chapter 2 and Chapter 3, respectively). The objective now was to find an answer to question 5 (page 11, Chapter 1.2.):

5a. Is it possible to design an experimental setup in which living subjects perform movements in a manner comparable with the post-mortem experiments, and how can these movements be recorded without use of intra-osseous measuring pellets?
 b. Are the movements that are made in vivo and recorded with this test setup comparable with the movements recorded during experiments with cadaver preparations?

By necessity, the method of outline analysis introduces an element of subjective interpretation.

4.2. Method

For the roentgen-cinematography we used the Siemens Siregraph (generator: Gigantos E 150 kV, intensifying screen 25/15 cm, focus 0.6–1.2 mm, film size 70 mm) of the Department of Radiology of the University Hospital of Leiden.

With this equipment it was not possible to take exposures in two directions at the same time, so that we had to make consecutive horizontal and dorso-plantar X-ray films. The same inner frame and measuring equipment as for Parts 1 and 2, were used in this part of the study. However, with the existing outer frame, the distance between the back of the inner

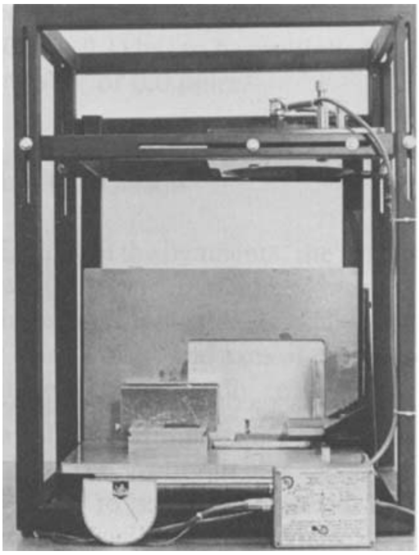

Fig. 4.1. Frontal view of the test apparatus for the in-vivo registrations.

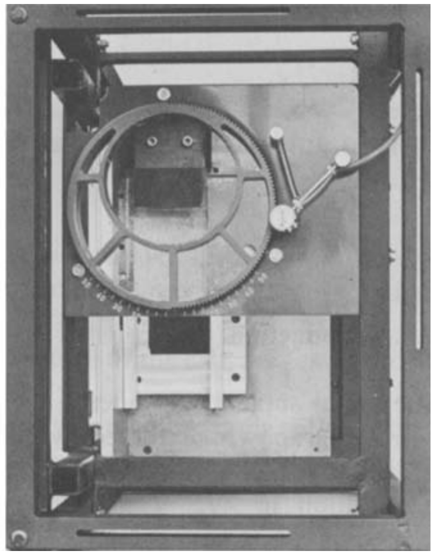

Fig. 4.2. View from above of the test apparatus for the in-vivo registrations.

frame and the intensifying screen was too long for the horizontal projection. This would have led to magnification and distortion that would have precluded comparison with the standard X-rays. For this reason, a second cage was constructed (Figs. 4.1. and 4.2.) in which the measuring frame could be placed directly *against* the roentgen table, which had the intensifying screen behind it, for the horizontal projection, and subsequently *on* the roentgen table for the dorso-plantar projection.

In this way it was possible to record on 70 mm film the tarsal supination carried out in one flowing movement by exorotation of the leg. In order to establish the degree of exorotation of the tibia that corresponded to a particular supinated position of the foot, we constructed a rotation meter, its graduation marked with roentgen contrast medium. This rotation meter consisted of a ring for the leg, a potentiometer, a switchbox and a voltmeter. A wide PVC ring, with an opening in the dorsal direction for the proximal part of the test subject's lower leg, kept the tibia in a central position. The raised rim of the ring was toothed (a in Fig. 4.2.). The opening for the lower leg was lined on the inside with coarse emery paper. After the test subject put the lower leg through the ring, the leg was fixed with wedges of balsa wood. The ring could turn around its axis in a round window in a PVC holder which could be adjusted up and down and front to back, and was fitted with ballbearings and a gradation (Fig. 4.4.).

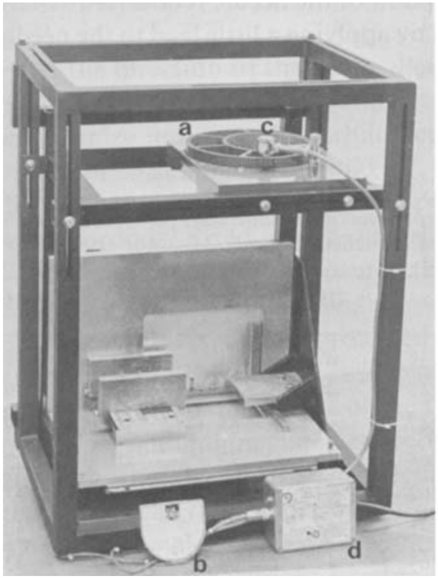

Fig. 4.3. Voltmeter equipment with ring (a), voltmeter (b), 'potmeter' (c), switchbox (d).

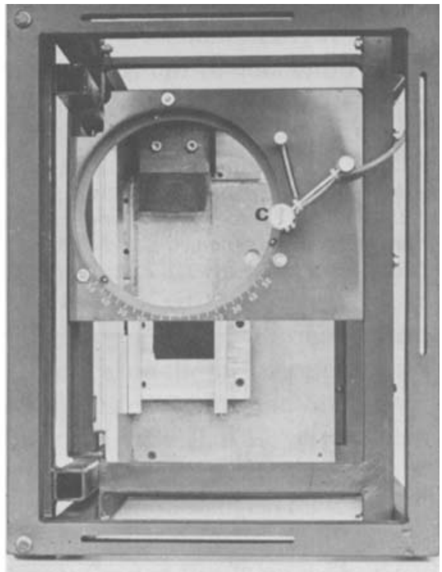

Fig. 4.4. 'Potmeter' (c) viewed from above.

Three bearings on the floor of the holder and three in its wall made possible rotation with little friction and allowed vertical displacement.

For practical reasons, the apparatus was so constructed that only the right leg could be X-rayed in the test setup. The electronic part of the rotation meter was developed in the Department of Electronics of the Laboratory for Physiology and Physiological Physics of the University of Leiden. It consisted of a low-friction potentiometer (c in Figs. 4.2. and 4.4.) with a cog-wheel on its axle, the toothing fitting that on the PVC ring (a in Fig. 4.2.). The cog-wheel of the potentiometer was pulled against the ring by a spring. By including a voltmeter (b in Fig. 4.3.) in the X-rays in both projections, the movements of the pointer could be recorded radiologically so that for every supinatory position of the tarsus, the corresponding degree of exorotation of the lower leg could be read.

A buffer amplifier in a switchbox (d in Fig. 4.3.) made it possible to eliminate the current consumption in the voltmeter (moving-coil meter) and reduce the load on the Wheatstone bridge to a negligible amount. As a result, the response of the voltmeter was virtually linear. Using two variable resistors, the desired scale range for positive and negative angles could be adjusted for horizontal (Fig. 4.6.) as well as vertical (Fig. 4.5.) use of the voltmeter. The dial of the voltmeter was calibrated and fitted with three steel pellets at the calibration places (i.e. 0°, 20° and 40°).

A small amount of lead fixed to the point of the needle rendered it visible in the X-ray. The balance was restored by applying a little lead to the needle on the other side of the fulcrum as well.

TABLE 4.1.

Various data for eight test subjects (t.s.)
L/R: left/right, L_f: foot length (mm), H_{tn} : height of navicular tuberosity (mm), H_{lm}: height of lateral malleolus (mm), H_{mm}: height of medial malleolus (mm), M_s: shoe size

t.s.	sex	age (yrs)	L/R	L_f	H_{tn}	H_{lm}	H_{mm}	M_s
1	f	19	R	246	29	51	64	38
2	f	19	R	245	40	58	71	39
3	f	26	R	247	51	65	77	39
4	m	19	R	264	45	73	80	43
5	m	20	R	262	47	65	74	42
6	m	24	R	241	47	62	78	40
7	m	20	R	264	49	64	78	43
8	f	20	R	230	45	61	71	39

TABLE 4.2.

Cad. nr	sex	age (yrs)	L/R
492	m	52	R

4.3. Test subjects

The eight test subjects, four men and four women, were all healthy physiotherapy students who as far as we know had normal feet. Their ages ranged from 19 to 26 years with a mean age of 21 years. Foot length (L_f), height of the navicular tuberosity (H_{tn}), height of the lateral malleolus (H_{lm}) and height of the medial malleolus (H_{mm}) were measured in mm, and shoe size (M_s) was recorded (Table 4.1.). The lower leg foot-preparation (cad. nr 492) had already been part of the material for Part 1, thus allowing a comparison to be made with the findings obtained at that time (Table 4.2.).

This specimen also made it possible for us to calibrate our in-vivo setup.

4.4. Procedure

First, the direction of the beam was adjusted with the fluoroscopic image on the monitor, using the sighting system (page 24). Subsequently, in order to optimize image quality while keeping the radiation dose minimal, we opted for 'blacking 2 + 0' at 60 kV, focus 0.6 mm and intensifying screen diameter 25 cm. Rate was 3 frames per second, and the duration of rotation was 6 seconds. Fixed source-intensifier distance was 106 cm.

To minimize X-ray exposure, the movements to be performed were thoroughly practised beforehand.

The test subject, gonads protected with lead, put S his leg through the ring and the opening in the plate, and placed the heel on the heel support in such a way that, when the outside of the forefoot rested against the vertical support of the aluminium plate, the second ray was parallel to the vertical plate, and in the same position as the specimens in the test setup. The ring was then fixed proximally round the lower leg with balsa wood wedges (Figs. 4.5. and 4.6.). While maintaining it horizontal, the height of the PVC plate was then adjusted so that the weight-bearing calcaneus rested firmly on the heel support. The plate was then fixed in place with four locking pins. Against this ring, which could now turn in and on the bearings, the potentiometer was placed.

After adjustment of the voltmeter, and a few test rotations, the film was recorded. With the test leg extended, tarsal supination was elicited by rotation of the leg in the hip and with the hip muscles. Thereafter, the test subject, with the ring in place stepped out of the test apparatus and took a position in relation to the X-ray apparatus that permitted exposures in another projection. For the osteo-ligamentous specimen (cad. nr 492) a separate construction was designed. By using an adaptor with teeth around the vertical shaft, with the same diameter and teeth ratio as the ring for the in-vivo experiments, the voltmeter registration could be used also for the cinematographic exposures of this specimen. Here, a 3 + 0 blacking was preferred to 2 + 0, but in all other respects the technique was identical. The specimen was rotated by the electric motor described before (page 22), the load was 340N, the duration of the rotation 6 seconds. Of the test subjects as well as of the specimen, only the exorotatory movement was recorded.

4.5. Processing the material

Of the films taken, the images of the starting position (0°), and of the 10°, 20° and 30° positions were placed together in one mask, following which a contact print and a contact film were made by means of a logotron ap-

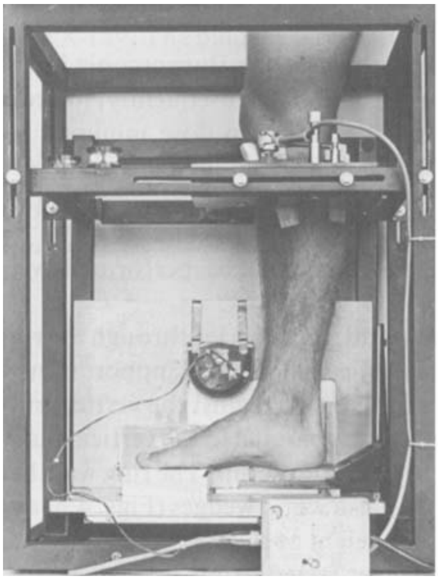

Fig. 4.5. Medial view of the horizontal projection, including voltmeter equipment.

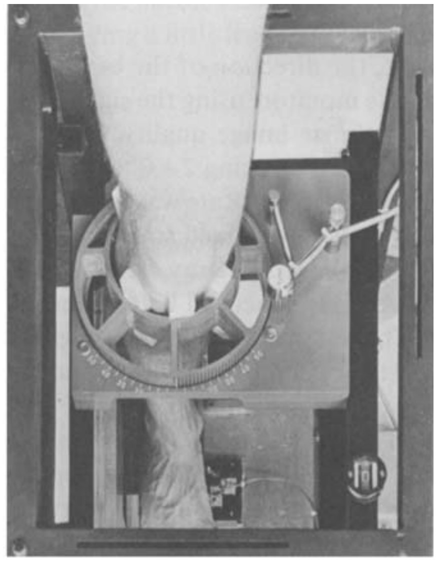

Fig. 4.6. View from above for the dorsoplantar projection, including voltmeter equipment.

paratus in the Department of Radiology. This apparatus heightened the contrast somewhat, simplifying the graphic processing (Figs. A.1.-A.8., Appendix).

With a distortion-free overhead projector, the 70 mm images were magnified until the reference system (the brass strips X, Y and Z of the cassette,

TABLE 4.3.

X-ray data for eight text subjects (t.s.)

Talo-calcaneal angle of inclination ϵ, calcaneal overlap P_C, talar length L_T and tarsal index i_t. S_v is tibial climbing in-vivo = measured tibial climbing in the enlarged 70 mm X-ray film divided by talar length × 100

t.s.	ϵ	P_C	L_T	i_t	S_v
1	33	11	54	13	8
2	28	8	55	8	5
3	20	6	54	4	3
4	24	10	64	7	6
5	25	9	67	6	5
6	24	13	59	10	6
7	26	10	62	8	4
8	22	9	59	6	4 (max. 28° exo.)

see page 21) had the same dimensions as in the 18 × 24 cm films of Parts 1 and 2 of the study. The outlines of the tarsal bones, tibias and fibulas were traced and compared for the several steps, both intra- and interindividually.

On the enlargement of the 70 mm image of the starting position, the tarsal index could be determined with the equation $i_t = 100 \times \frac{P_C}{L_T} \times tg\ \epsilon$ (Chapter 2.5.2., page 34), and the climbing of the tibia (S) could be found by measuring the distance between the tip of the concave distal end of the tibia and the basal reference line. The purpose was to find a correlation between the tarsal index and the climbing of the tibia.

4.6. Results and discussion

4.6.1. Huson's outline analysis

Huson (1961) has presented a detailed description of the movements of the live foot as a whole and of the tarsal bones in relation to each other during tarsal supination under a vertical load. These movements were brought about by exorotation of the leg, without the foot as a whole following this movement. Using medio-lateral and dorso-plantar X-rays of the starting position and the supination position, and combining them with specimen data, he made a number of observations.

In the medio-lateral X-rays he could see, as a result of supination:

a. the exorotation of the talus, rendered visible by the change of shape (widening) of the projection of the inlet of the tarsal canal and by the shift of the arch-shaped edges of the talar trochlea;
b. the elevation of the talus and calcaneus on the one hand and the first tarsal bone on the other: the medial arch of the foot has grown higher;
c. the downward tilting of the cuboid and of the fifth metatarsal bone owing to which the projection of the staircase-shaped outline of calcaneus, cuboid and fifth metatarsal bone becomes clearer and more angular: the lateral arch of the foot has descended;
d. the inversion of the calcaneus, deducible from the facts that the sustentaculum of the talus with the anterior articular surface rises in relation to the floor of the inlet of the tarsal canal;
e. the (further) inversion which the navicular and cuboid bones have undergone in relation to the talus and the calcaneus, deducible from the reduction in size of the projection of the navicular bone (its dorso-plantar dimensions). This is because the tuberosity of the navicular bone, having

turned into the projection plane, has become visible from the relative changes of the medial and lateral arches of the foot and from the shift of the cuboid bone in relation to the fifth metatarsal bone.

In the dorso-plantar X-rays he noted:

a. a turning away in a lateroposterior direction of the head of the talus from the socket of the navicular bone, due to exorotation of the talus;
b. a lateral bulging of the lateral edge of the foot, deducible from the fact that the anterior process of the calcaneus points in a more lateral direction, and from the adduction of the cuboid in relation to the calcaneus;
c. the supinatory tilting (inversion) of the forefoot, deducible from the overlapping of the projections of the cuboid and navicular bones, from the lengthening of the projection of the navicular bone, from the overlapping of the projections of the cuboid bone and the fifth metatarsal bone, from the partial overlapping of the images of the other metatarsal bones, and finally from the increased kink in the medial arch of the foot.

Huson states correctly that the magnitudes of the changes that are visible in the projections depend on the mobility of the foot examined, and that this will undoubtedly show individual variation.

A characterization of these individual differences in structure and mode of foot movement, and a characterization of the relation between these various characteristics of shape and function in terms of usable units, was not possible at that time. Our own technique of in-vivo recording (with the X-ray film showing the voltmeter, the deflection of which corresponded to the degree of exorotation) has allowed us to determine the supinatory positions corresponding to 0°, 10°, 20° and 30° exorotation for each individual subject and compare them with each other.

4.6.2. Further development of the outline analysis

To Huson's description of the roentgen image, which is generally applicable to the end position of the supinatory deformation, we can add the following:

A. For the *medio-lateral projection:*

In the starting position, with the beam direction we use, the malleolus tertius of the tibia is projected to a varying extent over the posterior edge of the fibula.

The tip of the lateral process of the talus extends to a point deep in the calcaneal sulcus.

The overlapping of the talar head over the anterior surface of the calcaneus, and the angle of inclination of the talo-calcaneal joint (determined by the combined tangents of the anterior and posterior joints) show individual variability. As we have seen, both are determined by the tarsal index.

The projection of the talar sustentaculum overlaps that of the calcaneal sulcus; we also note the angle between the inferior surface of the calcaneus and the horizontal reference strip. When we include the projection of the tuberosity of the navicular bone in our observations, we note first that its size is rather variable but that, as a rule, its tip is projected below or is level with the inferior one-third of the talo-navicular joint. This is not the case in test subject 3 (Fig. A.5., Appendix) having an index of 4. In this subject the tuberosity was situated higher. The cranial part of the cuboid is hidden because its projection overlaps that of the inferior surface of the navicular.

The projection of the centre-line of the fifth metatarsal bone touches the inferior surface of the calcaneo-cuboid articulation.

With the lower leg in *10° exorotation*, the projection of the posterior edge of the malleolus tertius nearly always coincides with that of the posterior edge of the fibula, or lies just outside it. The two curved edges are now seen separately, although only slightly as yet, with the medial edge (i.e. the medial edge on the trochlea tali) projected just below the lateral edge. This, together with the fact that the lateral process of the talus withdraws obliquely upward from the calcaneal sulcus, show clearly that the talus, held between tibia and fibula, rotates and is everted slightly.

As exorotation proceeds, rotation and eversion of the talus grow more pronounced. The overlap of the talar head and the anterior surface of the calcaneus grow smaller, proving that apart from exorotation and a slight eversion of the talus, a relative elevation of the talus is also involved: the angle of talo-calcaneal inclination appears to grow smaller. The shadow of the talar sustentaculum now becomes better visible above the calcaneal sulcus, and its distance to the calcaneo-cuboid joint grows slightly smaller. This means that the calcaneus also rotates but, unlike the talus, is slightly inverted. The calcaneus rises slightly, as shown by the widening of its angle with the horizontal strip.

The projection of the tuberosity of the navicular bone has moved up a little, to the boundary between the lower and middle third of the projection of the talo-navicular joint (In test subject 5, halfway to this projection, Fig. A.5., Appendix).

The anteroposterior diameter of the navicular is slightly reduced and a larger part of the cuboid is now visible.

The centre-line of the fifth metatarsal bone is projected below the calcaneo-cuboid joint; the base of the fifth metatarsal lies nearer the horizontal reference strip.

Since the medial arch possesses one segment more, it rises markedly, whereas the lateral arch descends only very little because the foot mostly rests with the lateral arch on the bottom, which also prevents sag.

At *20° exorotation*, all the changes mentioned grow even clearer and in test subjects 3, 4, 5, 7 and 8 (Figs. A.3.-A.5., A.7. and A.8., Appendix) we can observe the beginning of the *opening of the tarsal canal*, which is especially noticeable in feet with a lower tarsal index. This phenomenon is even clearer at *30° exorotation*. In several cases (test subjects 3, 4 and 5) an almost perfectly circular opening has appeared, without any overprojection of bones. This opening shows up best in feet with a low index (higher arches). Although feet with higher indexes also show a good oval-shaped through-view of the tarsal canal, this view is bisected by the anteromedial articular surface between the talar head and the talar sustentaculum.

From an anatomical viewpoint, it is to be expected that the tarsal canal will open sooner in feet with a low index than in feet with a high index. This can be related to the different starting positions of the tarsal bones. In the first case, the talar head, as it were, rests a little more on the top of the calcaneus. In flatter feet this situation is reached only after some supination (Fig. 2.18., page 33). Whereas the higher-arched foot has reached its maximal supination at 30°, the flatter foot can presumably still supinate more. That this hardly ever occurs with the living flatter foot in a real situation, such as on uneven ground, could be because the first peak of the moment curve (Fig. 2.19., page 36) may well be an insuperable barrier. If the foot were to supinate further after this point, it would 'tip over' (in about the same way as the specimens did in the test setup under a load of 340N). A ruptured ligament is not inconceivable on uneven ground where the rate of supination cannot be controlled so precisely as in the test setup. In our opinion, the barrier constitutes a built-in safety device for the lateral ligamentous system.

In addition to the above observations we notice that, at *30° rotation*, the two curved edges of the talar trochlea are lying quite far apart. In most cases one is situated above the other. The projections of the lateral and posterior processes overlap. In three of the eight cases, the overlap of the talar head and the calcaneus has disappeared entirely.

The projection of the tuberosity of the navicular bone is now everywhere above or level with the borderline of the middle and upper thirds of the talo-navicular joint. The anteroposterior diameter has been reduced to its minimum.

Practically the entire cuboid is visible. The base of the fifth metatarsal

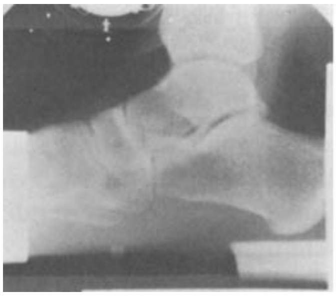

Fig. 4.7a. 70 mm X-ray film test of subject 7.

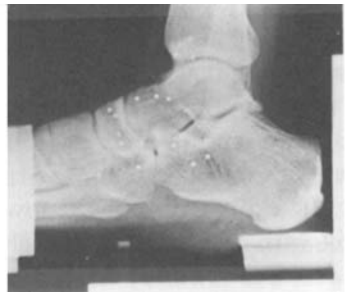

Fig. 4.7b. X-ray of specimen ♀ 29, reduced to 70 mm.

bone has moved even close to the horizontal reference strip, indicating that the lateral arch has sunk even more.

B. To Huson's observations of the changes in the *dorso-plantar projection* the following may be added:

The most striking phenomenon is that with increasing exorotation the skeleton of the foot grows steadily narrower because of the overlap of the talus and navicular on the one hand and the cuboid and calcaneus on the other, with the foot assuming a distinct 'comma shape'.

In all cases, the X-rays show clearly that, while in the starting position there is complete congruence in the talo-navicular joint, in subsequent positions the talar head turns away from the navicular.

Since in this small series the differences between the extreme values of the tarsal index are not very large, no statements can be made concerning the position and direction of the body and neck of the talus in relation to each other and in relation to the calcaneus.

TABLE 4.4.

Tabular comparison of the biological and roentgen-morphometric parameters of test subject 7 and amputation specimen ♀ 29

	sex	age	L/R	P_C	L_T	ϵ	i_t	S
test subject 7	m	20	R	10	62	25°	8	3
amputation prep. ♀ 29	f	29	L	9.5	56	24°	8	3

Passing from low (i_t = 4) to high (i_t = 13) talar indexes, the visible part of the calcaneus grows slightly larger.

Correspondingly, the overlap between the navicular and the cuboid is smaller in the foot with a tarsal index of 13 (test subject 1) than in the foot with i_t = 4 (test subject 3).

In feet with higher arches, the talus starts to turn away from the navicular at 10° exorotation of the lower leg. At this stage it does not yet do so in feet with a lower medial arch.

In all cases, the visible part of the anterior surface of the calcaneus grows smaller because the head of the talus turns away obliquely in the latero-posterior direction.

The distance from the lateral edge of the foot to the horizontal reference strip decreases.

At 20° rotation, these phenomena grow more pronounced, and the talar head is turning away from the navicular in feet with lower arches as well. We notice, however, that this turning away cannot be discerned on the medial side of the talo-navicular joint, because of the antero-medial extension of the articular surface, nor does any incongruence occur in that part of the joint where contact is maintained.

4.6.3. Application of outline analysis to compare a living test subject (nr 7) with an amputation specimen (♀ 29)

As we have seen in Chapter 3, the movements and the biomechanical behaviour of the tarsus during supination undergo no essential changes in the various stages of dissection of the fresh amputation specimens as we can outline in Figs. 3.6. and 3.7. (page 63).

Still, when we compare a dead leg, although completely intact and very fresh, with a living leg, we have to take into account the possible influence of muscular activity. Ambagtsheer (1978) demonstrated in his electromyographic study that his test subjects, whose feet were left unrestrained during supination just as in Huson's setup, used the posterior tibial muscle, the flexor muscles of the toes and of the great toe, and the anterior tibial muscle.

The influence of muscular activity on supination is actually only relative since we can induce supination in osteoligamentous specimens, as well.

There are three ways to induce supination of a tarsus. Supination is induced by muscular activity in a freely suspended non-weightbearing foot by tautening the posterior and anterior tibial muscles and the long and short flexor muscles.

Supination can be induced in the weight-bearing, free-standing foot in the absence of a stop against the lateral edge, by muscular activity of the muscles of the hip, thigh, lower leg and foot.

During this type of supination, the aim of the muscular activity in the foot and part of the activity in the lower leg is to keep the forefoot from turning aside and, depending on the instructions given the test subject, to keep the forefoot fully in contact with the supporting surface by pronating it in relation to the hind foot.

We may reason that muscular activity changes the shape of the subtalar foot structure so that the talus is forced into exorotation and through the talo-crural joint takes the lower leg with it.

The third type of supination is the main one in our study; it differs from the two others in that the use of muscular activity in the foot and lower leg can be eliminated.

By affixing one stop against the lateral edge of the forefoot and another to prevent the first metatarsal from rising, we can abolish the activating and correcting muscular forces. Thus we ought to be able to bring about supination by using only the ligament-operated system, in the same way that we observed in our specimens. Electromyography would be the only way to demonstrate this beyond doubt. When we exorotate the extended leg with the hip muscles, we convert the rotation of the 'mortise' by way of the talus into a supinatory deformation of the skeleton of the foot, without having to worry about the forefoot turning away or rising. This takes some practice, as we ourselves and the test subjects found out.

Huson (1961) argued that the tarsus is a mechanism with one degree of freedom of movement, and Van Langelaan's analysis has corroborated this. Thus it is highly unlikely that during supination in the weight-bearing situation in the presence or absence of a stop against the lateral edge of the foot, changes may occur in the pattern of movement of the tarsal bones. This argument supports our statement that, by bringing about supination in cadaver specimens as well as in live test subjects by way of the ligament-operated mechanism, we have established comparable situations in which the covering soft tissues do not materially affect the movement and the biomechanical behaviour of the tarsus.

It is therefore justified to compare test subject 7 with the fresh amputation specimen ♀ 29.

As we can see in Fig. 4.15a., Fig. 4.15b. and Table 4.4., a comparison of the two feet shows that there is a striking morphological similarity. The tarsal indexes are identical (both 8) and the shape of the tarsal bones are similar, as well. An interesting detail is that both feet contained a separate os trigonum. The phenomena that occur during supinatory deformation of these two feet, as seen in the medio-lateral and dorso-plantar X-ray films, are also virtually identical (Figs. 4.8. and 4.9.).

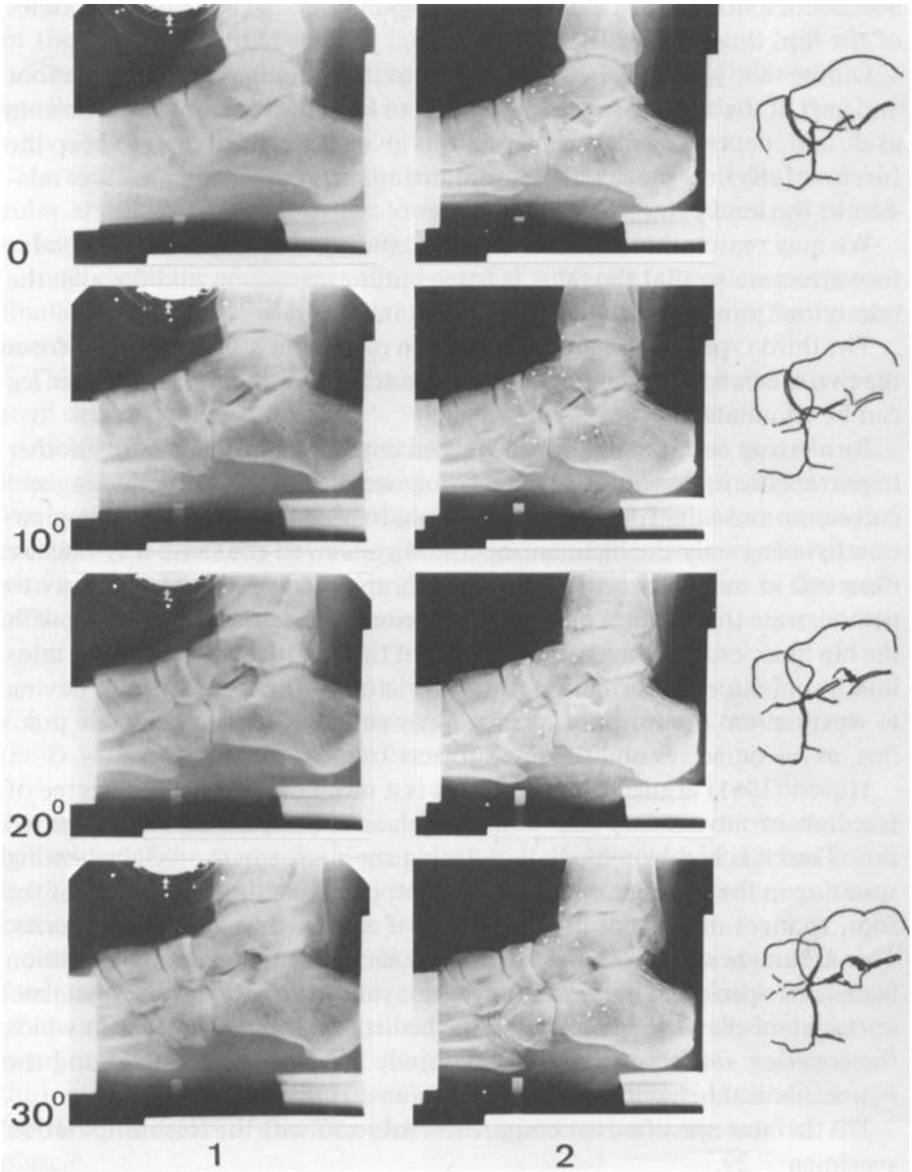

Fig. 4.8. Comparison for the horizontal projections of the 0°, 10°, 20° and 30° positions of test subject 7 (1), selected with the aid of the voltmeter and preparation ♀ 29 (2), reduced from 18×24 cm.

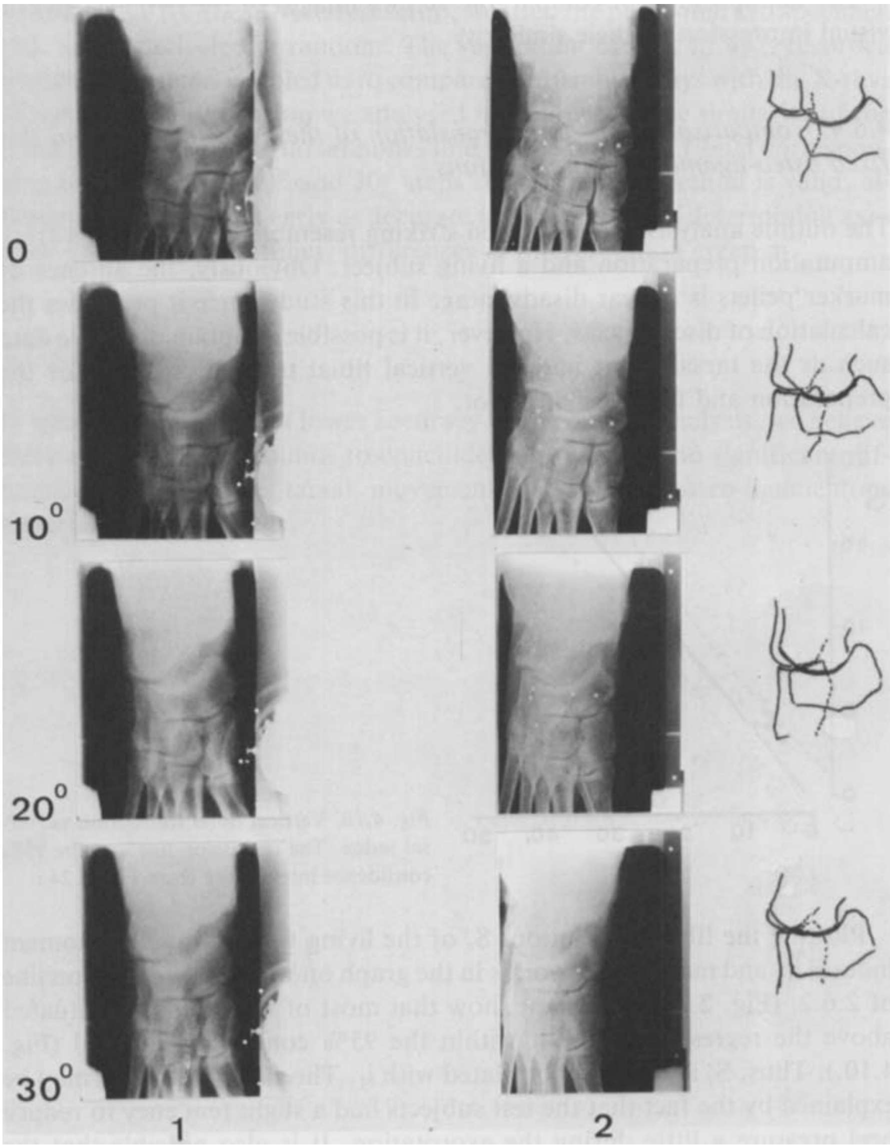

Fig. 4.9. Comparison for the dorso-plantar projections of the 0°, 10°, 20° and 30° positions of test subject 7 (1), selected with the aid of the voltmeter and preparation ♀ 29 (2), reduced from 18 × 24 cm and reversed.

The juxtaposition of comparable 70 mm images of the two legs gives a visual impression of their similarity.

4.6.4. Comparison of the tibial translation of the living subjects and the fixed osteo-ligamentous preparations

The outline analysis above showed striking resemblances between a fresh amputation preparation and a living subject. Obviously, the absence of marker pellets is a clear disadvantage in this study since it precludes the calculation of discrete axes. However, it is possible to obtain objective data such as the tarsal index and the vertical tibial translation both for the preparation and for the living foot.

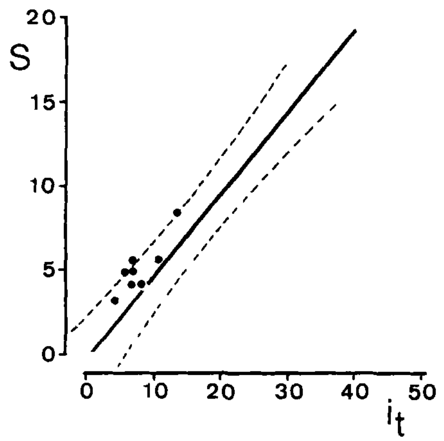

Fig. 4.10. Vertical tibial translation vs. tarsal index. The regression line and the 95% confidence interval are from Fig. 2.24.

Plotting the tibial translations S_v of the living feet against the moment indexes i_t, and marking the points in the graph on which the regression line of 2.6.2. (Fig. 2.24.) is drawn, show that most of the points are situated above the regression line but within the 95% confidence interval (Fig. 4.10.). Thus, S_v is strongly correlated with i_t. The slight deviation may be explained by the fact that the test subjects had a slight tendency to reduce heel pressure a little during the exorotation. It is also possible that the height of the arch was increased somewhat by active support of the foot muscles.

If we regard S_v as one of the expressions of the biomechanical behaviour, then the strong correlation with the tarsal index i_t and the moment index M, as well as the similarity of the phenomena in the X-ray films, indicate strongly that the mechanical behaviour of the two tarsi should resemble each other. That is, the tarsal bones will move around absolute and relative helical axes of comparable direction.

As a gauge for the in-vivo test setup, we used the pellet-marked specimen cad. nr 492, selected at random. The supination of cad. nr 492, recorded with the voltmeter, enabled us to compare the 70 mm X-rays with the X-rays of the stepwise supination we analysed in Chapter 2. The similarity of the spatial positions of the tarsal bones and of the tibia and fibula corresponding to the 0°, 10°, 20° and 30° steps show that this method is valid, although naturally not nearly as accurate as the method of determining axes since in looking at outlines, differences in interpretation creep in.

4.7. Conclusion

In spite of the somewhat lower accuracy of the outline analysis, we believe there are sufficient grounds to conclude that there are no significant differences between the tarsal movement patterns in osteo-ligamentous material and in live legs.

FIVE

Clinical relevance

The objective of this investigation was, initially at least, to pursue the development of understanding the biomechanical nature of the tarsus. In that we have to some extent succeeded.

Beyond the purely scientific aspects of such an investigation, it is always gratifying to the investigator if some of the new understanding can be shown to have practical implications, for example in aiding or preventing orthopedic surgery.

Le Lièvre (1961) showed with the aid of foot-prints, that feet with a low longitudinal arch, and thus apparently flat, may nevertheless give the imprint of a hollow foot. In this way he showed that one cannot conclude simply from appearance if a foot is flat or not.

In our investigation we had one specimen with a foot that looked completely flat (Fig. 5.1.). However, applying our new X-ray based tarsal index to this foot, we would expect it to be hollow from the biomechanical viewpoint. In fact, when the input moment necessary to supinate the foot, as well as the vertical tibia displacement are plotted against the tibia rotation (Fig. 5.2.), the result is indeed that of a very hollow foot.

It seems clear that these findings could have practical consequences for orthopedic surgery. Many patients suffer from acute or chronical lateral ligament injuries, almost always the result of a forced supination trauma. We have noticed that, in general, hollow feet are more prone to such accidents than are more flat feet. After we standardized the loaded mediolateral X-rays, we remarked that feet with a low tarsal index ($i_t < 8$) scored higher and in general had more severe damage to the ligaments than those with a high tarsal index. It should be possible, using the standardized X-ray technique in studies of patients who have been operated for acute ligament injures, to determine whether or not there is a correlation between the degree of the lesion and the magnitude of the tarsal index. Perhaps would the conclusion of such an investigation allow us to better prevent such accidents, by giving the correct sport-medical advise to athletes such as in the choice of shoe-type and the necessity of prophylactic taping.

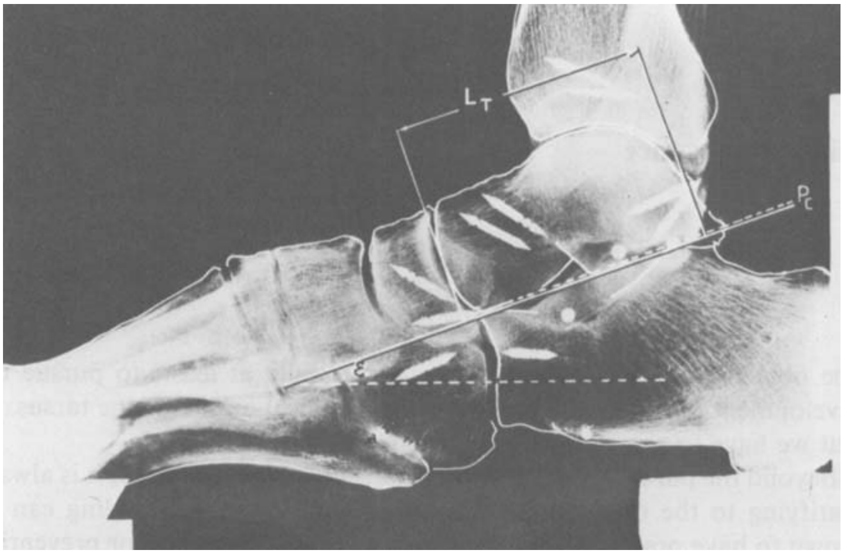

Fig. 5.1. Determination of tarsal index of a foot that appears to be flat. According to the index and moment and tibial translation however it is a very 'hollow' one.

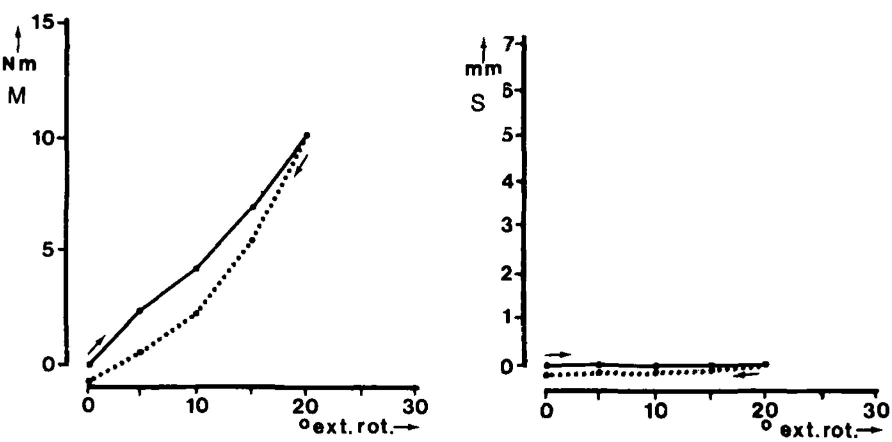

Fig. 5.2. Moment curve (left) and tibial translation curve (right). Notice: the moment (M) raises immediately; rotation only up to 20°, there is no displacement of the tibia (S).

SIX

Summary

The main purpose of this investigation was to extend the work of Huson, Ambagtsheer and Van Langelaan to living subjects. It may thus be regarded as the logical continuation of Van Langelaan's study.

The investigation consists of three main parts:

In part 1 (Chapter 2), stepwise supination of the tarsus of *fixed osteo-ligamentous preparations* (the mode of supination studied by Van Langelaan) was compared with continuous supination.

We found that stepwise supination of lower leg foot-preparations differs little from the continuous supination. The speed at which the continuous movement is carried out, and the amount of vertical loading, have only very slight effects. We could discern clearly that the visco-elastic properties of the tissues caused a difference in the paths of the supinating and pronating movements, the hysteresis effect.

During this investigation we discovered by coincidence that the input moment to be applied to the tibia to supinate the tarsus by rotation varied greatly from one individual to another. The same was true for the vertical tibial translation during supination. This finding that differently shaped feet also differ in biomechanical behaviour prompted an extra line of investigation with which we attempted to quantify this biomechanical behaviour by measuring moments and recording vertical tibial translations, combining the two and relating them to a new roentgenological classification of the tarsus. The traditional specification criteria were found to be unsuitable.

A strong correlation was found to exist between moment (M) and vertical tibial translation (S). Another strong correlation was observed between M and S and the tarsal index i_t, calculated with the equation $i_t = 100 \times \frac{P_C}{L_T} \times tg\epsilon_{TC}$. The index is determined entirely by the relative positions of the talus and calcaneus.

Part 2 (Chapter 3) comprises a study of *fresh amputation material*, as a step in the direction of live material.

Two amputated lower legs were analyzed *kinematically*, according to Van Langelaan and Spoor's photogrammetric method; *dynamically*, by measuring moments (M) and recording vertical tibial translations (S); and finally by comparing the *stepwise* and *continuous* supination and pronation of one specimen (♀ 29). Each method was applied both to the completely intact specimen and to the dissected osteo-ligamentous preparations.

As *kinematic* parameters we used the helical axes. We calculated both the relative axes (of the movements of one tarsal bone in relation to another) and the absolute discrete axes (of the tarsal bones in relation to the fixed reference system in the test setup) of supination from 0° – 30° and return. This included both the movement as a whole and steps of 10°.

We found that the patterns of the bundles of axes of the supinatory and return movements are comparable; and that the patterns for different loads and different phases of preparation of the specimen (intact and osteo-ligamentous) are also comparable.

The differences between corresponding phases (steps of 10° or the total 0° – 30° movement) were smaller in specimen ♀ 29 than in specimen ♂ 14.

This observation is not easily explained but three factors may be important: tarsal indexes i_t were very different, 8 and 25, respectively. The amplitudes of the movements of the tarsal bones in the boy's foot were larger than those in the woman's foot (difference in 'acceleration' between 15° and 25° on the tibial translation curve, tg 70° and tg 40°, respectively). At 30°, the return point, supination of the woman's tarsus was complete whereas that of the boy's was far from complete. Finally, the play in the test setup may have increased during the 4 years that separated the two experiments.

The *dynamic* parameters (M and S) served as an extra aid in studying the effect of the stage of preparation of the specimen. There was very little difference between the pre- and post-dissection findings regarding both the moment registration (M) and the vertical tibial translation (S). This showed clearly that the removal of the skin, the subcutaneous layer and the muscles caused no changes in the pattern of the movement.

A comparison of the stepwise movement from 0° to 30° and return with the same movement carried out continuous, both before and after dissection into osteo-ligamentous preparations, showed once again that, as in the fixed osteo-ligamentous material, there were hardly any differences to be observed between the intact specimen and the same specimen after removal of skin and muscles.

The results of the first two parts of this investigation demonstrate that the supination and *the return to the starting position* take place according to a particular fixed pattern which is little influenced by the speed at which the movement is carried out. The method of fixation or the stage of dissection appear to make little difference, provided the osteo-ligamentous apparatus remains intact.

Part 3 of this investigation (Chapter 4) focuses on the study of live legs, for which we could make use of the results of the first two parts.

In a test setup similar to that of Chapters 2 and 3, but including a voltmeter, we matched as accurately as possible a number of exorotation positions (0°, 10°, 20° and 30°) of the tibias of 8 healthy volunteers with the corresponding supination positions of the tarsus, selected from a 70 mm X-ray film in two projections. The matching sets were placed in a mask and compared.

From this it was possible to calculate the tarsal indexes and to measure the vertical tibial translations.

Comparing test subject 7 with the amputation specimen ♀ 29, we found striking resemblance. The similarities of the positions and shapes of the tarsal bones in the comparable positions showed clearly that the pattern of the movement of the tarsus in vivo does not differ from that of a dead specimen.

An important conclusion of this study is that every foot is unique. Differences in shape affect strongly the biomechanical behaviour of the tarsus and in consequence also higher articular systems. It should be possible to find out with retrospective studies if persons with low tarsal indexes (biomechanically 'cavus' feet) sustain lesions of the lateral ligaments of the ankle more readily than those with higher indexes (biomechanically 'flat' feet). The tarsal index can be determined from one standardized mediolateral X-ray of the weight-bearing foot.

In the final chapter, (Chapter 5) we reflect on the relative value of the study and consider in what direction we shall have to work and think to make the tarsal index clinically relevant.

Samenvatting

Het doel van het onderzoek was de bevindingen van Huson, Ambagtsheer en Van Langelaan te toetsen aan levende benen. Ons werk kan als een directe voortzetting van de theorie van Van Langelaan worden beschouwd.

Het onderzoek was in drie hoofddelen opgebouwd:

In deel 1 (Hoofdstuk 2), wordt de stap-voor-stap uitgevoerde supinatie van de voetwortel van *gefixeerde skeletbandenpreparaten* (de door Van Langelaan onderzochte wijze van supineren) vergeleken met de continue supinatie.

We constateerden dat de stap-voor-stap uitgevoerde supinatie van gefixeerde skeletbandenpreparaten weinig verschilde van de continue supinatie. Ook de invloed van de snelheid waarmee de continue beweging werd uitgevoerd bleek gering te zijn. Dit gold eveneens voor het effect van de grootte van de verticale belasting. We vonden dat de visco-elastische eigenschappen van de weefsels verschillen in de bewegingsbanen veroorzaakten tussen de heen- en teruggaande beweging: het "hysteresis effect".

Bij toeval werd ontdekt dat het invoerend moment op de tibia (om via rotatie de tarsus te supineren) interindividueel sterk verschilde en leek samen te hangen met de vorm van de voet. Ditzelfde gold voor de verticale verplaatsing van de tibia tijdens de supinatie. De bevinding, dat verschillend gevormde voeten zich biomechanisch verschillend gedragen, leidde tot een extra onderzoekslijn. Hierin werd getracht dit biomechanisch gedrag te kwantificeren middels momentmetingen en verticale tibiaverplaatsingsregistraties.

Beiden werden aan elkaar en aan een nieuwe röntgenologische indeling van de tarsus gerelateerd. Deze nieuwe indeling was noodzakelijk omdat de gebruikelijke indelingscriteria niet toepasbaar waren.

Er bleek een sterk verband te bestaan tussen momentgedrag (M) en de verticale tibiaverplaatsing (S). Eveneens was er een sterke correlatie tussen M en S en de tarsaalindex i_t, die in de nieuwe formule

$i_t = 100 \times \frac{P_C}{L_T} \times \text{tg}\, \epsilon_{TC}$, geheel wordt bepaald door de positie van talus en calcaneus t.o.v. elkaar.

In hoofdstuk 3 wordt het 2e deel van de studie beschreven. Dit deel gaat over de analyse van 2 door amputatie verkregen onderbenen als volgende stap in de richting van levende benen.

Deze geamputeerde onderbenen werden *kinematisch* onderzocht volgens de fotogrammetrische methode van Van Langelaan en Spoor: bij 50N en 340N axiale belasting en na verwijderen van huid en spieren bij 340N; *dynamisch*, d.m.v. momentmetingen (M) en verticale tibiaverplaatsingsregistratie (S); en tenslotte door vergelijking van de *stapsgewijze* en *continue* supinatie en pronatie van één preparaat (♀ 29).

Als *kinematische* parameters werden schroevingsassen gebruikt. Zowel relatieve assen (van het ene os tarsale ten opzichte van het andere) als absolute discrete assen (van de tarsalia ten opzichte van het vaste assenstelsel in de proefopstelling) werden berekend van de supinatiebeweging van 0° – 30° en van de teruggaande beweging van 30° – 0°, voor de totale beweging en in stapjes van 10°. We vonden dat de patronen van de assenbundels vergelijkbaar zijn voor de heen- en teruggaande beweging en dat de patronen eveneens vergelijkbaar zijn voor de verschillende belastingen en fasen van bewerking van het preparaat.

De onderlinge verschillen van de overeenkomstige fasen (stappen van 10° of de totale beweging 0° – 30°) waren bij het preparaat ♀ 29 kleiner dan bij preparaat ♂ 14.

Een verklaring hiervoor is niet eenvoudig te geven maar mogelijk zijn een 3-tal factoren belangrijk: de tarsaalindices verschillen sterk, resp. 8 (♀ 29) en 25 (♂ 14). De bewegingsuitslagen van de tarsalia in de jongensvoet waren groter dan die in de vrouwenvoet, (verschil in "versnelling" tussen 15° en 25° op de tibiaverplaatsingscurve, tg 70° resp. tg 40°). Bij 30°, het omkeerpunt, was de supinatie van de vrouw voltooid, bij de jongen echter nog in volle gang. Tenslotte toename van enige speling in de proefopstelling in de 4 jaar die tussen beide experimenten lag.

De *dynamische* parameters (M en S) waren een extra hulpmiddel bij de bestudering van de invloed van het bewerkingsstadium van het preparaat. Voor zowel de momentregistratie (M) als de verticale tibiaverplaatsing (S) gold, dat ze een sterke overeenkomst vertoonden. Het maakte ons duidelijk dat het ontdoen van huid, subcutis en spieren geen verandering in het patroon van de beweging teweeg bracht.

Een vergelijking van de discontinu uitgevoerde beweging van 0° – 30° en weer terug van 30° – 0° met dezelfde, maar continu uitgevoerde beweging, voor en na bewerking tot skeletbandenpreparaat maakte ons duidelijk, dat ook hier, net als in het gefixeerde skeletbandmateriaal, nauwelijks verschillen konden worden waargenomen tussen het intacte preparaat en hetzelfde preparaat na verwijderen van huid en spieren.

Uit de hoofdstukken 2 en 3 blijkt dat de supinatie en terugkeer naar de uitgangspositie volgens een bepaald vaststaand patroon verloopt en weinig afhankelijk is van de snelheid waarmee de beweging wordt uitgevoerd. Ook de wijze van fixatie en de bewerkingsfase lijken weinig uit te maken, mits het osteoligamentaire apparaat intact blijft.

In deel 3 (Hoofdstuk 4) worden levende benen bestudeerd. In een vergelijkbare proefopstelling als in de hoofdstukken 2 en 3 worden met behulp van een voltmeter zo nauwkeurig mogelijk de bij een bepaalde exorotatiestand van de tibia (0°, 10°, 20° en 30°) van 8 gezonde proefpersonen, de bijpassende supinatiestanden van de tarsus in 2 richtingen uit een 70 mm film geselecteerd, in een masker geplaatst en vervolgens met elkaar vergeleken. Het bleek mogelijk hieruit de tarsale indices te berekenen en de verticale tibiaverplaatsingen te meten.

Uit de vergelijking van proefpersoon 7 met het amputatiepreparaat ♀ 29 blijkt een zeer opvallende gelijkenis. De overeenkomsten van de posities en vorm van de tarsalia van de vergelijkbare standen maakten duidelijk dat het bewegingspatroon van de tarsus in vivo op de door ons onderzochte manier niet verschilt van dat van een dood preparaat.

Maar wat ons tot slot vooral duidelijk is geworden is, dat iedere voet uniek is en de onderlinge vormverschillen grote invloed hebben op het biomechanisch gedrag van de tarsus en dus op dat van de hoger gelegen gewrichtsketen. Uit retrospectief onderzoek moet kunnen blijken, of mensen met lage tarsale indices (biomechanisch "holle" voeten) eerder een laterale enkelbandlaesie krijgen dan mensen met hoge indices (biomechanisch "platte" voeten). Via één gestandaardiseerde mediolaterale belaste voetopname kan deze index worden bepaald.

In het laatste hoofdstuk (5) geven we een korte terugblik op de studie en overdenken in welke richting gedacht en gewerkt moet worden om de tarsale index ook klinisch toe te passen.

REFERENCES

Ambagtsheer, J.B.T. (1978) The function of the muscles of the lower leg in relation to movements of the tarsus. Thesis, University of Leiden. Acta Orthop. Scand. Suppl. no. 178.

Barnett, C.H. and Napier, J.R. (1952) The axis of rotation of the ankle joint in man. J. Anat. (Lond.) 86, 1.

Barnett, C.H., Davies, D.V. and McConaill, M.A. (1961) Synovial joints. London, Longmans.

Benink, R.J. (1977) A roentgenographic study of the continuous motion of the tarsal bones. J. Anat. (Lond.) 124, 252.

Benink, R.J. (1978) A localizing device for X-ray sources. Radiology 128 (2), 508 – 509.

Benink, R.J. (1982) Biomechanical behaviour of the human tarsus related with a new radiological index. Biomechanics: Principles and applications. Developments in Biomechanics 1, 191 – 197.

Benink, R.J. and Huson, A. (1977) Een röntgenologische studie van de continue beweging van de tarsale beenstukken. Ned. T. Geneesk. 121, 652.

Benink, R.J. and Huson, A. (1977) A roentgenographic study of the continuous motions of the tarsal bones. Acta Morphol. Neerl.-Scand. 15, 321.

Benink, R.J. and Spoor, C.W. (1978) Bewegingsonderzoek van de supinatoire vervorming van de tarsus. Ned. T. Geneesk. 122, 455.

Close, J.R. and Inman, V.T. (1953) The action of the subtaler joint. Prosth. Dev. Res. Proj., Univ. Calif., Berkeley, Ser. II, Issue 24, 1 – 19.

Elftman, H. (1960) The transverse tarsal joint and its control. Clin. Orthop. 16, 41 – 45.

Hicks, J.H. (1953) The mechanics of the foot I. The joints. J. Anat. (Lond.) 87, 345 – 357.

Hicks, J.H. (1954) The mechanics of the foot II. The plantar aponeurosis and the arch. J. Anat. (Lond.) 88, 25 – 31.

Hicks, J.H. (1955) The mechanics of the foot III. The foot as a support. Acta Anat. 25, 34 – 45.

Huson, A. (1961) Een ontleedkundig-functioneel onderzoek van de voetwortel. Thesis, University of Leiden, Luctor et Emergo.

Huson, A. (1966) L'interdépendance des mouvements du tarse. Extrait du Bulletin de l'Ass. des Anatomistes. C.R. Ass. Anat. 51, 509 – 514.

Huson, A. (1973) La chaine cinématique fermée. Bulletin de l'Association des Anatomistes, 57, 887 – 894.

Huson, A. (1982) Perspectives in human-joint kinematics. Biomechanics: Principles and applications. Developments in Biomechanics, 1, 31 – 46.

Huson, A., Benink, R.J., Langelaan, E.J. van and Spoor, C.W. (1977) Die Bewegungsart der tarsalen Gelenke. Proc. 4e Europ. Anat. Congr. Basle. Acta Anat. 99, 279.

Inman, V.T. (1976) The joints of the ankle. The Williams and Wilkins Company. Baltimore.

Jones, R.L. (1945) The functional significance of the declination of the axis of the subtalar joint. Anat. Rec. 93, 151 – 159.

Langelaan, E.J. van (1983) A kinematical analysis of the tarsal joints. Thesis, University of Leiden. Acta Orthop. Scand. Suppl. no. 204, vol. 54.

Langelaan, E.J., van and Spoor, C.W. (1975) Een kinematische analyse van de tarsus. Ned. T. Geneesk. 37, 1437.

Langelaan, E.J. van, Spoor, C.W. and Huson, A. (1974) A kinematical analysis of the tarsal joints. J. Anatomy 117, 650.

Lelièvre, J. (1961) Pathologie du pied, Masson et Cie, Editeurs, Paris.

Manter, J.T. (1941) Movements of the subtalar and transverse tarsal joints. Anat. Rec. 80, 4, 397 – 410.

Sachers, W. (1949) Die Form des Fersenbeines und ihre Beziehung zu den Fußtypen. Arch. Orthop. Unfallchir. 44, 226 – 234.

Sammarco, G.J., Burstein, A.H. and Frankel, V.H. (1973) Biomechanics of the ankle: A kinematic study. Orthop. Clin. North Am. 4, 75 – 96.

Schmidt, H.M. (1981) Die Artikulationsflächen der menschlichen Sprunggelenke. Advances in anatomy, embryology and cell biology 66.

Spoor, C.W. (1984) Explanation, verification and application of helical-axis error propagation formulas. Human Movement Science 3, 95 – 117.

Stewart, S.F. (1970) Human gait and the human foot: An ethnological study of flat foot. Clinical Orthopedics and Related Research 70, 111 – 123.

Vogel, P.L. de, (1970) Enige functioneel-anatomische aspecten van het bovenste spronggewricht. Thesis, University of Leiden, Drukkerij Groenendijk. Rotterdam.

APPENDIX

Contents

List of abbreviations and symbols used

App.	: appendix
L	: left
R	: right
rad	: radial
Nm	: newton meter
N	: newton
I	: vertical load of 50 N on the driving shaft
II	: vertical load of 160 N on the driving shaft
III	: vertical load of 340 N on the driving shaft
X	: edge of brass rod in X direction
Y	: edge of brass rod in Y direction
Z	: edge of brass rod in Z direction
d	: distance in mm from pellet centre to centre-line of the pellet trajectory
•	: symbol for two experiments performed separately (just ♂ 14, 340N, return movement)
*	: marker or marker trajectory not clearly visible
i_s	: interrupted (stepwise) supination
i_r	: interrupted (stepwise) return to starting position
u_s5	: uninterrupted (continuous) supination in 5 seconds
u_s8	: uninterrupted (continuous) supination in 8 seconds
u_s60	: uninterrupted (continuous) supination in 60 seconds
u_r5	: uninterrupted (continuous) return to starting position in 5 seconds
u_r60	: uninterrupted (continuous) return to starting position in 60 seconds
i_t	: tarsal index
ϵ_{TC}	: talo-calcaneal inclination angle in the longitudinal direction of the foot in degrees
P_C	: overprojection of the talar head and the calcaneus in mm
L_T	: length of talus in mm
$\overline{i_t}$	: mean tarsal index
SD	: standard deviation
tg	: tangent
M	: exorotating moment (in Nm) on the driving shaft required to rotate the tibia
S	: vertical tibial translation in mm
H.A.	: helical axis
π	: angle between the projection of the helical axis on the basal plane (XY), and the sagittal plane (XZ) (deviation angle)
φ	: angle between the helical axis and the basal plane (XY) (inclination angle)
t	: translation along the helical axis
α	: rotation angle (in degrees) round the helical axis
γ	: angle (in degrees) between two helical axes
β	: deviation angle (in degrees) of the directional vector
ϱ	: square root of the mean square of the distances between the pellets and the rotation axis through the centre of gravity in mm
σ	: standard deviation per co-ordinate in mm
N_i	: vertical load in newtons on the 'intact' specimen
N_o	: vertical load in newtons on the specimen after removal of skin and muscles
TACA	: talo-calcaneal joint
TANA	: talo-navicular joint
CUNA	: cuboideo-navicular joint
NACA	: naviculo-calcaneal junction
CUCA	: cuboideo-calcaneal joint
PVC	: polyvinylchloride
kV	: kilovolt
mA	: milliampere
L_f	: foot length (mm)

H_{tn} : height of navicular tuberosity (mm)
H_{lm} : height of lateral malleolus (mm)
H_{mm} : height of medial malleolus (mm)
M_s : shoe size

Protocol/measuring procedure.
Experiments to compare stepwise and continuous movements under different loads at different speeds, and to determine the rotating moment and the tibial translation.

step number	time scale (min.)	nr of X-rays	
			A. Adjustment
1	0		Mount the yoke with 160N (II) on the vertical shaft. Assess the sag on the vertical translation meter. Mean sag after approx 7 min: 0.01 mm in 14 seconds.
			The position which the tarsus itself assumes under the influence of the vertical load is regarded as the starting position of the tibia.
3			The adjustable base ring with graduation is fixed at 0°.
			B. Recording of moment and tibial translation
4	5		Read simultaneously the *moment magnitude* and *vertical tibial translation* as functions of the rotation angle from 0° to 30° and from 30° to 0°, in steps of 5°.
			C. Recording of marker positions of the stepwise movement
6	11	1[a]	Place envelopes with roentgen films in the cassettes, apply lead numbers.
7			Exposure the 0° position in both directions *simultaneously*. Distance 106 cm, exposure: 3 sec., 90 kV and 33 mA.
8	12		Remove films, insert new ones, change lead numbers.
			Four exposures are now superimposed on each other, each exposure being made with both roentgen tubes simultaneously.
9		2	0° position 1 sec., 86 kV, 33 mA
10		2	10° exorotation position 1 sec., 86 kV, 33 mA
11		2	20° exorotation position 1 sec., 86 kV, 33 mA
12		2	30° exorotation position 1 sec., 86 kV, 33 mA
13	15		Change X-ray films and lead numbers.
14		3[b]	30° position, exposure: 3 sec., 90 kV, 33 mA
15	17		Change X-ray films and lead numbers.
			Four exposures are now superimposed on each other, each exposure being made with both roentgen tubes simultaneously.

[a] X-ray 1 serves for the determination of the starting position of the markers and for the determination of the tarsal index.
[b] X-ray 3 serves for the determination of the position of the markers after supination.
[c] X-ray 5 serves for the determination of the marker position after return to the starting position.

step number	time scale (min.)	nr of X-rays	
16		4	30° exorotation position 1 sec., 86 kV, 33 mA
17		4	20° exorotation position 1 sec., 86 kV, 33 mA
18		4	10° exorotation position 1 sec., 86 kV, 33 mA
19		4	0° position 1 sec., 86 kV, 33 mA
			D. Recording of marker pellets paths of the continuous movement
20	20		Change X-rays and lead numbers.
21		5[c]	0° position, exposure: 3 sec., 90 kV, 33 mA
22	22		Change X-rays and lead numbers.
23			Adjust the electric motor for the rapid movement (6°/sec) from 0° to 30° by means of the microswitches.
24		6	U_s5 II; exposure: 5 sec., 86 kV, 33 mA in both directions
25			0.4 sec., 86 kV, 33 mA pre- and after-exposure
26	26		Change X-rays and lead numbers and for the rapid movement (6°/sec) from 30° – 0°.
27		7	U_r5 II; exposure: 5 sec., 86 kV, 33 mA in both directions
28			0.4 sec., 86 kV, 33 mA pre- and after-exposure
29	28		Change X-rays and lead numbers.
30			Adjust the electric motor to the slow movement (0.5°/sec) from 0° to 30° by means of the microswitches.
31			U_s60 II; 0.4 sec., 86 kV, 33 mA pre-exposure, then expose every 5 seconds for 0.4 sec., 86 kV, 33 mA with after-exposure for 0.4 sec., 86 kV, 33 mA.
34	34	9	Change X-rays and lead numbers, then for the slow movement (0.5°/sec) from 30° to 0°.
35			U_r60 II; pre-exposure for 0.4 sec., 86 kV
36			33 mA, then exposures every 5 seconds for 0.4 sec., 86 kV, 33 mA and
37			after-exposure for 0.4 sec., 86 kV, 33 mA.
38	37		Remove X-rays.

TABLE A.1.

Spec. nr 548 tarsal index 10		i_s II versus u_s5 II								i_s II versus u_s60 II							
		horizontal				dorso-plantar				horizontal				dorso-plantar			
bone	pellet nr	degrees ext. rot.				degrees ext. rot.				degrees ext. rot.				degrees ext. rot.			
		0	10	20	30	0	10	20	30	0	10	20	30	0	10	20	30
tibia	1	0	0	0	0	0	−0.2	−0.1	0	0	0	−0.1	0	−0.1	−0.3	−0.2	−0.2
	1	0	+0.1	+0.1	0	0	0	0	0	0	0	0	0	+0.1	0	0	+0.1
talus	2	0	+0.1	+0.1	0	0	0	−0.1	0	0	0	+0.1	0	+0.1	+0.1	0	0
	3	0	0	0	0	0	+0.2	0	0	0	0	0	0	−0.2	0	−0.2	−0.2
	1	+0.1	−0.1	0	0	0	0	0	+0.1	0	−0.1	+0.1	+0.2	0	−0.1	−0.1	0
calcaneus	2	+0.1	+0.1	0	0	0	0	0	0	+0.1	+0.1	0	0	0	0	−0.1	0
	3	0	0	0	0	+0.1	+0.1	0	0	0	0	0	0	0	+0.1	−0.1	0
	1	0	0	0	0	0	+0.2	+0.1	0	0	−0.2	0	0	0	+0.1	+0.1	0
navicular	2	0	0	0	0	0	0	0	0	0	0	−0.1	0	0	0	0	0
	3	+0.1	0	0	0	0	0	0	0	0	0	0	0	0	0	0	0
	1	0	0	−0.1	−0.1	0	0	0	0	0	+0.1	−0.1	0	0	0	0	0
cuboid	2	0	0	0	0	0	0	0	0	0	0	0	0	0	0	+0.1	0
	3	0	+0.1	0	0	−0.1	0	0	−0.1	0	0	+0.1	0	0	0	0	−0.1

TABLE A.2.

Spec. nr 506 tarsal index 13		i_sII versus u_s5 II								i_sII versus u_s60 II							
		horizontal				dorso-plantar				horizontal				dorso-plantar			
bone	pellet nr	degrees ext. rot.				degrees ext. rot.				degrees ext. rot.				degrees ext. rot.			
		0	10	20	30	0	10	20	30	0	10	20	30	0	10	20	30
tibia	1	−0.1	0	0	0	−0.2	−0.1	−0.1	−0.1	−0.1	−0.1	0	0	−0.2	−0.2	−0.1	0
	1	0	0	−0.1	−0.1	0	0	0	0	−0.1	−0.1	0	0	0	−0.1	0	0
talus	2	0	0	−0.1	−0.1	*	*	*	*	0	0	0	0	*	*	*	*
	3	0	0	0	0	0	0	0	0	−0.1	−0.1	0	0	0	0	−0.1	0
	1	0	−0.2	−0.1	0	0	0	0	0	+0.2	+0.2	+0.1	0	0	0	0	0
calcaneus	2	0	0	0	0	0	0	0	0	0	0	0	0	0	0	0	0
	3	*	*	*	*	*	*	*	*	*	*	*	*	*	*	*	*
	1	0	0	−0.1	0	0	+0.1	+0.1	0	−0.2	−0.1	0	0	0	+0.1	0	−0.1
navicular	2	0	0	0	+0.1	0	0	0	0	−0.2	−0.1	+0.2	+0.2	0	0	−0.1	−0.1
	3	0	0	0	0	0	0	0	0	0	0	+0.1	*	0	0	−0.1	−0.2
	1	0	0	0	0	−0.1	−0.1	−0.1	0	0	0	+0.1	0	0	0	0	0
cuboid	2	0	0	0	0	0	0	0	0	−0.1	0	+0.1	0	0	0	0	0
	3	0	0	0	0	−0.1	−0.1	−0.1	−0.1	0	0	+0.1	0	0	0	−0.1	−0.2

TABLE A.3.

Spec. nr 349 tarsal index 10		i_s II versus u_s5 II								i_s II versus u_s60 II							
		horizontal				dorso-plantar				horizontal				dorso-plantar			
bone	pellet nr	degrees ext. rot.				degrees ext. rot.				degrees ext. rot.				degrees ext. rot.			
		0	10	20	30	0	10	20	30	0	10	20	30	0	10	20	30
tibia	1	0	0	0	0	−0.2	−0.1	−0.1	0	0	0	−0.1	0	−0.2	−0.2	−0.1	0
	1	−0.1	−0.1	−0.1	−0.1	*	*	*	*	0	0	0	0	*	*	*	*
talus	2	0	0	0	−0.1	0	0	0	0	0	0	−0.1	−0.2	0	−0.1	−0.1	0
	3	0	0	0	0	0	0	0	+0.1	0	−0.2	0	0	+0.1	0	−0.1	0
	1	0	−0.2	−0.1	0	0	0	0	+0.2	−0.1	−0.3	−0.2	0	0	0	0	0
calcaneus	2	0	0	0	0	0	0	0	*	−0.1	−0.1	−0.1	0	0	0	0	*
	3	0	0	0	0	0	0	0	+0.1	0	0	0	−0.1	0	0	0	+0.1
	1	0	0	−0.1	0	0	+0.1	+0.1	+0.2	0	−0.1	0	+0.1	+0.2	+0.2	+0.1	0
navicular	2	0	0	−0.1	−0.1	0	+0.1	+0.1	+0.2	0	0	0	−0.1	0	+0.1	+0.1	0
	3	+0.1	0	0	0	+0.1	0	*	*	0	0	0	0	+0.1	+0.1	*	*
	1	0	0	0	0	0	0	0	0	−0.1	0	+0.1	+0.1	0	−0.1	0	0
cuboid	2	0	+0.2	+0.1	0	0	0	0	0	−0.1	+0.1	+0.2	0	0	0	0	0
	3	0	0	0	0	0	0	0	0	0	+0.1	+0.1	0	0	0	0	0

TABLE A.4.

Spec. nr 342 tarsal index 11		i_s II versus u_s 5 II								i_s II versus u_s 60 II							
		horizontal				dorso-plantar				horizontal				dorso-plantar			
bone	pellet nr	degrees ext. rot.				degrees ext. rot.				degrees ext. rot.				degrees ext. rot.			
		0	10	20	30	0	10	20	30	0	10	20	30	0	10	20	30
tibia	1	−0.1	−0.1	0	0	−0.2	−0.3	−0.1	−0.1	−0.2	−0.3	−0.2	−0.1	−0.3	−0.2	−0.1	−0.1
	1	−0.1	+0.1	+0.1	0	0	0	+0.1	*	0	+0.2	+0.2	+0.3	0	0	+0.2	*
talus	2	−0.1	0	0	0	0	0	+0.1	0	+0.1	+0.3	+0.2	+0.1	0	+0.1	+0.2	+0.1
	3	0	+0.1	0	0	0	0	0	*	0	+0.1	+0.2	+0.2	0	+0.1	+0.1	*
	1	0	+0.1	0	0	0	−0.1	0	−0.1	0	+0.1	−0.2	0	0	0	0	−0.2
calcaneus	2	0	0	0	−0.1	0	−0.1	−0.1	0	0	+0.1	+0.1	+0.1	0	−0.1	−0.1	0
	3	0	0	0	−0.1	+0.1	0	+0.1	*	−0.1	+0.1	0	0	+0.1	0	+0.1	*
	1	0	0	+0.1	0	+0.1	+0.1	0	0	0	+0.1	+0.1	+0.2	+0.1	+0.1	+0.1	0
navicular	2	0	0	+0.1	0	0	0	+0.1	*	0	+0.2	+0.2	+0.2	0	0	+0.1	*
	3	0	0	0	0	0	−0.1	+0.1	+0.2	0	0	+0.1	+0.1	0	0	+0.1	+0.2
	1	−0.1	0	0	−0.2	0	0	0	−0.1	−0.1	+0.2	+0.2	+0.1	0	0	0	−0.1
cuboid	2	0	0	0	0	0	−0.1	0	0	0	+0.1	+0.1	+0.1	0	−0.1	0	0
	3	0	0	0	0	0	0	+0.1	+0.2	0	+0.1	+0.1	+0.1	0	0	+0.1	+0.2

TABLE A.5.

Spec. nr 492 tarsal index 13		i_sII versus u_s5 II								i_sII versus u_s60 II							
		horizontal				dorso-plantar				horizontal				dorso-plantar			
bone	pellet nr	degrees ext. rot.				degrees ext. rot.				degrees ext. rot.				degrees ext. rot.			
		0	10	20	30	0	10	20	30	0	10	20	30	0	10	20	30
tibia	1	0	0	−0.1	−0.2	0	0	+0.1	+0.1	0	0	−0.1	−0.2	0	+0.1	+0.2	0
	1	−0.1	−0.1	0	0	0	0	+0.1	0	−0.1	0	0	0	0	+0.1	0	0
talus	2	0	0	0	+0.1	0	0	0	0	0	0	0	+0.1	0	+0.1	0	0
	3	0	0	0	0	0	*	*	*	0	0	0	0	0	*	*	*
	1	+0.1	+0.1	0	−0.1	+0.1	+0.1	0	0	+0.1	+0.1	0	0	+0.1	0	0	0
calcaneus	2	+0.1	0	0	0	0	0	0	0	0	0	0	0	0	0	0	0
	3	0	0	0	0	0	0	+0.1	0	0	0	0	0	0	0	+0.1	+0.1
	1	−0.1	0	0	0	0	0	+0.1	+0.1	−0.1	0	0	0	0	0	+0.1	+0.2
navicular	2	0	0	0	0	0	0	0	+0.1	−0.1	0	0	−0.1	0	0	0	+0.2
	3	0	0	0	0	0	0	+0.1	+0.1	0	0	0	0	0	+0.1	+0.1	+0.1
	1	0	0	0	0	0	0	0	+0.1	0	0	0	0	0	0	0	+0.1
cuboid	2	+0.1	+0.1	0	0	0	+0.1	0	0	+0.1	+0.1	0	0	0	+0.1	0	0
	3	0	0	0	0	0	0	0	0	0	0	0	0	0	0	0	0

TABLE A.6.

Spec. nr 511 tarsal index 23		i_sII versus u_s5 II								i_sII versus u_s60 II							
		horizontal				dorso-plantar				horizontal				dorso-plantar			
bone	pellet nr	degrees ext. rot.				degrees ext. rot.				degrees ext. rot.				degrees ext. rot.			
		0	10	20	30	0	10	20	30	0	10	20	30	0	10	20	30
tibia	1	+0.1	0	0	0	−0.1	−0.2	−0.2	−0.2	−0.1	0	+0.1	+0.2	−0.2	−0.2	−0.1	−0.1
	1	0	+0.1	0	−0.1	0	0	+0.1	+0.1	0	0	−0.1	−0.2	−0.1	0	0	0
talus	2	0	+0.1	+0.1	0	0	0	+0.1	0	+0,1	0	0	−0.1	−0.1	0	0	−0.1
	3	0	0	0	0	0	0	0	0	0	−0.1	−0.1	−0.1	0	−0.1	0	0
	1	+0.1	+0.1	+0.1	0	0	0	+0.1	+0.1	+0.1	−0.1	−0.1	−0.2	0	0	0	0
calcaneus	2	0	0	0	0	0	0	0	−0.1	0	0	0	0	−0.1	0	0	0
	3	0	+0.1	0	0	0	0	0	0	0	0	+0.1	+0.2	0	0	0	0
	1	0	0	+0.1	+0.1	0	+0.1	+0.1	0	0	0	−0.1	−0.2	+0.1	+0.2	0	0
navicular	2	+0.1	0	0	*	−0.1	0	+0.1	0	0	−0.1	−0.1	*	0	+0.1	0	0
	3	0	+0.1	*	*	−0.1	0	0	0	0	+0.1	*	*	0	+0.1	0	−0.1
	1	0	+0.1	+0.1	0	−0.1	−0.1	−0.1	−0.2	+0.1	+0.2	+0.2	+0.3	−0.1	−0.2	−0.3	−0.4
cuboid	2	+0.1	+0.1	0	0	0	−0.1	0	−0.1	0	+0.1	+0.1	+0.2	−0.1	−0.2	−0.2	−0.3
	3	+0.1	0	0	0	−0.1	−0.1	−0.1	−0.2	+0.1	+0.2	+0.2	+0.3	−0.1	−0.2	−0.1	−0.3

TABLE A.7.

Spec. nr 548 tarsal index 10		i_rII versus u_r5 II								i_rII versus u_r60 II							
		horizontal				dorso-plantar				horizontal				dorso-plantar			
bone	pellet nr	degrees ext. rot.				degrees ext. rot.				degrees ext. rot.				degrees ext. rot.			
		30	20	10	0	30	20	10	0	30	20	10	0	30	20	10	0
tibia	1	0	−0.1	−0.2	0	0	0	−0.1	−0.2	0	0	−0.1	0	−0.1	0	−0.1	−0.1
	1	0	0	−0.1	0	0	0	0	0	0	0	0	0	0	0	0	0
talus	2	0	0	0	0	0	0	0	0	0	0	0	0	0	0	0	0
	3	0	0	−0.1	−0.2	0	0	0	0	0	0	0	0	0	0	0	0
	1	0	0	0	0	0	0	0	0	+0.1	+0.1	0	0	0	0	0	0
calcaneus	2	0	0	0	0	0	0	0	0	0	0	0	0	0	0	0	0
	3	0	−0.1	0	0	0	+0.1	0	0	0	0	0	0	0	0	0	0
	1	0	−0.1	0	0	0	0	0	0	0	0	0	0	0	0	0	0
navicular	2	0	0	−0.1	0	0	+0.1	0	0	0	0	+0.1	0	0	0	+0.1	0
	3	0	0	0	0	0	0	0	0	0	0	0	0	0	0	0	0
	1	0	0	0	0	0	−0.1	0	0	0	0	0	0	0	0	0	0
cuboid	2	0	0	0	0	0	−0.1	0	0	0	0	0	0	0	0	0	0
	3	0	0	0	0	0	0	0	0	0	0	0	0	0	0	0	0

TABLE A.8.

Spec. nr 548 tarsal index 10		i_s III versus u_s5 III								i_s III versus u_s60 III							
		horizontal				dorso-plantar				horizontal				dorso-plantar			
bone	pellet nr	degrees ext. rot.				degrees ext. rot.				degrees ext. rot.				degrees ext. rot.			
		0	10	20	30	0	10	20	30	0	10	20	30	0	10	20	30
tibia	1	0	0	0	0	0	−0.2	−0.1	0	0	0	0	0	0	−0.2	−0.1	−0.1
	1	0	0	+0.1	0	0	−0.1	0	0	0	+0.1	0	0	+0.1	0	0	0
talus	2	0	−0.1	0	0	0	0	−0.1	0	0	0	0	0	+0.1	+0.1	0	0
	3	−0.1	−0.1	−0.1	−0.1	0	0	0	0	0	0	0	0	0	0	0	0
	1	0	0	−0.1	0	0	0	0	0	0	−0.1	−0.1	0	0	0	0	0
calcaneus	2	0	0	0	0	+0.1	0	0	0	0	0	0	0	0	0	0	0
	3	0	+0.1	0	0	+0.1	+0.1	0	0	0	0	−0.1	0	0	0	0	0
	1	0	−0.1	−0.1	0	0	+0.1	+0.1	0	0	−0.1	0	0	0	0	0	0
navicular	2	0	0	0	0	0	0	+0.1	0	0	0	0	0	0	0	0	0
	3	0	0	0	0	−0.1	0	0	0	0	0	0	0	0	0	0	0
	1	0	0	0	0	0	−0.1	0	0	0	0	0	0	0	0	−0.1	0
cuboid	2	−0.1	−0.2	−0.1	−0.1	0	−0.1	0	0	0	−0.1	0	0	0	0	−0.1	0
	3	0	0	0	0	0	−0.1	0	0	0	0	0	0	0	0	−0.1	0

TABLE A.9.

Spec. nr 548 tarsal index 10		i_rIII versus u_r5 III								i_rIII versus u_r60 III							
		horizontal				dorso-plantar				horizontal				dorso-plantar			
bone	pellet nr	degrees ext. rot.				degrees ext. rot.				degrees ext. rot.				degrees ext. rot.			
		30	20	10	0	30	20	10	0	30	20	10	0	30	20	10	0
tibia	1	0	0	−0.1	−0.1	0	0	0	0	−0.2	−0.1	0	0	0	0	0	0
	1	0	0	0	0	0	0	0	0	0	0	0	0	0	0	0	0
talus	2	0	0	0	0	0	0	*	*	0	0	−0.1	0	0	+0.1	*	*
	3	0	0	0	0	0	0	0	−0.1	0	0	0	0	0	0	0	0
	1	0	0	0	0	0	0	0	0	0	0	0	0	0	0	0	0
calcaneus	2	0	0	0	0	0	−0.1	0	0	0	0	0	0	0	0	0	0
	3	−0.1	−0.1	−0.1	−0.1	0	0	*	*	0	0	0	0	0	0	*	*
	1	0	0	0	0	0	0	0	0		0	0	0	0	+0.1	+0.1	0
navicular	2	0	0	0	0	0	0	0	0	0	0	0	0	0	0	0	0
	3	0	0	0	0	0	0	0	0	0	0	0	0	0	0	0	0
	1	0	0	0	0	0	0	0	0	0	0	0	0	0	0	0	0
cuboid	2	0	0	0	0	0	0	0	0	0	0	0	0	0	0	0	0
	3	0	0	0	0	0	0	0	0	0	0	0	0	0	0	0	0

TABLE A.10.

Spec. nr 349 tarsal index 10		i_s II versus u_s8 II							
		horizontal				dorso-plantar			
bone	pellet nr	degrees ext. rot.				degrees ext. rot.			
		0	10	20	30	0	10	20	30
tibia	1	0	0	0	0	−0.2	−0.2	−0.1	0
	1	−0.1	−0.1	−0.1	0	*	*	*	*
talus	2	0	0	0	0	0	0	0	0
	3	−0.1	0	0	0	0	0	0	0
	1	0	−0.1	−0.1	0	0	0	0	+0.1
calcaneus	2	−0.1	0	0	0	0	0	0	*
	3	0	0	0	0	0	0	0	0
	1	0	−0.1	−0.1	−0.2	0	+0.1	0	−0.1
navicular	2	0	−0.1	0	0	0	+0.1	0	0
	3	0	0	0	0	0	0	0	0
	1	0	0	0	0	0	0	0	0
cuboid	2	0	0	0	0	0	0	0	0
	3	0	0	0	0	0	0	0	0

TABLE A.11.
Relative TACA

		♀ 29			♂ 14		
Phase		*50N* fresh un-dissected	*340N* fresh un-dissected	*340N* fresh dissected	*50N* fresh un-dissected	*340N* fresh un-dissected	*340N* fresh dissected
1	t	−0.07	−0.18	−0.06	0.24	0.13	−0.12
	α	8.44	5.91	6.05	3.72	1.27	0.81
2	t	−0.45	−0.37	−0.31	0.16	−0.02	−0.23
	α	7.43	10.55	9.73	11.86	4.09	4.77
3	t	0.01	−0.12	−0.36	1.66	0.71	−0.32
	α	3.27	4.02	6.17	12.69	14.79	14.21
4	t	0.07	0.01	−0.18	0.65	★ 1.25	−0.43
	α	2.89	2.76	3.76	8.19	11.58	12.93
5	t	−0.23	−0.40	−0.45	1.11	0.13	−0.09
	α	6.75	8.10	9.89	13.13	10.04	5.90
6	t	−0.38	−0.19	−0.29	0.34	0.01	−0.05
	α	8.25	7.54	6.01	5.89	2.79	0.81
	$\bar{\alpha}$	6.17	6.48	6.93	9.25	7.38	6.57

TABLE A.12.
Relative TACA

	♀ 29			♂ 14		
Phase	50N fresh un-dissected	340N fresh un-dissected	340N fresh dissected	50N fresh un-dissected	340N fresh un-dissected	340N fresh dissected
	π	π	π	π	π	π
1	−20.74 (339.26)	−23.01 (336.99)	−21.45 (338.55)	39.48	34.89	14.76
2	−16.88 (343.12)	−20.56 (339.44)	−22.70 (337.30)	38.87	39.53	34.64
3	−5.97 (354.03)	−12.71 (347.29)	−15.62 (344.38)	27.57	40.17	39.30
4	−5.53 (354.47)	−21.19 (338.81)	−12.00 (348.00)	25.97	* 35.10	39.38
5	−12.80 (347.20)	−16.43 (343.57)	−20.69 (339.31)	37.27	44.25	37.18
6	−21.20 (338.80)	−24.14 (335.86)	−26.38 (333.62)	35.32	37.13	30.01
	φ	φ	φ	φ	φ	φ
1	40.39	36.78	34.39	30.49	25.16	34.39
2	43.46	42.34	38.52	31.96	30.16	26.88
3	53.21	49.25	43.84	29.93	28.27	29.13
4	52.97	53.13	42.54	34.29	* 27.86	29.98
5	46.16	43.45	40.58	28.67	29.66	23.90
6	37.90	40.63	33.08	30.07	33.56	27.18

TABLE A.13.
Relative TACA

	♀ 29			♂ 14		
Phase	50N fresh un-dissected	340N fresh un-dissected	340N fresh dissected	50N fresh un-dissected	340N fresh un-dissected	340N fresh dissected
	γ	γ	γ	γ	γ	γ
1–6	2.51°	3.95°	4.31	3.62	8.64	14.93
2–5	3.96°	3.22°	2.58	3.57	4.14	3.76
3–4	0.60°	6.58	2.94	4.57	4.49	0.85
1–2	4.20	5.87	4.25	1.56	6.46	18.64
2–3	12.12	8.81	7.53	9.89	1.96	4.69
4–5	8.04	10.18	6.79	11.15	8.22	6.38
5–6	10.83	6.38	8.77	2.20	7.20	7.25

TABLE A.14.
Relative TANA

Phase		♀ 29 50N fresh un-dissected	♀ 29 340N fresh un-dissected	♀ 29 340N fresh dissected	♂ 14 50N fresh un-dissected	♂ 14 340N fresh un-dissected	♂ 14 340N fresh dissected
1	t	0.61	0.48	0.53	−0.36	−0.30	−0.11
	α	13.81	11.25	10.09	9.55	4.21	2.00
2	t	0.60	0.82	0.91	−0.69	−0.20	−0.06
	α	16.03	19.64	18.71	20.96	9.85	7.55
3	t	0.21	0.38	0.51	−0.84	−0.68	−0.69
	α	7.59	11.43	14.79	25.08	27.07	23.27
4	t	0.25	0.39	0.43	−0.63	⋆ −1.01	−0.68
	α	7.32	8.45	10.94	16.81	28.75	21.79
5	t	0.48	0.58	0.85	−1.00	−0.46	−0.10
	α	13.14	16.56	17.58	24.39	18.21	8.60
6	t	0.60	0.62	0.58	−0.36	+0.01	0.03
	α	14.76	14.48	11.94	11.97	5.92	1.60
	$\bar{\alpha}$	12.1	13.7	14.0	18.2	15.7	10.8

TABLE A.15.
Relative TANA

Phase	♀ 29 50N fresh un-dissected	♀ 29 340N fresh un-dissected	♀ 29 340N fresh dissected	♂ 14 50N fresh un-dissected	♂ 14 340N fresh un-dissected	♂ 14 340N fresh dissected
	π	π	π	π	π	π
1	348.75	352.21	353.83	25.18	9.81	13.52
2	353.82	349.45	346.08	27.86	31.45	38.86
3	355.22	355.11	358.90	18.25	28.68	32.36
4	351.83	351.67	353.85	20.31	23.65	34.05
5	352.92	348.38	348.29	22.86	31.64	33.26
6	354.15	354.91	355.74	21.10	24.74	32.91
	φ	φ	φ	φ	φ	φ
1	35.34	32.14	29.33	37.31	37.72	32.99
2	29.90	33.58	37.59	33.62	32.43	31.71
3	24.52	21.33	27.03	19.72	28.97	29.96
4	25.75	21.58	27.70	23.31	⋆ 30.72	32.81
5	32.63	31.66	36.71	30.97	29.17	23.96
6	32.56	31.80	28.10	32.26	27.28	29.66

TABLE A.16.

Relative TANA

	♀ 29			♂ 14		
Phase	50N fresh un-dissected	340N fresh un-dissected	340N fresh dissected	50N fresh un-dissected	340N fresh un-dissected	340N fresh dissected
	γ	γ	γ	γ	γ	γ
1–6	5.26	2.32	2.08	6.05	16.32	17.86
2–5	2.83	2.12	1.97	4.99	3.27	9.19
3–4	3.31	3.21	4.53	4.07	4.70	3.19
1–2	6.91	2.73	10.48	4.29	18.44	21.39
2–3	5.52	13.23	15.10	16.32	4.20	5.84
4–5	6.94	10.49	10.16	7.99	7.70	8.88
5–6	1.03	5.55	10.65	1.98	6.37	5.71

TABLE A.17.

Relative CUNA

		♀ 29			♂ 14		
Phase		50N fresh un-dissected	340N fresh un-dissected	340N fresh dissected	50N fresh un-dissected	340N fresh un-dissected	340N fresh dissected
1	t	−0.18	−0.32	−0.10	−0.46	−0.57	−0.35
	α	0.76	0.95	1.04	0.37	0.74	0.33
2	t	−0.14	−0.17	−0.06	0.99	−0.10	0.27
	α	4.05	3.31	2.27	2.38	0.81	1.08
3	t	0.11	+0.09	−0.19	0.50	1.11	0.76
	α	2.46	4.73	5.24	6.78	3.38	2.06
4	t	−0.05	0.01	−0.16	0.06	⋆ 1.20	0.44
	α	2.62	3.23	3.62	4.44	3.95	1.28
5	t	−0.01	0.09	−0.13	1.38	0.85	0.10
	α	2.52	3.17	2.51	3.89	1.25	0.89
6	t	−0.28	−0.32	−0.12	0.63	−0.37	−0.10
	α	2.19	2.53	2.12	0.70	0.95	0.37
	$\bar{\alpha}$	2.40	3.0	2.8	3.1	1.9	1.0

TABLE A.18.
Relative CUNA

Phase	♀ 29 50N fresh undissected	♀ 29 340N fresh undissected	♀ 29 340N fresh dissected	♂ 14 50N fresh undissected	♂ 14 340N fresh undissected	♂ 14 340N fresh dissected
	π	π	π	π	π	π
1	17.18 (197.18)	29.04 (209.04)	44.18 (224.18)	66.40 (246.40)	56.75 (236.75)	39.89 (219.89)
2	25.86 (205.86)	13.48 (193.48)	13.84 (193.84)	155.44 (335.44)	335.28 (155.28)	347.53 (167.53)
3	23.72 (203.72)	26.45 (206.45)	27.84 (207.84)	161.42 (341.42)	172.75 (352.75)	181.03 (1.03)
4	21.36 (201.36)	28.72 (208.72)	25.40 (205.40)	156.10 (336.10)	* 163.15 (343.15)	166.47 (346.47)
5	16.89 (196.89)	4.16 (184.16)	15.77 (195.77)	164.61 (344.61)	211.72 (31.72)	302.54 (122.54)
6	33.97 (213.97)	30.49 (210.49)	37.97 (217.97)	124.02 (304.02)	341.89 (161.89)	297.57 (117.57)
	φ	φ	φ	φ	φ	φ
1	−31.57	−10.88	− 5.16	−40.99	− 8.48	18.69
2	+ 9.33	+ 9.72	+35.84	− 2.21	+47.41	51.83
3	−22.91	−24.44	−15.52	7.92	− 3.81	−14.76
4	−30.60	−31.26	−23.74	17.87	* −13.01	− 5.35
5	3.88	− 4.48	+28.24	−10.45	− 6.76	+49.50
6	0.58	+ 4.98	10.95	−10.09	43.73	− 1.45

TABLE A.19.
Relative CUNA

Phase	♀ 29 50N fresh undissected	♀ 29 340N fresh undissected	♀ 29 340N fresh dissected	♂ 14 50N fresh undissected	♂ 14 340N fresh undissected	♂ 14 340N fresh dissected
	γ	γ	γ	γ	γ	γ
1–6	34.72	15.92	17.26	59.75	84.93	39.06
2–5	10.44	16.92	7.77	13.28	117.28	29.16
3–4	7.98	7.11	8.54	12.23	13.21	19.14
1–2	23.65	25.76	49.90	87.83	90.53	72.18
2–3	13.73	36.43	53.04	11.75	133.87	39.61
4–5	27.05	35.95	52.81	29.55	48.19	67.53
5–6	17.38	27.95	27.04	39.87	122.97	51.13

TABLE A.20.
Relative NACA

		♀ 29			♂ 14		
Phase		50N fresh un-dissected	340N fresh un-dissected	340N fresh dissected	50N fresh un-dissected	340N fresh un-dissected	340N fresh dissected
1	t	0.43	0.31	0.19	−0.17	−0.30	0.02
	α	5.62	5.66	4.46	6.01	3.10	1.20
2	t	0.84	0.74	0.54	0.02	0.00	0.14
	α	9.09	9.50	9.17	9.44	5.82	2.85
3	t	0.30	0.76	0.70	−1.71	−0.20	0.58
	α	4.86	8.02	9.17	12.95	12.78	9.25
4	t	0.38	0.55	0.61	−1.17	★ −0.78	0.38
	α	4.83	6.20	7.31	8.79	13.61	8.97
5	t	0.65	0.94	0.59	−0.59	0.04	0.10
	α	6.71	8.69	7.95	11.95	8.59	2.74
6	t	0.42	0.26	0.17	−0.15	0.13	0.07
	α	7.03	7.64	6.61	6.34	3.25	0.80
	$\bar{\alpha}$	6.4	7.0	7.5	9.3	7.9	4.3

TABLE A.21.
Relative NACA

	♀ 29			♂ 14		
Phase	50N fresh un-dissected	340N fresh un-dissected	340N fresh dissected	50N fresh un-dissected	340N fresh un-dissected	340N fresh dissected
	π	π	π	π	π	π
1	2.09	7.00	13.03	15.54	−2.08 (357.92)	12.68
2	5.03	1.68	−1.74 (358.26)	14.28	26.02	47.37
3	3.87	−2.93 (357.07)	4.94	2.70	15.41	22.27
4	−1.51 (358.49)	−4.76 (355.24)	−3.41 (356.59)	11.57	★ 14.20	28.85
5	1.07	4.37	4.80	6.65	16.34	23.64
6	12.00	11.67	15.31	7.31	14.90	35.38
	φ	φ	φ	φ	φ	φ
1	27.78	26.75	21.40	41.19	41.39	32.05
2	22.29	27.56	40.78	37.84	34.24	38.28
3	11.29	11.12	17.79	21.14	32.94	32.30
4	14.26	12.87	25.40	24.11	★ 40.76	37.42
5	23.46	27.03	38.35	37.56	29.59	23.23
6	26.74	23.11	22.55	34.78	21.56	31.46

TABLE A.22.
Relative NACA

	♀ 29			♂ 14		
Phase	50N fresh un-dissected	340N fresh un-dissected	340N fresh dissected	50N fresh un-dissected	340N fresh un-dissected	340N fresh dissected
	γ	γ	γ	γ	γ	γ
1–6	8.87	5.58	2.40	9.11	24.45	19.27
2–5	3.84	5.40	5.60	6.04	9.42	25.14
3–4	6.02	2.51	10.86	8.71	7.88	7.43
1–2	6.11	4.80	23.07	3.49	23.21	28.77
2–3	11.05	17.00	23.69	19.46	8.93	2.19
4–5	9.53	14.17	14.69	14.09	11.30	14.88
5–6	10.42	15.03	18.18	2.82	8.14	13.27

TABLE A.23.
Relative CUCA

		♀ 29			♂ 14		
Phase		50N fresh un-dissected	340N fresh un-dissected	340N fresh dissected	50N fresh un-dissected	340N fresh un-dissected	340N fresh dissected
1	t	0.65	0.56	0.39	−0.73	−0.48	−0.18
	α	5.30	5.02	3.73	5.99	3.39	1.37
2	t	0.68	0.75	0.53	−0.57	−0.41	0.02
	α	6.36	6.51	6.99	8.12	6.46	3.71
3	t	0.42	0.48	0.67	−2.16	−1.23	−0.30
	α	3.31	5.52	6.05	8.44	10.23	7.46
4	t	0.46	0.49	0.60	−0.97	⋆ −1.39	−0.04
	α	3.67	4.86	5.92	6.93	10.94	8.21
5	t	0.57	0.75	0.62	−1.62	−0.85	−0.36
	α	4.72	6.17	5.55	8.98	7.49	3.19
6	t	0.64	0.58	0.36	−0.81	−0.52	−0.15
	α	5.38	5.46	4.78	6.05	4.06	0.84
	$\bar{\alpha}$	4.8	5.6	5.5	7.4	7.1	4.1

TABLE A.24.
Relative CUCA

Phase	♀ 29 50N fresh undissected	♀ 29 340N fresh undissected	♀ 29 340N fresh dissected	♂ 14 50N fresh undissected	♂ 14 340N fresh undissected	♂ 14 340N fresh dissected
	π	π	π	π	π	π
1	0.28	2.60	3.96	18.34	11.20	3.19
2	−8.12 (351.88)	−3.68 (356.32)	−7.55 (352.45)	27.32	21.07	34.21
3	−1.94 (358.04)	−16.65 (343.35)	−6.49 (353.51)	9.38	21.79	28.25
4	−11.17 (348.83)	−14.73 (345.27)	−14.61 (345.39)	25.81	* 27.32	36.21
5	− 5.91 (347.20)	− 6.12 (343.57)	− 1.36 (339.31)	17.18	12.90	10.82
6	1.89	2.40	4.64	14.39	8.79	5.39
	φ	φ	φ	φ	φ	φ
1	34.86	33.16	27.82	38.44	35.21	22.77
2	42.01	36.86	42.20	46.60	36.51	44.46
3	38.64	44.22	49.35	48.68	42.90	37.34
4	44.69	42.68	53.67	51.98	* 51.08	41.36
5	37.58	42.05	42.92	49.30	32.73	32.81
6	37.23	31.19	27.36	35.64	26.94	28.72

TABLE A.25.
Relative CUCA

Phase	♀ 29 50N fresh undissected	♀ 29 340N fresh undissected	♀ 29 340N fresh dissected	♂ 14 50N fresh undissected	♂ 14 340N fresh undissected	♂ 14 340N fresh dissected
	γ	γ	γ	γ	γ	γ
1–6	2.71	1.97	0.76	4.21	8.56	6.27
2–5	4.75	5.52	4.62	7.30	7.70	22.55
3–4	9.15	2.08	6.64	10.97	9.94	7.35
1–2	9.71	6.34	17.16	10.49	8.10	33.38
2–3	5.78	12.28	7.20	12.23	6.42	8.42
4–5	8.14	6.39	13.86	6.09	21.17	21.89
5–6	6.21	12.82	16.31	13.81	6.80	6.20

TABLE A.26. Tibia.

Spec.		α 30° computed		t direct measurement		t computed	
		sup.	ret.	sup.	ret.	sup.	ret.
♀ 29	50N_i	29.9	28.4	2.38	2.17	2.82	2.26
i_t = 8	340N_i	27.3	27.8	1.86	1.34	0.70	1.47
L	340N_o	28.9	29.3	1.70	1.22	1.46	1.43
♂ 14	50N_i	28.8	28.7	5.12	4.35	5.23	4.55
i_t = 25	340N_i	27.3	* 28.5	5.56	5.27	5.36	* 6.07
R	340N_o	27.1	27.3	5.32	5.43	5.26	5.62

TABLE A.27. Talus.

Spec.		α 30°		t	
		sup.	ret.	sup.	ret.
♀ 29	50N_i	27.6	26.3	−0.84	−0.18
i_t = 8	340N_i	27.5	26.6	−1.68	−0.95
L	340N_o	26.8	25.5	−1.59	−0.80
♂ 14	50N_i	32.2	31.3	4.30	4.08
i_t = 25	340N_i	26.5	* 29.5	2.14	* 3.91
R	340N_o	23.1	22.4	0.01	0.79

TABLE A.28. Calcaneus.

Spec.		α 30°		t	
		sup.	ret.	sup.	ret.
♀ 29	50N_i	17.4	16.8	−0.24	−0.27
i_t = 8	340N_i	17.0	16.3	−0.52	−0.16
L	340N_o	18.0	17.4	−0.10	−0.02
♂ 14	50N_i	20.0	19.6	1.80	1.67
i_t = 25	340N_i	16.3	* 17.6	0.60	* 1.07
R	340N_o	15.0	14.6	0.07	0.15

TABLE A.29. Cuboid.

Spec.		α 30°		t	
		sup.	ret.	sup.	ret.
♀ 29	$50N_i$	22.7	22.0	1.17	1.22
i_t = 8	$340N_i$	24.5	23.5	1.66	1.66
L	$340N_o$	25.9	23.7	1.61	1.62
♂ 14	$50N_i$	29.5	28.5	−2.17	−2.30
i_t = 25	$340N_i$	24.5	● 27.9	−2.31	★ −2.55
R	$340N_o$	20.3	19.9	−0.75	−0.77

TABLE A.30. Navicular.

Spec.		α 30°		t	
		sup.	ret.	sup.	ret.
♀ 29	$50N_i$	29.7	28.2	0.17	0.26
i_t = 8	$340N_i$	32.9	31.0	0.50	0.82
L	$340N_o$	33.5	31.2	−0.10	−0.20
♂ 14	$50N_i$	38.0	36.6	2.06	1.71
i_t = 25	$340N_i$	26.9	● 32.0	0.76	★ 0.37
R	$340N_o$	21.3	20.7	0.48	0.09

TABLE A.31.

$50 N_i$	♀ 29 i_t = 8		♂ 14 i_t = 25	
α	0–30	30–0	0–30	30–0
TACA	19.1	17.8	28.2	27.1
TANA	37.3	35.2	55.0	53.1
CUNA	7.2	7.1	9.1	8.6
NACA	19.5	18.4	27.9	26.9
CUCA	14.9	13.7	22.4	21.8

TABLE A.32.

340 N_i	♀ 29 $i_t = 8$		♂ 14 $i_t = 25$	
α	0–30	30–0	0–30	★ 30–0
TACA	20.4	18.3	20.1	24.3
TANA	42.1	39.3	40.9	48.8
CUNA	8.6	8.4	2.6	4.1
NACA	22.9	22.3	21.5	25.2
CUCA	16.9	16.4	20.0	22.0

TABLE A.33.

340 N_o	♀ 29 $i_t = 8$		♂ 14 $i_t = 25$	
α	0–30	30–0	0–30	30–0
TACA	21.9	19.2	19.7	19.6
TANA	43.3	40.6	32.7	31.9
CUNA	7.9	7.7	1.1	1.1
NACA	22.3	21.8	13.1	12.4
CUCA	16.6	16.2	12.4	12.0

TABLE A.34.

Spec. ♀ 29 i = 8 unprocessed		i_s III versus u_s60 III								i_r III versus u_r60 III							
		horizontal				dorso-plantar				horizontal				dorso-plantar			
bone	pellet nr	degrees ext. rot.				degrees ext. rot.				degrees ext. rot.				degrees ext. rot.			
		0	10	20	30	0	10	20	30	30	20	10	0	30	20	10	0
tibia	1	0	0	0	−0.1	0	0	−0.1	−0.1	0	0	0	0	0	0	+0.1	0
	1	0	0	0	0	0	0	−0.1	0	0	0	−0.1	0	0	0	0	0
talus	2	0	0	0	0	0	0	0	0	0	0	0	0	+0.1	0	0	0
	3	0	0	0	0	0	0	0	0	0	0	+0.1	0	0	−0.1	0	0
	1	0	+0.1	0	−0.1	0	0	0	−0.1	0	−0.1	0	0	0	−0.1	0	0
calcaneus	2	+0.1	0	0	0	0	0	0	0	0	−0.1	0	0	0	+0.1	+0.1	0
	3	0	0	+0.1	0	0	−0.1	0	0	0	−0.1	0	0	0	0	0	0
	1	0	+0.1	0	0	0	0	0	0	0	0	0	0	0	0	0	0
navicular	2	0	+0.1	+0.1	0	0	+0.1	0	0	−0.1	0	0	0	0	+0.1	0	0
	3	0	0	0	0	0	0	0	0	0	+0.1	0	0	0	0	0	0
	1	0	0	−0.1	0	0	−0.1	−0.2	−0.1	0	−0.1	0	0	0	0	−0.1	0
cuboid	2	0	−0.1	−0.2	0	0	0	−0.1	0	0	−0.2	−0.1	0	0	0	+0.1	0
	3	0	0	−0.1	0	0	0	0	0	0	0	0	0	0	0	+0.1	0

TABLE A.35.

Spec. ♀ 29 i_t = 8 osteo-ligamentous prep.		i_s III versus u_s60 III								i_r III versus u_r60 III							
		horizontal				dorso-plantar				horizontal				dorso-plantar			
bone	pellet nr	degrees ext. rot.				degrees ext. rot.				degrees ext. rot.				degrees ext. rot.			
		0	10	20	30	0	10	20	30	30	20	10	0	30	20	10	0
tibia	1	0	0	−0.1	−0.1	0	0	−0.1	0	0	+0.1	0	0	0	0	0	0
	1	0	0	0	0	0	0	0	0	0	0	0	0	0	0	+0.1	0
talus	2	0	0	0	0	0	0	−0.1	0	0	0	0	0	0	0	0	0
	3	0	0	0	0	0	0	0	0	0	0	0	0	0	+0.1	0	0
	1	0	0	−0.1	−0.1	0	0	0	0	0	−0.1	−0.1	0	0	−0.1	0	0
calcaneus	2	0	0	0	0	0	0	0	0	0	0	0	−0.1	0	0	0	0
	3	0	+0.1	0	0	0	0	−0.1	0	0	0	+0.1	0	0	0	+0.1	0
	1	0	0	0	0	0	0	0	0	0	0	0	0	0	0	0	0
navicular	2	0	+0.1	0	0	0	0	0	0	0	+0.1	0	0	0	0	+0.1	0
	3	0	+0.1	0	+0.1	0	0	0	0	0	0	0	0	0	0	0	0
	1	0	0	0	−0.1	0	−0.1	−0.2	−0.2	0	0	0	0	0	−0.1	0	0
cuboid	2	−0.1	0	−0.1	0	0	0	−0.1	0	0	0	−0.1	0	0	+0.1	0	−0.1
	3	0	0	0	0	0	+0.1	0	0	0	0	0	0	0	0	0	0

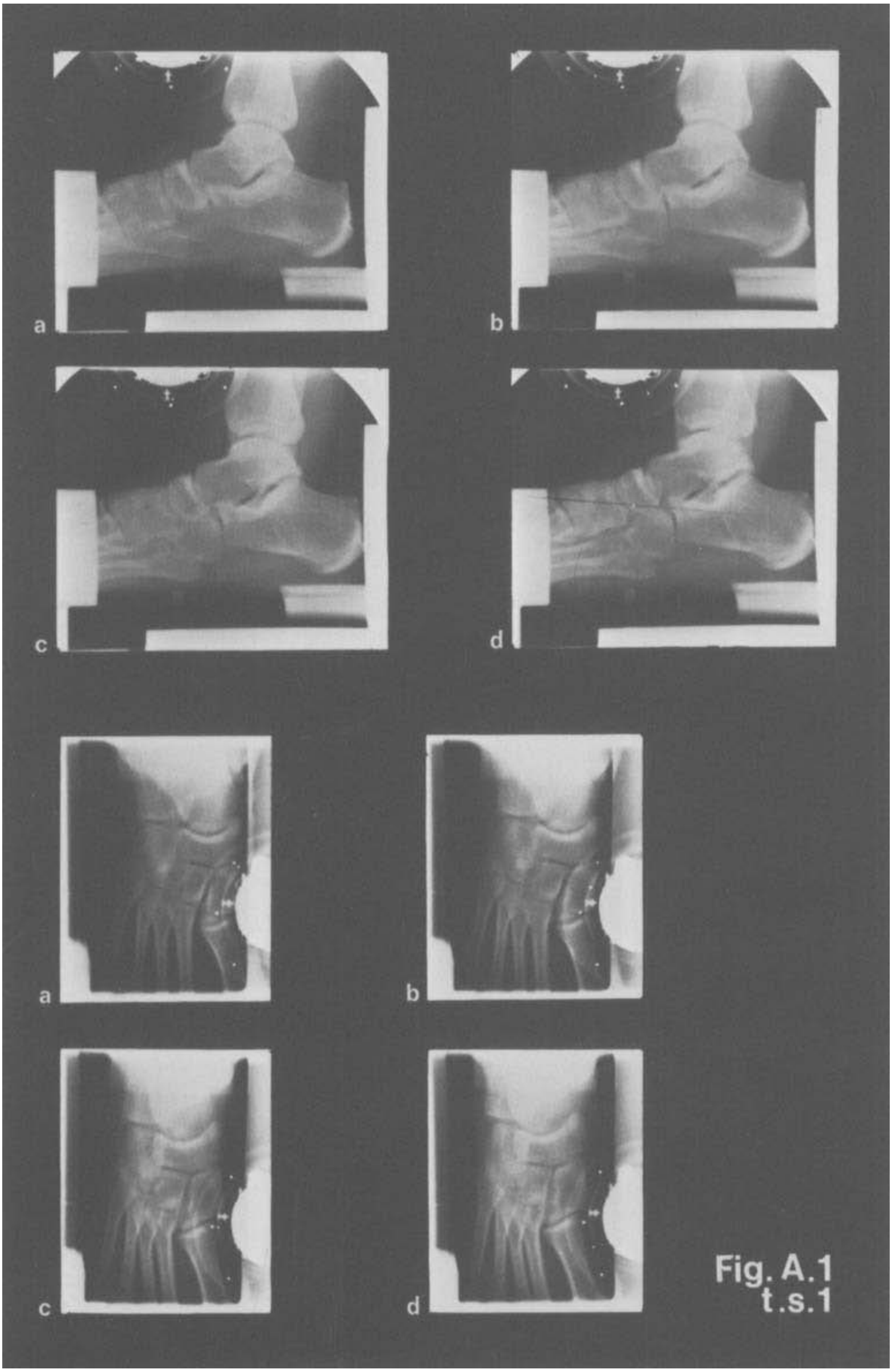

Fig. A.1
t.s.1

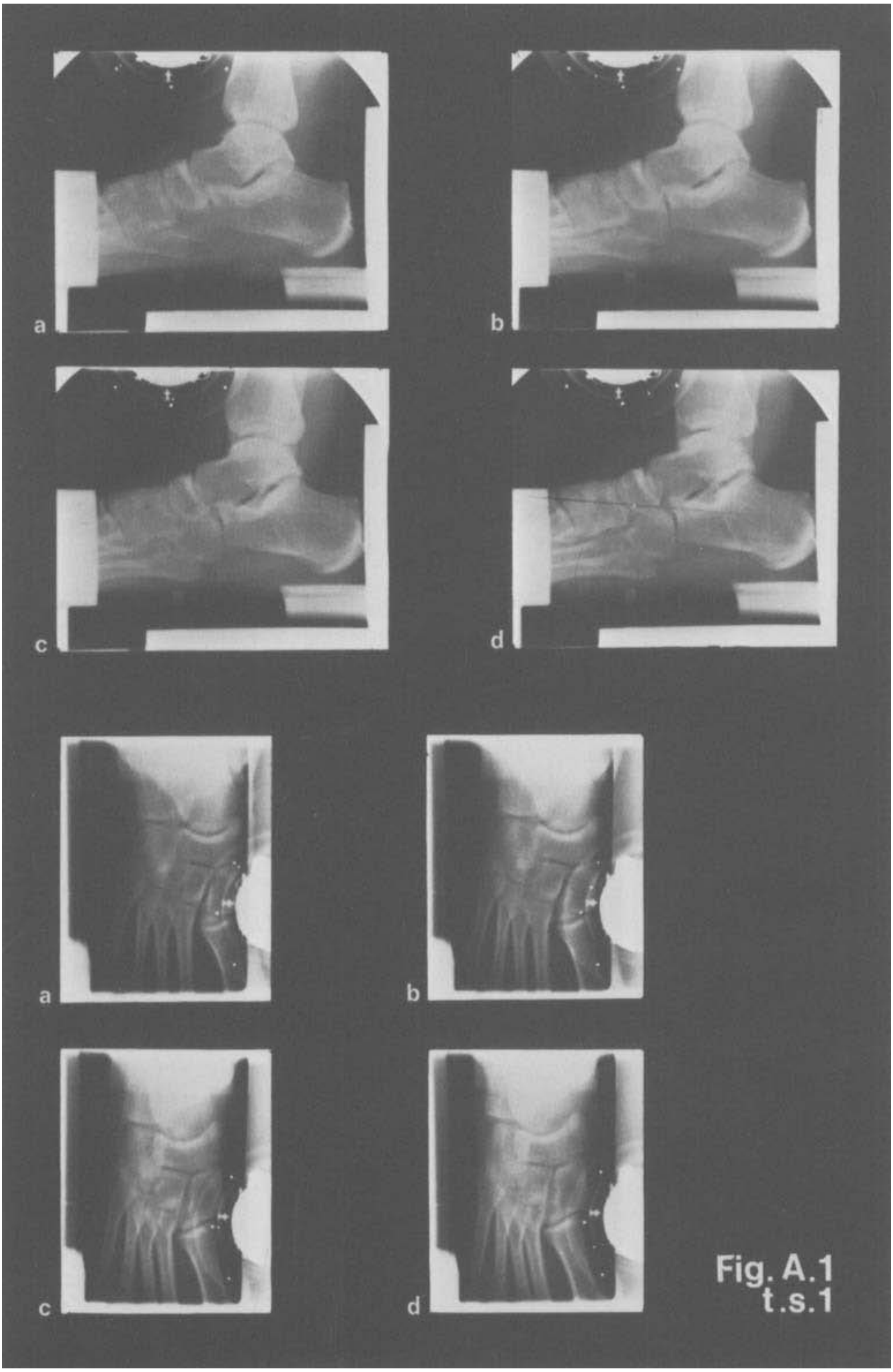

Fig. A.1
t.s.1

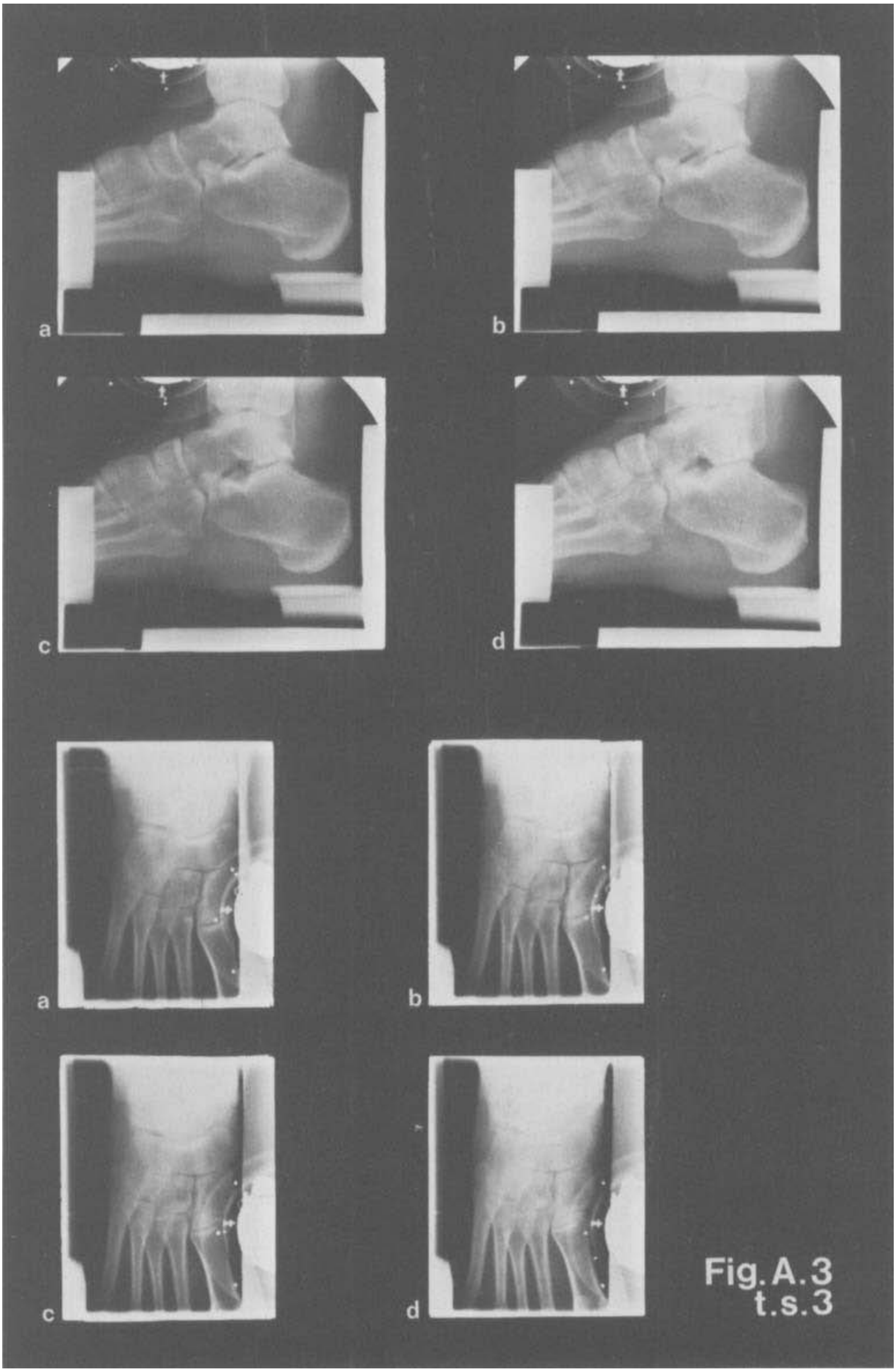

Fig. A.3
t.s.3

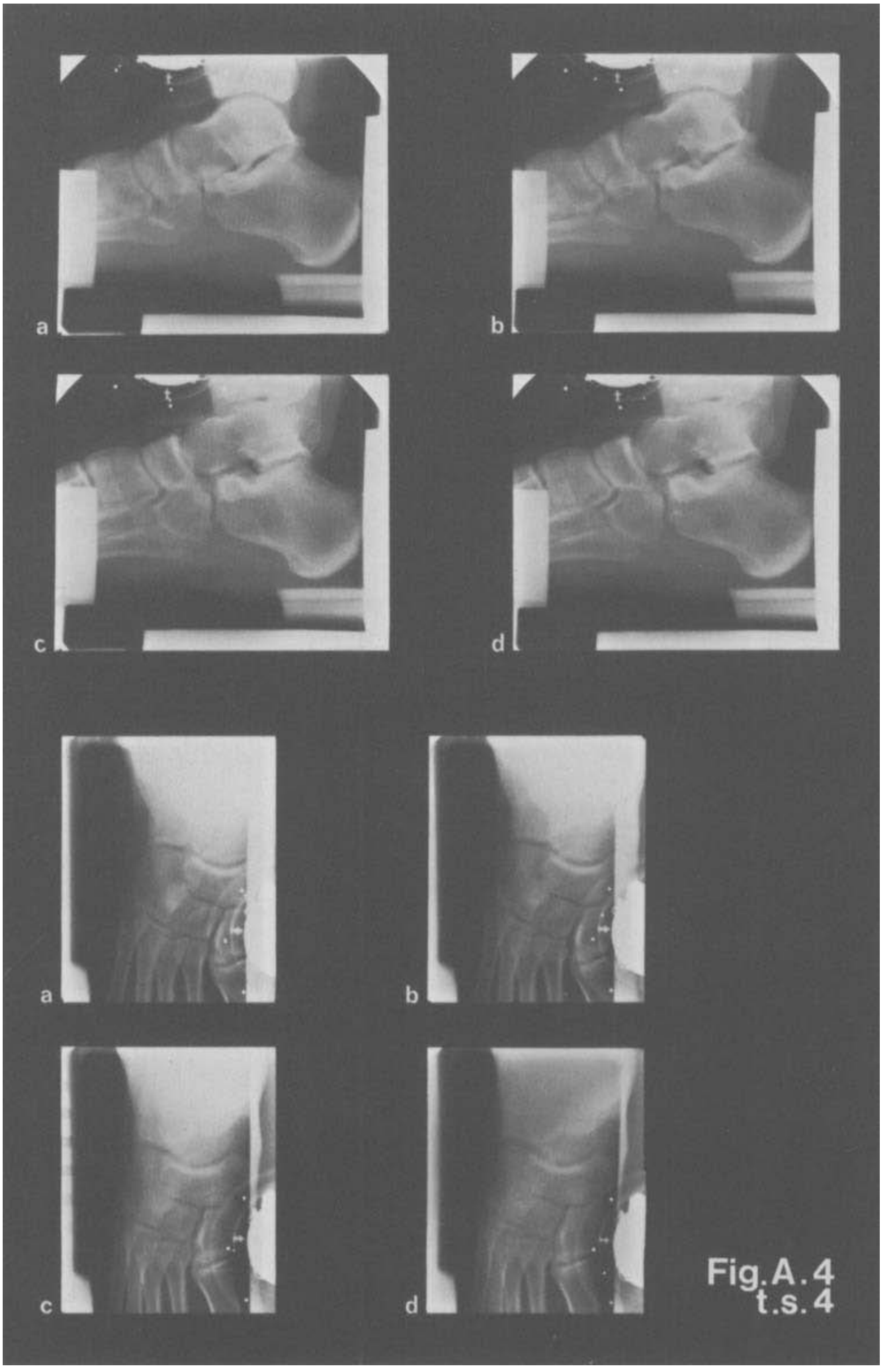

Fig. A.4
t.s. 4

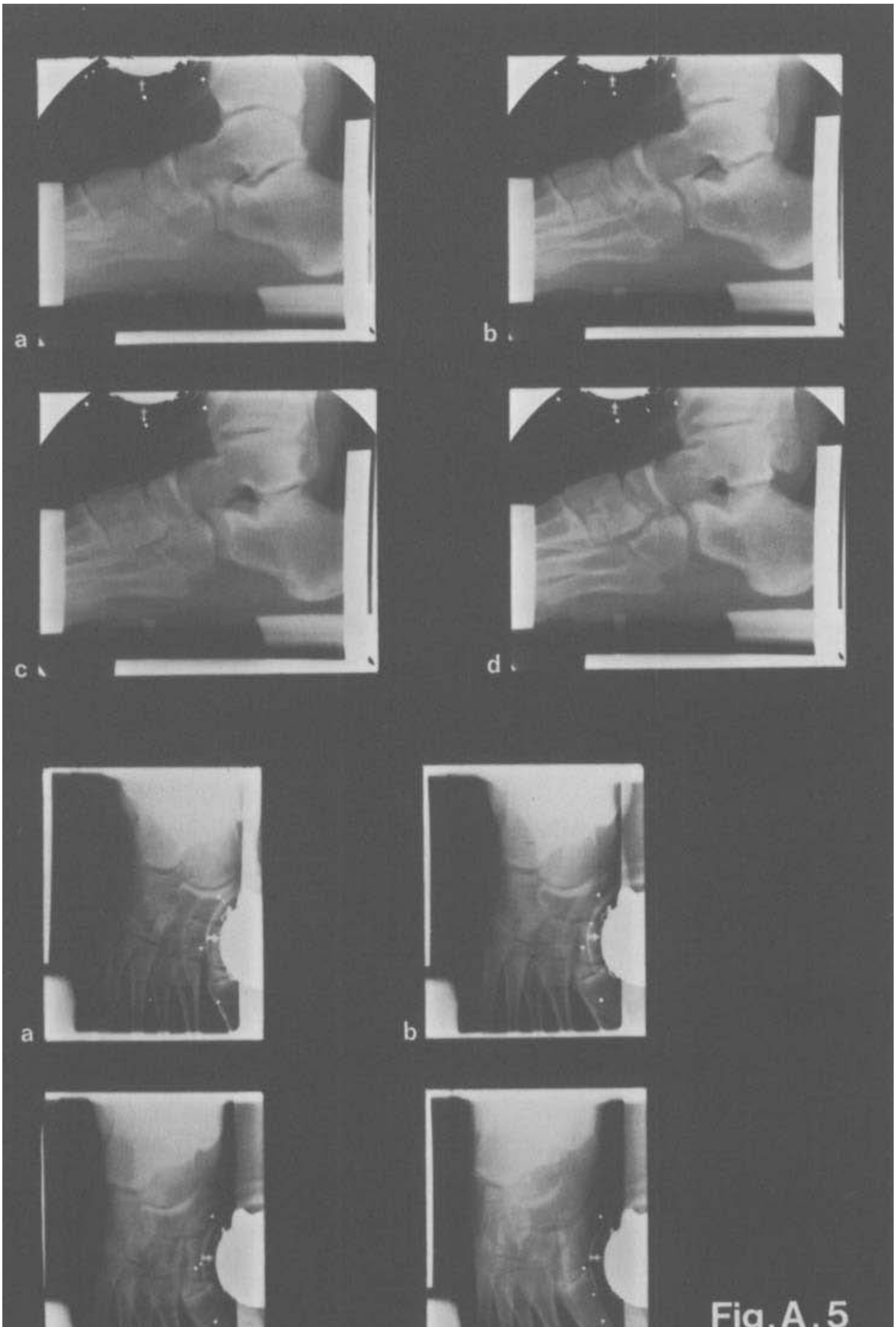

Fig. A. 5
t. s. 5

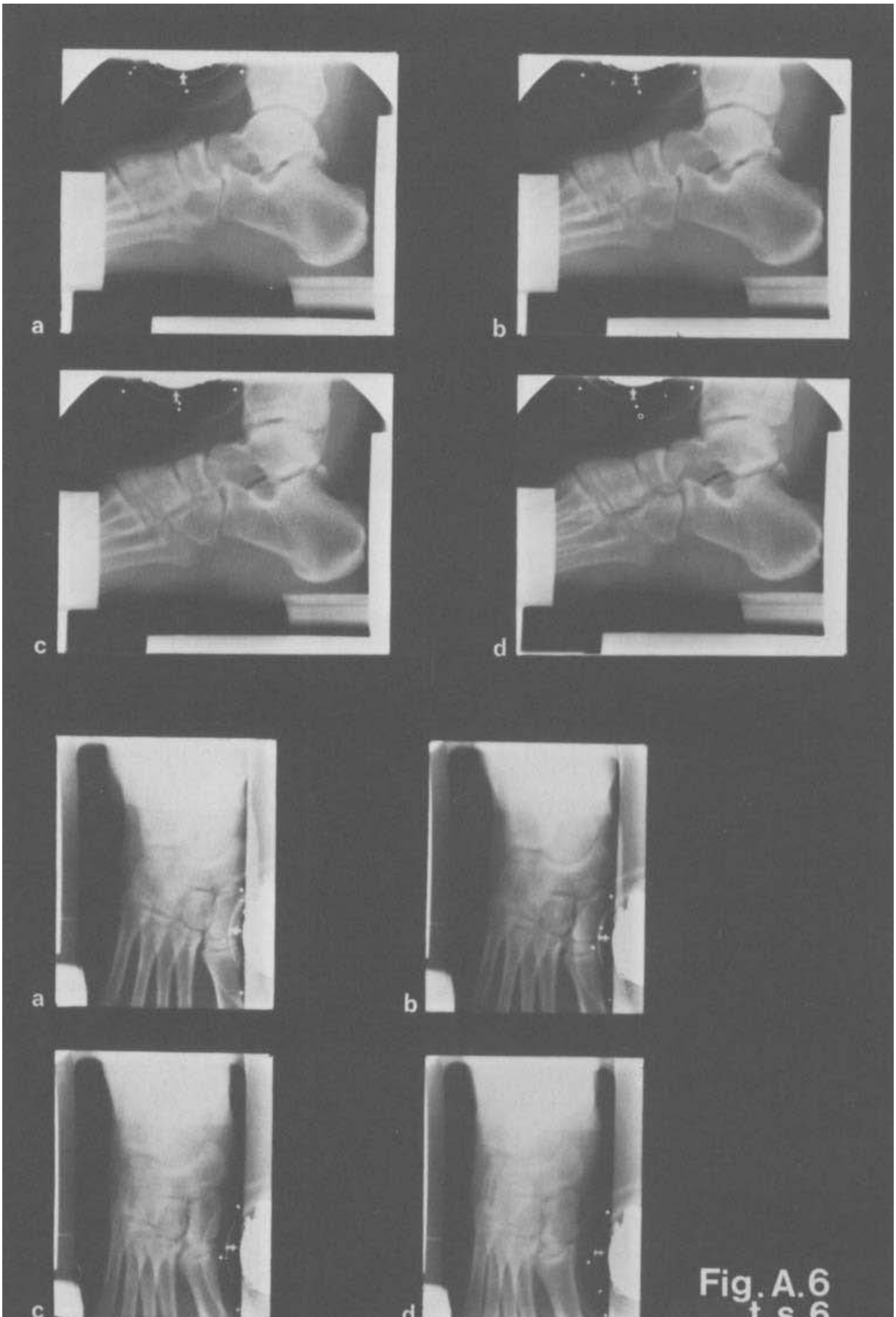

Fig. A.6
t.s.6

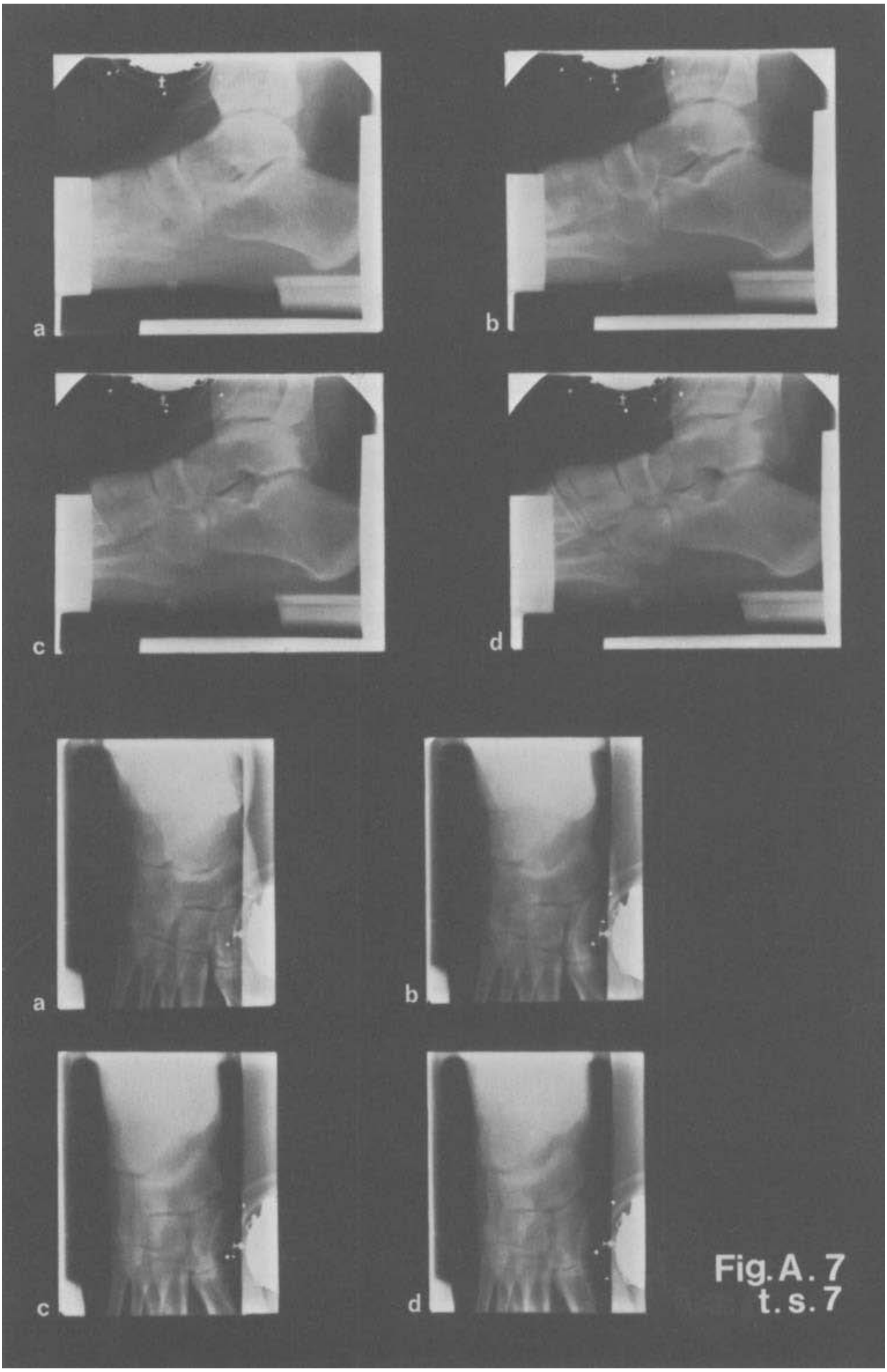

Fig. A. 7
t. s. 7

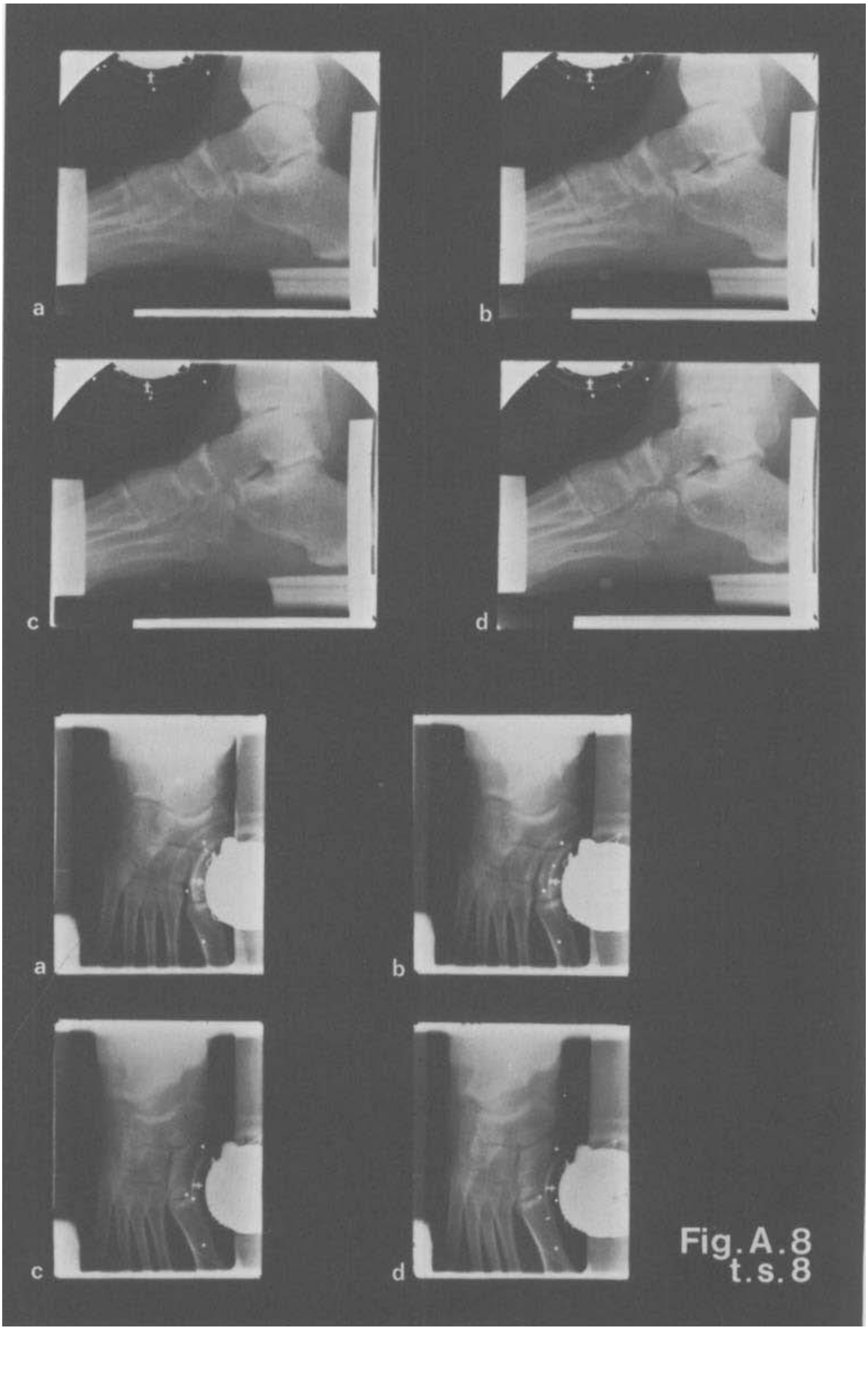

Fig. A.8
t.s. 8

Acknowledgments

The experimental work was performed at the Laboratory of Anatomy and Embryology of the University of Leiden (head Prof. Dr A. Huson).

The mechanical part of the already existing experimental setup was adapted by Mr. J. van der Kaai of the Anatomical Department; the electric unit was modified by the late Mr. C.G. Wouters of the Department of Physiology of the University of Leiden.

Mathematical support and technical advise were given by Ir C.W. Spoor, who also adapted the computerprograms and assisted with most of the experiments. Drs M. Schaafsma did some of the kinematical experiments.

The X-ray photographs were measured at the Laboratory of Geodesy, Delft University of Technology (head Prof. Dr Ir G.H. Ligterink) with the support of Mr. A. van Voorden. Fig. 2.8. was drafted by the late Mr. J. Tinkelenberg. Photographs were taken by Mr. J.H. Lens.

The X-ray photographs and 70 mm films were processed by Mr. M.G. Popkes and Mr. C.Th. Ruygrok at the Radiological Department of the Academic Hospital of Leiden (head Prof. Dr A.E. van Voorthuisen).

Statistical advise was given by Dr J. Hermans of Medical Statistics, University of Leiden.

The manuscript was typed by Mrs. W. Meijer-Bokhorst, Mrs. A. v.d. Heijde-Baltus, Mrs. D. v. Etten and Mrs. H.M. Nanninga-Visser. The Dutch text was translated by Mr. C. Visser and Mrs. M. Henkes.

The English text was edited by Dr B. Sundby, Netherlands Institute for Sea Research.

Curriculum vitae

The author was born in Amsterdam, The Netherlands, on the 26th of June 1947. After graduating secondary school from 1961 to 1967 at the Charlois Lyceum in Rotterdam, he fulfilled his military service as a Reserve-officer.

He studied medicine at the University of Leiden from 1969 to 1976. He graduated in 1976. Between 1974 and 1977 he worked two years at the Laboratory of Anatomy and Embryology (head Prof. Dr J.M.F. Landsmeer).

From 1977 to 1979 he underwent specialist training in General Surgery at the Bleuland Hospital in Gouda (head Dr J.D.C. Koch) and from 1979 to 1983 he received training as an orthopaedic surgeon in the Department of Orthopaedics of the University of Leiden (head Prof. Dr F. Duyfjes). During this four-year period, he trained during half a year at the Red Cross Hospital in The Hague with Mr. H.J. de Mol van Otterloo and Mr. L.J.C.D. Mol, orthopaedic surgeons.

Since 1983 the author is working as an orthopaedic surgeon at the Gemini Hospital in Den Helder in association with the orthopaedic surgeon Mr. P.J.M. Konings, and the general surgeons Mr. K.J. Boekhoudt, Mr. W.W.J. Clarijs and Mr. J.J.M. Jutte.